NTNU
Norwegian University of
Science and Technology

An empirical approach for determining the evolution and behavior of rockslide dams.

Development of a empirical tool based on geomorphic parameters of rockslide dams and impounded valleys to predict future rockslide dam heights and their relative longevity

Vegard Utstøl Jakobsen

Geotechnology
Submission date: February 2016
Supervisor: Reginald Hermanns, IGB
Co-supervisor: Thierry Oppikofer, NGU

Norwegian University of Science and Technology
Department of Geology and Mineral Resources Engineering

Abstract

The secondary consequences of rock slope failure pose a threat to people living in Norwegian valleys. Blockage of rivers cause upriver flooding. Catastrophic breaching of the dam poses a major threat to people living beneath the dam.

This master thesis introduces a tool that predicts the dam height of future rock slope failures. The tool is created on the basis of a geomorphic analysis of rockslide dams in the southwestern parts of Norway (Jakobsen, 2015). The tool is an empirical equation that considers "dam volume" and "valley width" as the major factors that influences "dam height". The parameters were chosen based on a 2-dimensional covariance-analysis. The database used to determine the empirical equation contains 19 elements.

$$dam\ height = \frac{dam\ Volume}{2{,}76E+05}\, e^{-\frac{valley\ width}{8{,}03E+02}} - \frac{valley\ width}{6{,}66E+01} + 31{,}12$$

Dimensionless blockage index considers "catchment area" (A_b), "dam volume" (V_d) and "dam height" as the main factors that determine the stability of rockslide dams (Ermini & Casagli, 2003). The stability of future rockslide dams can be assessed by replacing "dam height" with the equation above.

$$DBI = \log\left(\frac{A_b * \left(\frac{V_d}{2{,}76E+05}\, e^{\frac{W_v}{8{,}03E+02}} - \frac{W_v}{6{,}66E+01} + 31{,}12\right)}{V_d}\right)$$

Other factors influence the stability of rockslide dams. The character of the carapace governs the resistance of the dam against continuous erosion (Weidinger, 2011). Grainsize analysis of the rockslide dams; Månavatnet and Gloppedalsura illustrate how the character of the carapace influences the stability, and hence the longevity of rockslide dams.

Sammendrag

De sekundære konsekvensene av store fjellskred er en potensiell risiko for mennesker som bor i norske daler. Blokkering av dreneringssystemer fører til oversvømmelse oppstrøms. Dambrudd av dreneringsblokaden tillater frigivelse av enorme vannmasser nedstrøms, som utsetter mennesker som bor nedstrøm for en enorm risiko.

Denne masteroppgaven introduserer et verktøy som kan brukes for å estimere dam-høyde til framtidige fjellskred. Verktøyet er basert på geomorfologisk undersøkelse av skreddemninger i fylkene; Møre og Romsdal, Sogn og Fjordane, Hordaland og Rogaland (Jakobsen, 2015). Verktøyet er basert på empirisk data, og anser dam-volum og dal-bredde som de viktigste parameterne for å forutsi dam-høyde. Parameterne bestemt er basert ved hjelp av en 2-dimensional varians-analyse. Databasen som ble brukt i ligningen under består av 19 elementer.

$$dam\ høyde = \frac{dam\ Volum}{2{,}76E+05}\, e^{-\frac{valley\ width}{8{,}03E+02}} - \frac{dal\ bredde}{6{,}66E+01} + 31{,}12$$

DBI anser dreneringsareal (A_b), dam-volum (V_d) og dam-høyde som parametere for å bestemme stabiliteten av skreddemninger (Ermini & Casagli, 2003). Man kan forutsi stabiliteten til framtidige skreddemninger ved å erstatte dam-høyde med likningen ovenfor.

$$DBI = \log\left(\frac{A_b * \left(\frac{V_d}{2{,}76E+05}\, e^{\frac{W_v}{8{,}03E+02}} - \frac{W_v}{6{,}66E+01} + 31{,}12\right)}{V_d}\right)$$

Flere andre faktorer påvirker stabiliteten til skreddemninger. Det grove øverste laget til fjellskred kontrollerer avsetningens mottastand mot erosjon (Weidinger, 2011). Kornanalyser av skreddemningene; Gloppedalsura og Månavatnet illustrer hvordan karakteren til avsetninger påvirker dam-stabilitet, og levetiden til demningen.

Acknowledgement

I can't help but feel pride and accomplishment when sitting down, reading through my master-thesis. Five and a half years have been spent at NTNU. Things have changed, others have changed and I have changed. I am forever grateful to the IGB faculty for giving me the opportunity to grow as a person, as well as offering me the opportunity to gain valuable knowledge. I want to give my sincerest thanks to both my supervisors; Reginald Hermanns and Thierry Oppikofer for giving me the opportunity to work with them, withstanding countless stupid questions as well as well as accepting my moronic humor. Furthermore; I want to thank the entire geohazard-team at NGU for making me feel welcome, and for including me into the group.

The summer of 2015 was spent doing fieldwork, and engaging in countless discussions with my colleague Øyvind Rem. Well, I hope this is interpreted with a portion of humor, but "you were a star on the dark night-sky", haha. Well, I guess I have to mention the other stars as well. My brother Håvard Utstøl Jakobsen, Ivanna Penna and my cousin Sølve Pettersen whom have stuck up with correcting my numerous English errors, I promise I will help you with engineering-geological problems in the future. No acknowledgement can be written without mentioning a mother, so Ragnhild Utstøl Jakobsen (my mother), thank you for everything!

The first cornerstone has been laid, so with this;

Sayonara.

Vegard Utstøl Jakobsen

Table of Contents

1. Introduction

Rockslide dams form by catastrophic failure of rock slope instabilities in valleys. The glacially over-steepened valleys are an ideal setting in Norway considering dam formation, where potential unstable rock slope areas are in abundance. Systematic mapping of the southern and western parts of Norway resulted in the discovery of 72 landslide dams (Jakobsen, 2015). Further detailed analysis on the landslide dams revealed that 3 dams were related to glacial deposits. The remaining landslide dams have been analyzed according to dam stability, morphometry and geomorphology.

Rockslide dams pose a threat due to the potential catastrophic dam failure. The most critical parameter considering dam failure consequences is dam height since it controls lake volume. Several rockslide dams are situated closed to, or at inhabited areas, and poses a serious threat to people. For example, Onilsvatnet in Tafjord was formed by a 210Mm^3 rock avalanche, that after formation failed catastrophically (Hermanns et al., 2013). The residual lake is used today as a recourse for power production.

The goal of this master thesis is to establish a tool that predicts rockslide dam height of future catastrophic rock slope failures. The tool is to be constructed on the basis of the morphometric analysis of rockslide dams in southern and western Norway (Jakobsen, 2015). To investigate which parameters influence the formation of rockslide dams, geomorphic valley parameters and morphometric dam parameters are to be analyzed. The tool can be used as a preliminary method to determine the secondary consequences of rock slope failure in Norwegian valleys. The northern part of Norway is to be systematically mapped to locate suitable dams to test the tool against. Eventually, the tool is to be used to determine "dam height" of the potential rock slope areas; Gamanjunni, Mannen and Ivasnasen.

Several factors influence the stability and longevity of landslide dams. Dimensionless blockage index (DBI) is a method that considers; dam volume (m^3), dam height (m) and the size of the catchment area (m^2) to assess the stability of landslide dams. (Ermini & Casagli, 2003; Weidinger, 2011). The stability of future rockslide dams can be assessed by replacing dam height in the DBI-equation, with the tool proposed in this master-thesis. Grainsize analysis of rockslide dams can give additional information about the longevity of the lake, where the erosional resistance of the rockslide carapace plays an important role.

2. Theory

2.1. Formation of Rockslide Dams

Rockslide dams usually form when rock slope instabilities fail in a geomorphic domain that allows formation of rockslide deposits that block a preexisting drainage network, and result in upriver flooding, and changes to the all over erosional regime (Evans, Delaney, Hermanns, Strom, and Scarascia-Mugnozza (2011). The size and shape of the rockslide deposit depends on the mobility and size of the mass movement, and the geomorphological domain in which rock slope failure occur.

2.1.1 Types of Mass Movements that Form Rockslide Dams

Studies have shown that a broad range of mass movements are able to form landslide dams (Costa & Schuster, 1988). The study shows that; avalanches, slumps, slides, and flows formed most landslide dams based on an inventory of 180 dams (Figure 2.1). Generally, large dams form by complex landslides that start as slumps or slides, and transform into rock or debris avalanches (Costa & Schuster, 1988). Only a minority of the landslide dams investigated were formed by rock falls or sensitive clay failures (Figure 2.1) (Costa & Schuster, 1988) Systematic photo-interpretation in the southwestern parts of Norway resulted in an inventory of 72 landslide dams (Appendix. C-3). Further detailed analysis in the framework of the project-thesis revealed that 3 of the landslide dams were actually related to glacial deposits. Therefore, the resulting database contains 69 elements. Results show that 46% of the dams were formed by rockslides or massive rock falls, rock avalanches formed 53% and only 1% were formed by debris flows (Figure 2.2) (Jakobsen, 2015).

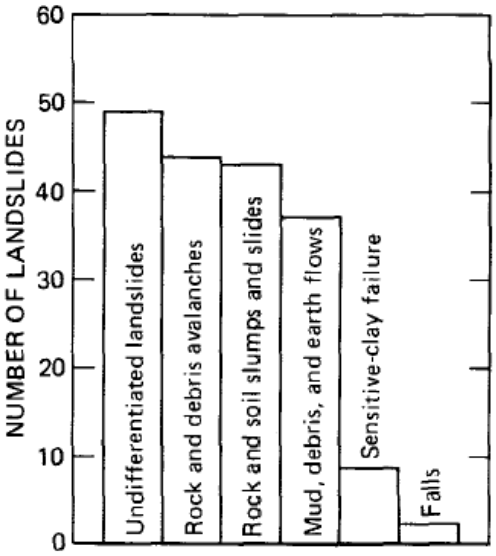

Figure 2.1:The distribution of mass movements that form landslide dams (Costa & Schuster, 1988).

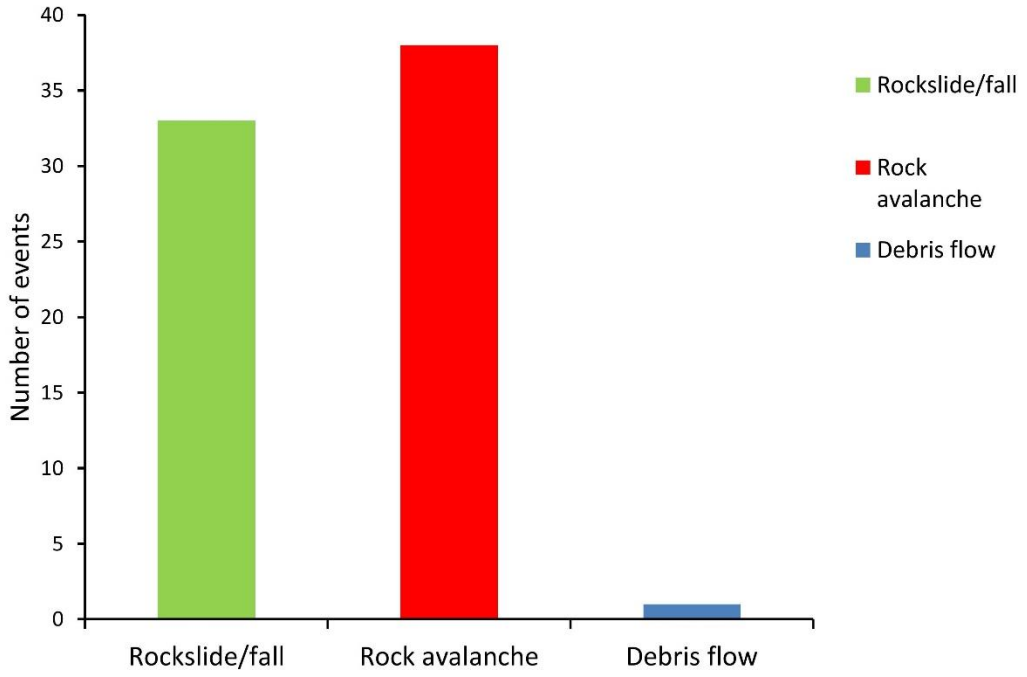

Figure 2.2: Distribution of landslides that have formed dams (Jakobsen, 2015).

The mobility of landslides depends on the volume of the initial failure, the height of the failure surface above the valley floor, the material composing the landslide and, constraints made by the geomorphology on the landslide (Nicoletti & Sorriso-Valvo, 1991). Concerning the volume of the initial failure, studies show that rockslide runoff increases with increasing rockslide volume (Nicoletti & Sorriso-Valvo, 1991). This has an implication on the final three dimensional shape and distribution of the rockslide deposit, and therefor effect the likelihood of rockslide dam formation (Evans et al., 2011).

2.1.2 Geomorphic Setting of Rockslide Dams

Rockslide dams form most frequent where narrow steep valleys are bordered by terrain with high relief (Costa & Schuster, 1988). The width of the valley determines the confinement on the rockslide mass (Clague, 1994). For example, rock slope failures in narrow valleys are more likely to result in debris deposits of greater thickness than identical failures in wide valleys (Clague, 1994). The location of the failure surface on the rock slope governs the potential energy of the mass movement and hence the initial mobility. This is represented by the fahrböschung, which represent the angle of reach as a function of volume (Corominas, 1996). If the valley-floor where rock slope failure occurs is steeply inclined, the mobility of the rockslide event increases, resulting in longer runoff distance down-valley (Nicoletti & Sorriso-Valvo, 1991).

The capability of the topography to constrain the mobility of rock slope failure influences the fahrböschung and the morphometry of the final deposit. If the rockslide debris is forced by the topography to channelize, the mobility of the rockslide increases, resulting in an "elongated hourglass shape" of the deposit. This situation is considered to be; low energy dissipative geomorphic control because it favors mobility (Figure 2.3; A)(Nicoletti & Sorriso-Valvo, 1991). When the rockslide material is unrestricted by topography, and the debris is able to spread out laterally while streaming downslope, the final debris formation is characterized by its "nearly oval, lengthened trapezium or tongue"-shape. This situation is considered to be; moderate energy dissipative geomorphic control (Figure 2.3; B)(Nicoletti & Sorriso-Valvo, 1991). If the rockslide is contained by opposing topography such as an opposing valley side in a narrow valley, the rockslide debris run-up the opposing valley side, hence constricting the mobility of the rockslide, resulting in a "deformed T-shape" of the deposit. This situation is considered to be; high-energy-dissipative geomorphic control (Figure 2.3; C)(Nicoletti & Sorriso-Valvo, 1991).

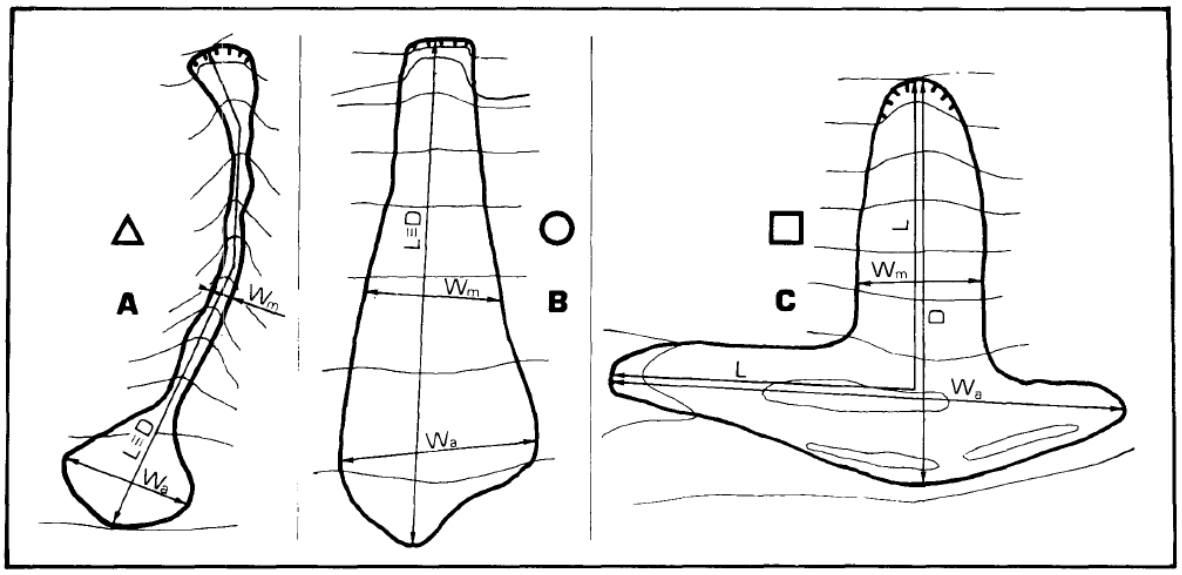

Figure 2.3: Three different situations of geomorphic control. A; Low energy dissipative geomorphic setting. B; moderate-energy dissipative geomorphic setting. C; High energy dissipative geomorphic setting (Nicoletti & Sorriso-Valvo, 1991).

The transport distance of rockslide debris during rockslide events has been investigated and described by among Albert Heim and Kenneth Hsu (Heim, 1932; Hsü, 1975). These studies show that the travel distance of rock slope failure is primarily a function of; the height of the release area and the volume of the rock slope failure (Figure 2.4). In other words, the travel distance during rock slope failure increases with increasing rockslide volume or increasing height of the release area (Heim, 1932; Hsü, 1975). Studies show that the correlation between

fahrböschung and the volume of the rockslide is nonlinear. This is related to incomplete fragmentation of the rockslide material during transportation (Corominas, 1996).

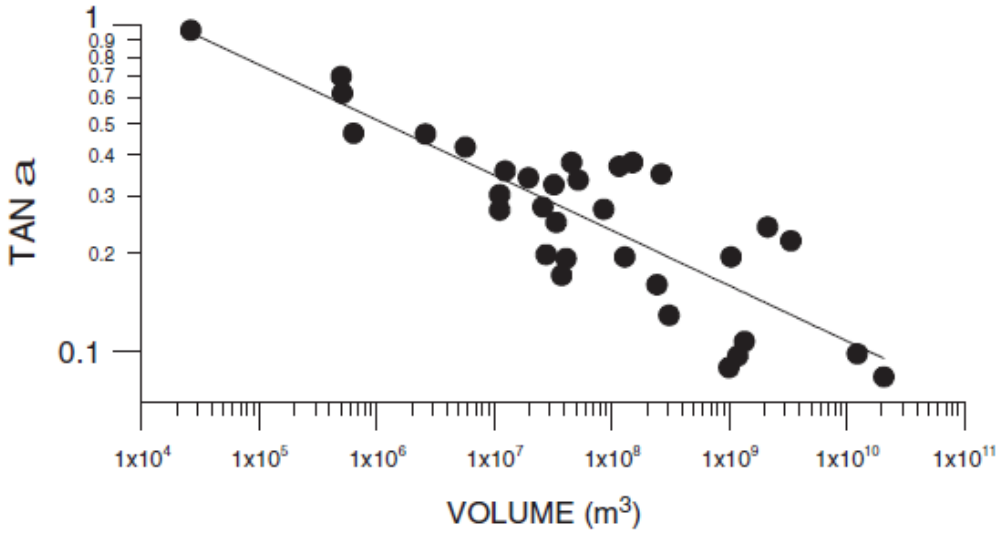

Figure 2.4:Graph illustrating the relationship between the tangent of fahrböschung and the volume of the rock slope failure (Hungr, 2006)

The elements described above characterize the general geomorphic elements affecting the distribution of rockslide deposits. Topographic irregularities such as hills or cliffs influence the displacement of the rockslide material, and hence effect the final form of the rockslide deposits. For example, hills in the direct travel path of a rock slope failure event forces divergence of transportation, and might result in the formation of several drainage blockades (Hermanns et al., 2011). Topographic irregularities are difficult to quantify, but affect the final form of the deposit.

2.2. Rockslide Dam Classification

Landslide dams can be classified according to the relation between the landslide deposit and valley geomorphology (Swanson, Oyagi, & Tominaga, 1986). The classification system proposed by Costa and Schuster (1998) distinguishes between different shapes of the landslide deposit related to the valley floor in two-dimensions (planar view) (Costa & Schuster, 1988). The classification system composes six different landslide dam classes. Type I dams are small compared to the valley width, and do not reach from one valley side to the other (Figure 2.5) (Costa & Schuster, 1988). Type II landslide dams are generally formed by larger landslides related to the valley width, filling the valley floor from one side to the other (Figure 2.5) (Costa & Schuster, 1988). Type III landslide dams are formed by high mobility landslides, allowing transportation of debris up-valley and down-valley, which can result in blockage of tributary valleys (Figure 2.5) (Costa & Schuster, 1988). Type IV landslide dams are formed by concurrent failure events from both sides of the valley that produces landslide deposits that connect in the valley (Figure 2.5) (Costa & Schuster, 1988). Type V landslide dams are formed when the landslides fail in a geomorphic domain that offers little to no confinement, resulting in dispersion of the landslide mass and the formation of several lobes of debris, enabling impoundment of multiple lakes (Figure 2.5) (Costa & Schuster, 1988). Type IV landslide dams form when the failure surface extend under the stream and emerges on the opposite valley, the formation of this class involve slow basal sliding that forms lakes by raising the elevation of the stream bed (Figure 2.5) (Costa & Schuster, 1988).

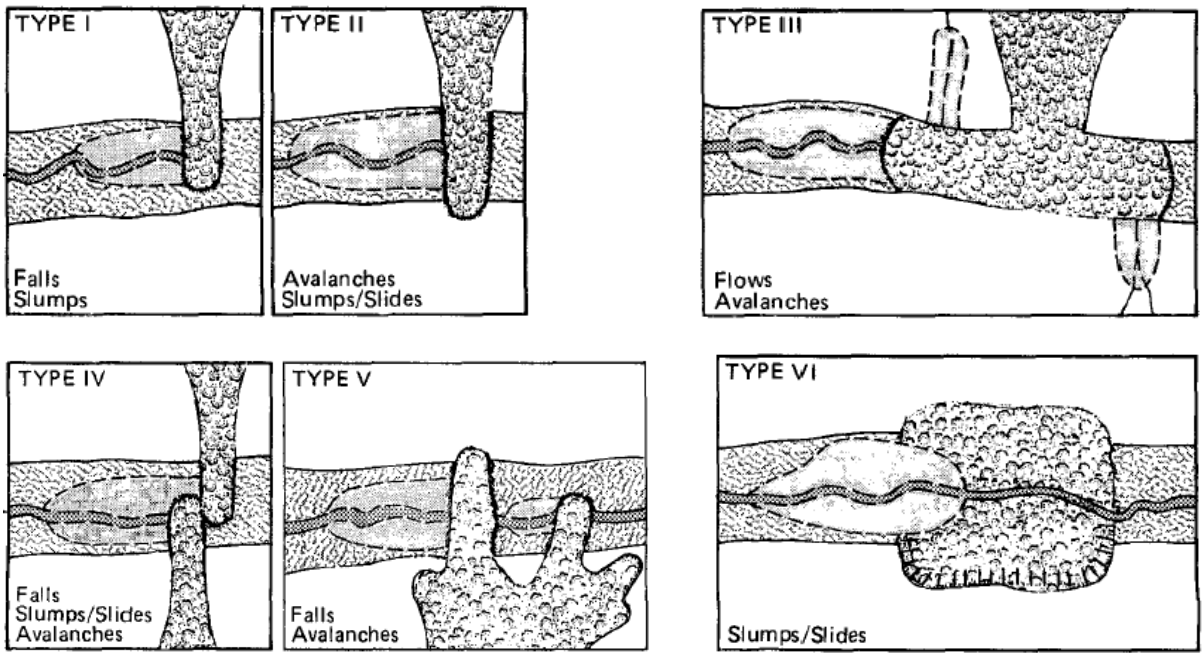

Figure 2.5: Traditional two-dimensional landslide dam classification (Costa & Schuster, 1988).

The classification-system proposed by Costa and Schuster (1988) focuses on the relation between the landslide deposit and the underlying geomorphology. It has been the classification preferred employed since its development in 1988, despite that general rockslide classification-systems have evolved (Cruden, 1996; Hungr, Leroueil, & Picarelli, 2014; Varnes, 1978). In recent years, limitations considering the classification-system proposed by Cosa and Schuster (1988), such as the fact that landslide dams are not two-dimensional features, have resulted in an updated landslide dam classification-system (Hermanns et al., 2011). The classification system proposed by Hermanns et al. (2011) emphasizes the fact that landslide dams are not two-dimensional features, and should therefore be classified according to the three-dimensional distribution of landslide deposits. The proposed classification system is a three-step system that considers; the two-dimensional planar distribution of the landslide deposits, which extends the classification system by Costa and Schuster (1998). A cross-valley profile of the landslide deposit and its relation to the underlying, buried valley morphology (Hermanns et al., 2011). An along-valley profile of the landslide debris and the underlying substrate (Hermanns et al., 2011).

2.2.1 Two-Dimensional (Plan View) Distribution of Rockslide Deposits

The two-dimensional distribution of rockslide deposits takes into account the phenomenon of landslide dams at confluences of two or more river valleys, and the rarer case of drainage divide (Hermanns et al., 2011). The two-dimensional classification is divided into five main distributions.

I. Ponds on large rockslide deposits are frequent. They are not connected to the river channel, and are therefore related to a limited drainage system, resulting in small scale lakes (Figure 2.6) (Hermanns et al., 2011).

II. Singular rockslide events can have different shapes based on rockslide volume, rockslide mobility and valley morphology. They can cross the entire valley, resulting in rockslide dams blocking the entire valley. Or they can partly cross the valley floor, resulting in imperfect damming of the valley (Hermanns et al., 2011). The singular rockslide barriers are divided into five subgroups based on the relation between; rockslide volume, valley morphology and rockslide mobility (Figure 2.6) (Hermanns et al., 2011).

III. Several rockslide dams might form as a consequence of a singular rockslide event. This depends on the size of the rockslide and the ability of the rockslide to spread out, creating multiple lobes or basins that enables accumulation of water. This class can be subdivided into two subgroups based on the morphology of the rockslide deposit (Figure 2.6) (Hermanns et al., 2011).

IV. Singular rockslide events may form contiguous dams in two or more valleys if the size and mobility is large enough to influence a confluence of valleys, or if the source location is favorable. Parts of the rockslide mass may run-up on the opposing valley side, and block tributary valleys. Five subtypes of this class can be derived based on the rockslide deposit and the valley system (Figure 2.6) (Hermanns et al., 2011).

V. Some rockslide events fail in a geomorphic domain that does not favor the formation of dams that absolutely block the drainage network, but allows the establishment of drainage divide. These incidents are rare, and are sub-classified in two classes. (Figure 2.6) (Hermanns et al., 2011).

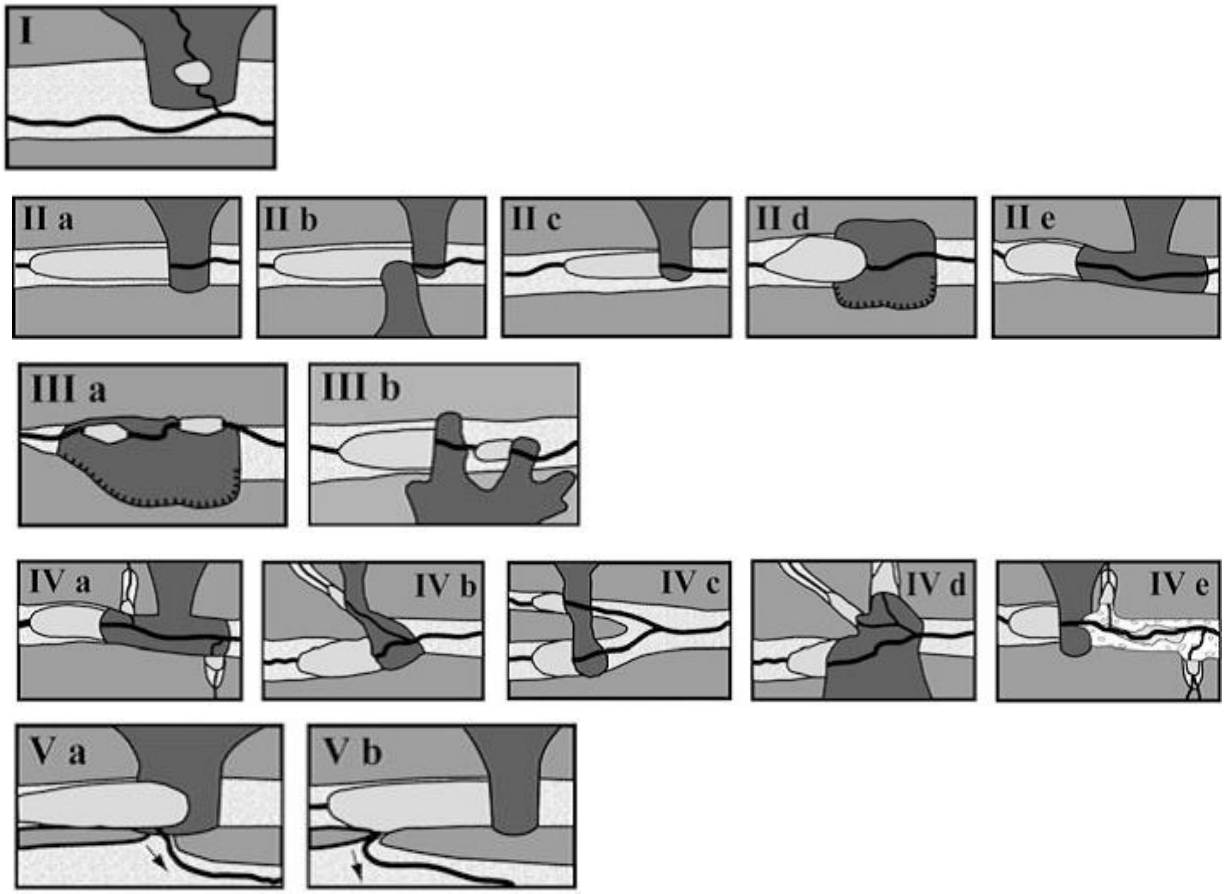

Figure 2.6: Two dimensional rockslide dam classification (Hermanns et al., 2011)

2.2.2 Cross-Valley Profile of Rockslide Deposits

The second part of the rockslide dam classification-system describes the relation between the rockslide deposit and the valley floor, by using an across valley profile. It takes into account the shape of the rockslide deposit and the symmetry of the valley.

i. The first type involves the symmetrical relation between the valley floor and the rockslide deposit in such a way that the lowest line of the deposit concurs with the lowest line of the valley (Figure 2.7) (Hermanns et al., 2011).
ii. The final of form of the deposit depends on the mobility of the rockslide; the mass may be deposited on either side of the valley depending on the mobility of the rockslide. In this case; the rockslide dam profile is asymmetrical to either side of the valley (Figure 2.7) (Hermanns et al., 2011).
iii. Class three represent rockslide dams in asymmetric valleys, where the lowest part of the dam does not correspond with the lowest part of the valley (Figure 2.7) (Hermanns et al., 2011).

iv. The fourth type represent rockslide dams where the initial rockslide only cover parts of the valley floor, and therefore allow drainage to diverge around the distal parts of the dam, creating an impoundment of limited depth (Figure 2.7) (Hermanns et al., 2011).

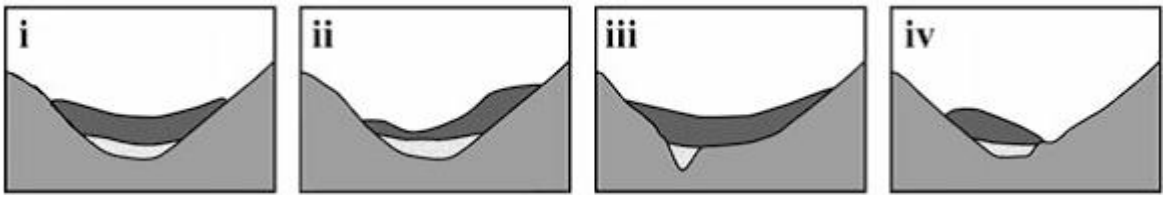

Figure 2.7: Cross-valley classification of rockslide deposits (Hermanns et al., 2011).

2.2.3 Along-Valley Profile of Rockslide Deposits

The third part of the rockslide dam classification-system describes the relation between the rockslide deposit and the valley floor by using an along-valley profile. It takes into account the shape of the rockslide dam and the geomorphology of the valley.

1. Rockslides of high mobility that do not experience major constraints by topographical constraints may spread over large areas to produce deposits of shallow thickness, hence form impoundments of limited depths (Figure 2.8) (Hermanns et al., 2011).
2. Rockslides that fails in a morphological domain that prohibits the rockslide mass to spread may form impoundments of great depths (Figure 2.8) (Hermanns et al., 2011).
3. In steeper valleys, the rockslide mass continues spreading along valley in thalweg direction. This results in a thin, often asymmetric deposit, where the major part rockslide is deposited in the frontal parts of the deposit. The impounded lake is often shallow due to the steepness of the valley floor (Figure 2.8) (Hermanns et al., 2011).
4. In some cases, the rockslide mass splits into two bodies. This can occur when the rockslide impacts an opposing slope, splits up and spreads in the thalweg direction with an offset between the rockslide bodies. Such slides often produce various dams in a singular valley (Figure 2.8) (Hermanns et al., 2011).

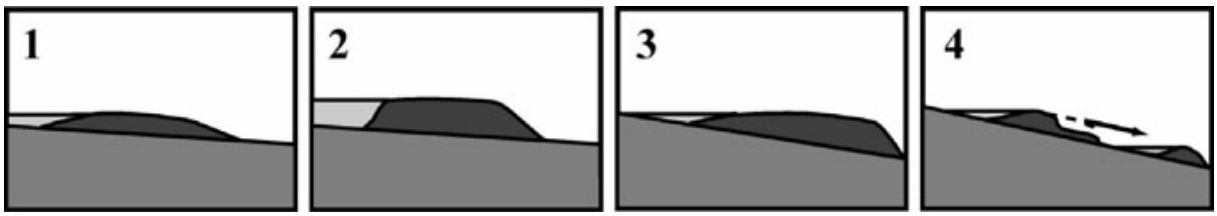

Figure 2.8: Along valley profile of the rockslide dam (Hermanns et al., 2011).

2.3. Morphological Parameters Controlling the Behavior of Rockslide Dams

2.3.1 Geomorphological Valley Parameters

Features such as valley width, slope angle and the height of the release area exert control on the distribution of the rockslide deposit, and indirectly control the likelihood of rockslide dam formation (Nicoletti & Sorriso-Valvo, 1991). Several parameters can be assessed to characterize the geomorphological predisposition of rockslide areas:

- Valley width (m): decided on the basis of the distance between equipotential lines, each dam has been considered as a unique case.
- Height of the release area (m): elevation difference between the back scarp and the valley floor.
- Gradient of the valley thalweg (degrees).
- Character of the unstable rock slope (Geological strength index, Rock mass rating or Q-value) (Stead D, 2013):
    - Orientation of planar structures (joints, bedding plane or faults).
    - Character of planar structures (roughness, spacing, waviness or persistence)
    - The character of the lithology (mineral composition, grade of metamorphosis or weathering).
    - The mechanical properties of the rock mass (rock mass modulus, uniaxial compressive strength or tensile strength).

The parameters describing the geomorphology of the valley can easily be assessed in a geographic information system (GIS).

2.3.2 Rockslide Dam Parameters

Rockslide dams can be characterized by morphological parameters such as; the size and shape of the depositional feature (Stefanelli, Catani, & Casagli, 2015). Similar work has been systematically carried out in New-Zealand by Oliver Korup (Korup, 2004), in Italy by Tacconi Steffanelli (Stefanelli et al., 2015) and in Japan (Swanson FJ, 1986). The most significant geomorphic parameters are listed below, and are illustrated in; Figure 2.9, Figure 2.10, and Figure 2.11

- Rockslide dam length: Maximum length of the rockslide dam, across valley.
- Rockslide dam width: Maximum width of the rockslide dam, along the valley thalweg.
- Rockslide dam mean height: The average thickness of the rockslide dam.
- Rockslide dam maximum height: The height of the rockslide dam where overtopping occurs.
- Rockslide dam area: Area of the rockslide mass contributing to blockage of the drainage network.
- Rockslide dam volume: Volume of the rockslide mass contributing to blockage of the drainage network.

The material that constitutes rockslide dams originates from rock slope failures. Parts of the rockslide mass are deposited on the proximal valley slope in the form of scree. Other parts of the rockslide mass are transported across the valley, to the distal valley side. The rockslide dam does therefore not constitute the entire rock slope failure (Figure 2.9, Figure 2.10 and Figure 2.11). The area of the rockslide dam is recognized to be the part of the rockslide deposit that influences the preexisting drainage network.

The maximum height of the rockslide dam is the thickness of the dam where overtopping occurs (S. Dunning, Petley, & Strom, 2005). If the rockslide is deposited symmetrical in a symmetric valley, the maximum height overlies the prior valley thalweg (Hermanns et al., 2011). However, if the rockslide is deposited asymmetrical in a valley, overtopping most likely occurs on the rockslide dam margins. This implies that the maximum height of the rockslide dam deviates from the maximum thickness of the dam (Hermanns et al., 2011).

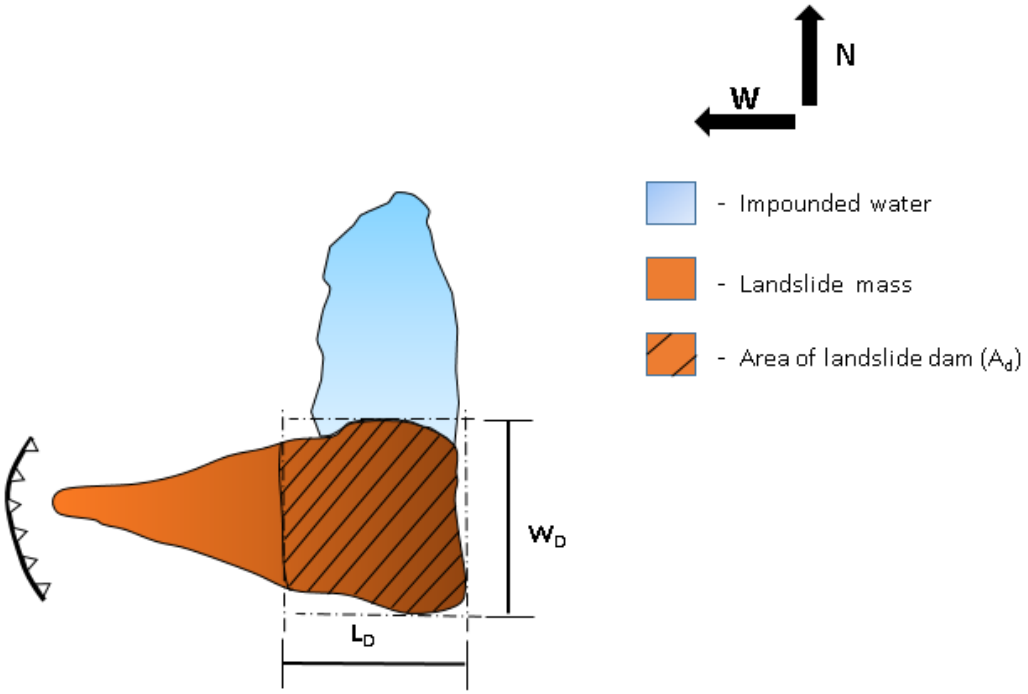

Figure 2.9: Two- dimensional distribution of a rockslide dam (Jakobsen, 2015).

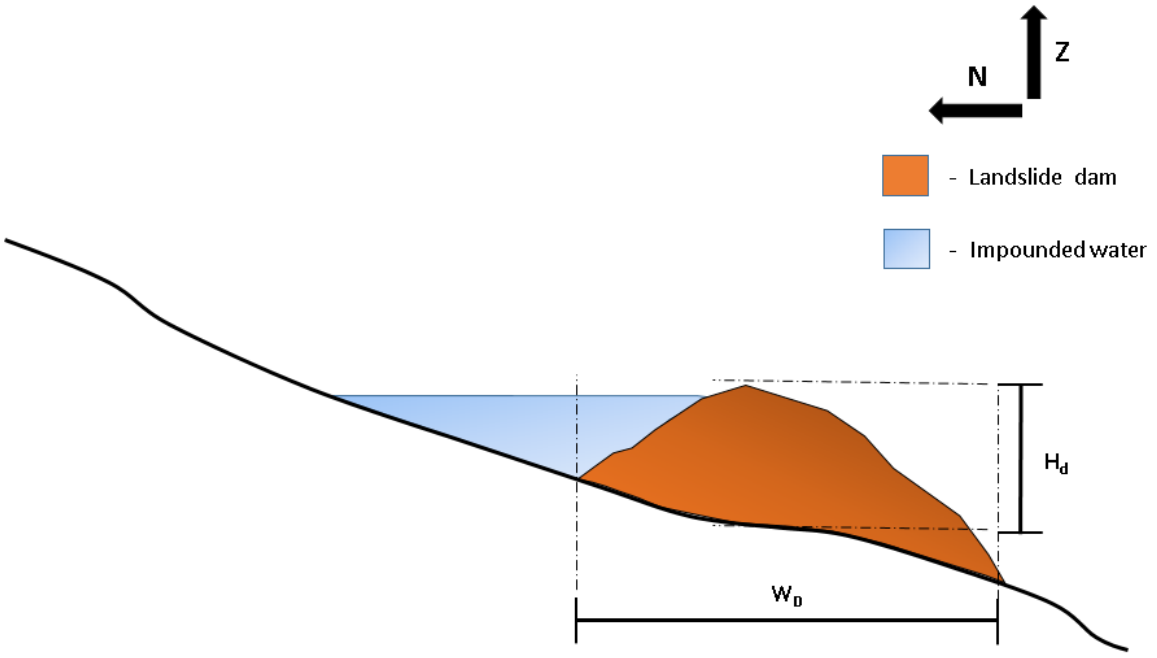

Figure 2.10: Along-valley distribution of a rockslide dam (Jakobsen, 2015).

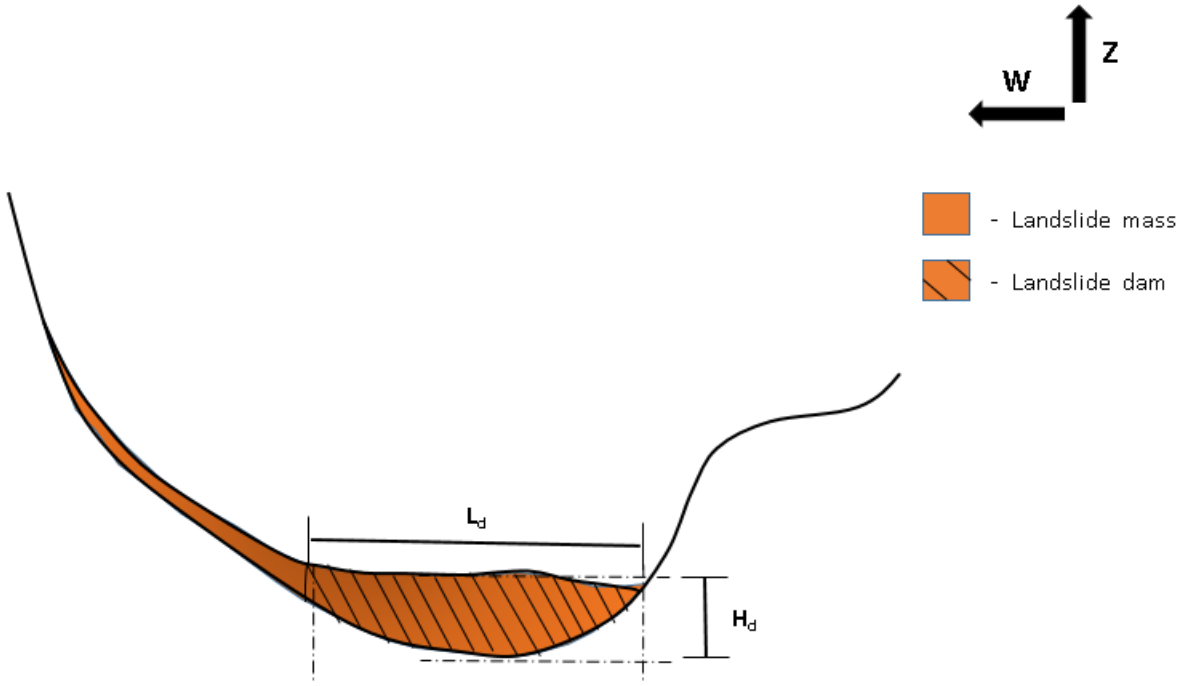

Figure 2.11: Cross-valley distribution of a rockslide dam (Jakobsen, 2015).

2.4. Evolution and Behavior of Rockslide Dam

2.4.1 Rockslide Dam Failure

Rockslide dams fail by a number of processes;

1. Overtopping which may lead to progressive upstream erosion and lateral widening of the overtopped channel (Evans et al., 2011).
2. Piping (Evans et al., 2011).
3. Sliding collapse of the distal portion of the rockslide dam due to high pore pressures or seepage (Evans et al., 2011).

Overtopping is initiated when the lake level reaches the rim of the rockslide dam (Evans et al., 2011). During overtopping failure, the overflow channel develops and enlarges by vertical down-cutting and subsequent lateral widening (Coleman, Webby, & Andrews, 2002). The widening of the spillway is accelerated by the collapse of the channel walls. Continued erosion allows further development of the channel cross-section, which again allows greater discharge and sediment transport until a stable lake level is reached (Evans et al., 2011).

The internal sedimentary structure of a rockslide deposit depends on the parent rockmass, mechanism of transportation and duration of transportation (Weidinger, 2011). If the properties of the sediments composing the rockslide dam favor high porosity and high permeability, continuous filtration through the dam might result in failure by the process of piping (Costa & Schuster, 1988). Piping is the process where granular material is eroded internally. It starts at the distal part of the dam by eroding granular particles, and gradually retrogresses towards the reservoir due to infiltration, resulting in a sudden outburst (Richards & Reddy, 2007). Failure due to slope collapse of the dam itself occurs if the rockslide dam is located in a steep valley and with high

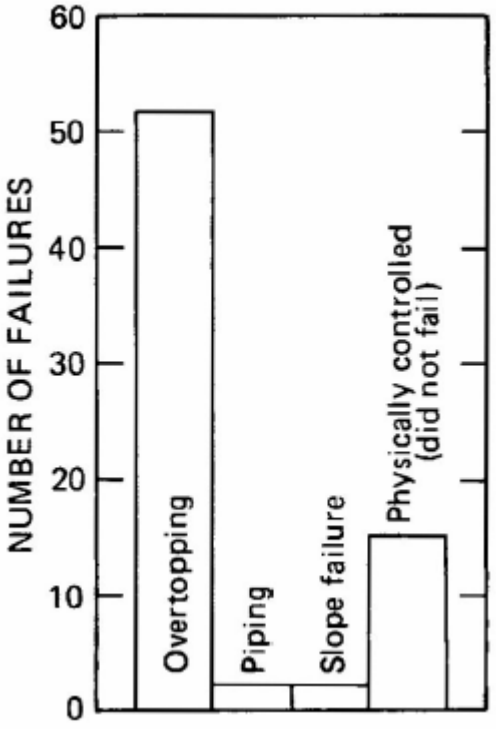

Figure 2.12: Distribution of failure process of 55 landslide dams (Costa & Schuster, 1988).

porepressure-difference across the dam, making it susceptible to slope failure. If the dam itself has a narrow cross section or if the slope failure itself is progressive, the crest may fail, leading to overtopping and breaching (Costa & Schuster, 1988).

Most dams fail by overtopping, followed by breaching by erosion (Costa & Schuster, 1988). Failure due to piping or slope failure are considered uncommon (Figure 2.12) (Costa & Schuster, 1988).

Analysis of rockslide dams in the southwestern part of Norway show that most dams remains stable. Some dams have been subjected by continuous erosion resulting in reduction of the lake capacity. Some dams are either entirely or partly filled in. Only a few dams have failed in a way that drastically reduces the capacity of the lake while transporting coarse material (Figure 2.13) (Jakobsen, 2015).

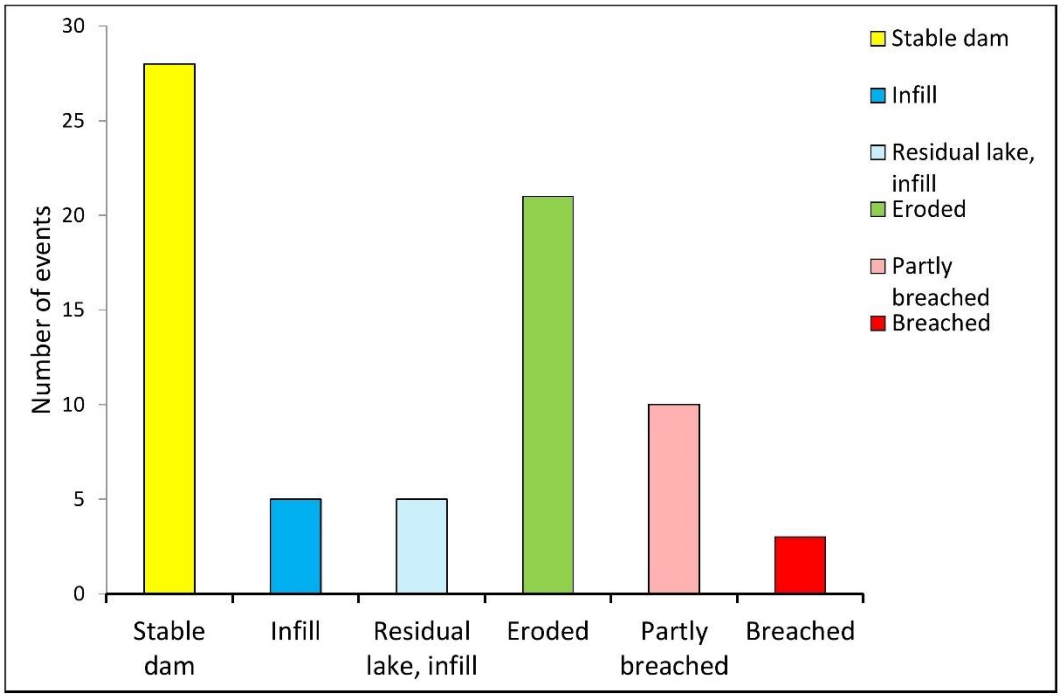

Figure 2.13: The distribution of failure process of dams in the southwestern Norway.

2.4.2 Rockslide Dam Longevity

Not all rockslide dams are unstable or have the potential to fail. Some rockslide dams exist for millennia leaving behind persistent geomorphic features that influences the evolution of the landscape as a whole. An example of such a landslide dam is the Phoksundo Lake, which was formed by the Ringmo rockslide more than 30.000 years ago (Weidinger, 2011). The sedimentological character of the landslide dam, the mineral composition of the host rock, the size of the catchment area, the volume of the rock slope failure event, the preexisting geomorphological domain where failure occurs, the climatic conditions, and the rate of sedimentation into the reservoir are all factors that influence the longevity of rockslide dams (Weidinger, 2011).

The grade of fragmentation of the rock mass during transportation plays an important role considering the longevity of rockslide dams since erosional processes occur much faster in fine-grained material than in coarse-grained material (Weidinger, 2011). The character of the deposit depends on transportation-type, the volume of the mass, mechanism of sliding, the distance traveled and the involved lithologies (Weidinger, 2011). During giant rock slope failures and long transportation, mechanical shattering causes the original intact rock to disintegrate; leaving behind a fine grained deposit. In addition to mechanical shattering, the mineral composition of the host material, and the climatic situation determines the rate of which weathering modifies the deposit. In other words; the mineral composition, together with the climatic regime governs the formation-rate of fines within the deposit, which influences the longevity of rockslide dams (Weidinger, 2011).

Field investigations on the interior of rockslide deposits reveal that rockslide deposits are not inversely graded, but show three distinct facie. A surface and near surface carapace facies, the main interior facies, and a basal facies (S. A. Dunning & Armitage, 2011). The carapace facies is the coarsest unit in a rock avalanche deposit, composing the material close to the surface. This facies is clast supported and preserves the original source stratigraphy (S. A. Dunning & Armitage, 2011). The main body facies lies below the carapace and makes up the majority of the rockslide deposit volume, the boundary is represented by a line where the material below is intensely fragmented and matrix supported (S. A. Dunning & Armitage, 2011). The basal facies includes material originating from the substrata as well as material from the rock avalanche, and is interpreted to be the smallest by volume within the deposit (S. A. Dunning & Armitage, 2011).

The coarse grained carapace is characterized as the major component considering rockslide dam stability due to overtopping. This is illustrated in the article "Stability and Lifespan of Landslide Dams in the Himalayas" where the authors recognized that greater the diameter of the components constituting the carapace, the longer the life span of the dam and the lake (Figure 2.14) (Weidinger, 2011). This relationship was suggested based on fieldwork conducted in the Himalayas, where the average grain, boulder and block size was visually estimated by analyzing different outcrops (Weidinger, 2011).

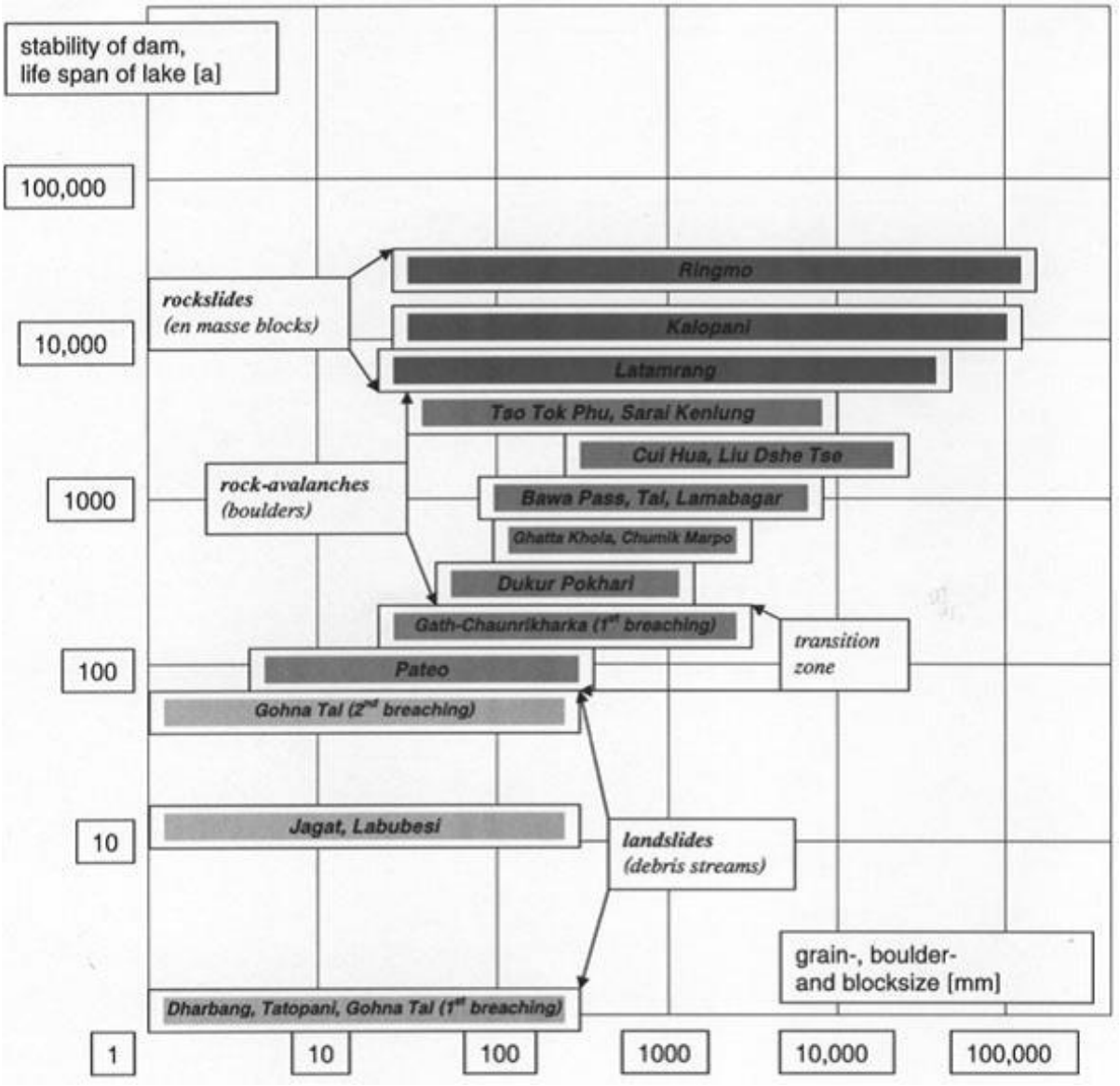

Figure 2.14: The longevity of rockslide dams as a function of the character of the carapace (Weidinger, 2011).

Costa and Schuster studied an inventory of 73 landslide dams with the intention to investigate the longevity of dams that fail. The investigation show that 27% of the dams fail within the first day, 41% within the first week, 80% within 6 months and 85% within the first year of existence (Figure 2.15)(Costa & Schuster, 1988). These percentages represent landslide dams that have failed, numerous other landslide have remained stable to this day, for example Phoksundo Lake (Weidinger, 2011). Landslide dam failure rate is between one third and one half of the landslide dam formation rate (Evans et al., 2011).

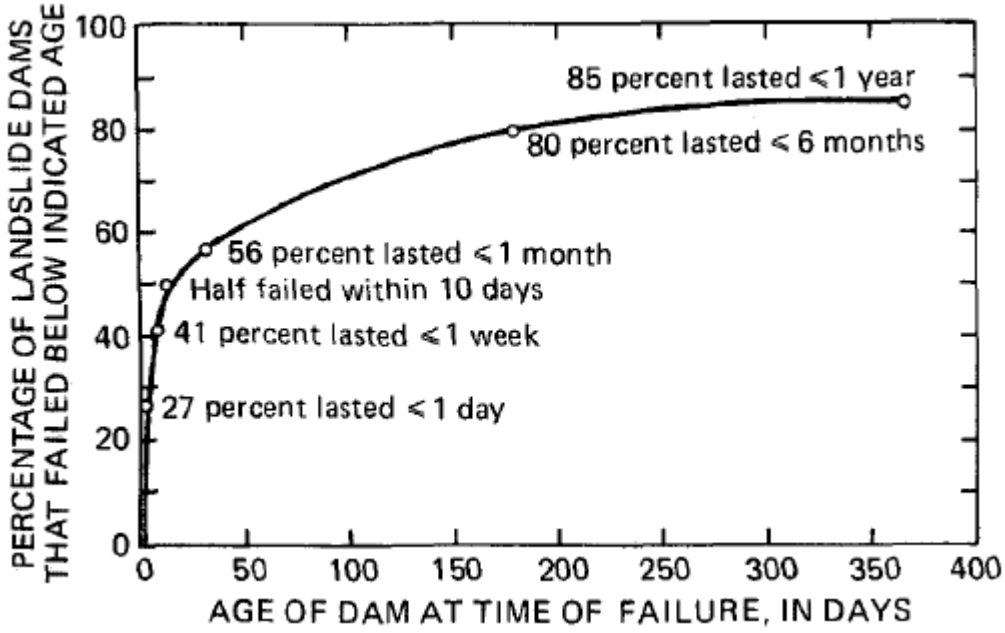

Figure 2.15: The longevity of rockslide dams that fail (Costa & Schuster, 1988).

2.4.3 Dimensionless Blockage Index

The stability of rockslide dams is related to the character of the debris composing the dam, the volume of the dam, the catchment area, the climatic situation and the geomorphic distribution of the rockslide deposit (Ermini & Casagli, 2003; Weidinger, 2011). The Dimensionless blockage index (DBI) is an empirical relation that describes the preliminary forecast of blockage evolution (equation 3.1). The dimensionless blockage index considers the volume as the main stabilizing factor, since it controls the dam self-weight, and the watershed area as the main destabilizing factor since it controls channel discharge and stream power (Canuti, Casagli, & Ermini, 1998; Casagli & Ermini, 1999). Dam height influences the stability of the dam considering both overtopping and piping (Ermini & Casagli, 2003).

$$(3.1) \quad DBI = \log\left(\frac{A_b * H_d}{V_d}\right)$$

Where H_d is the dam height (m), V_d the landslide dam volume (m^3) and A_b the catchment area (m^2). The stability domain is obtained by plotting V_d/H_d versus A_b log-log, and differentiating by the stability classes; stable dam (SD) and unstable dam (UD) (Figure 2.16). Analysis on DBI values show that the stability-instability domain varies on a global basis. This can be explained by regional variation in parameters such as the; climatic situation, the character of the debris composing the dam and the geomorphic setting of the landslide dams (Costa & Schuster, 1988). An analysis of 84 selected events worldwide, show the stability domain, the uncertain domain and the instability domain of global landslide dams (Figure 2.16) (Ermini & Casagli, 2003). The values of the domains are:

- Stability domain: DBI < 2,75
- Uncertain domain: 2,75 < DBI 3,08
- Instability domain: DBI > 3,08

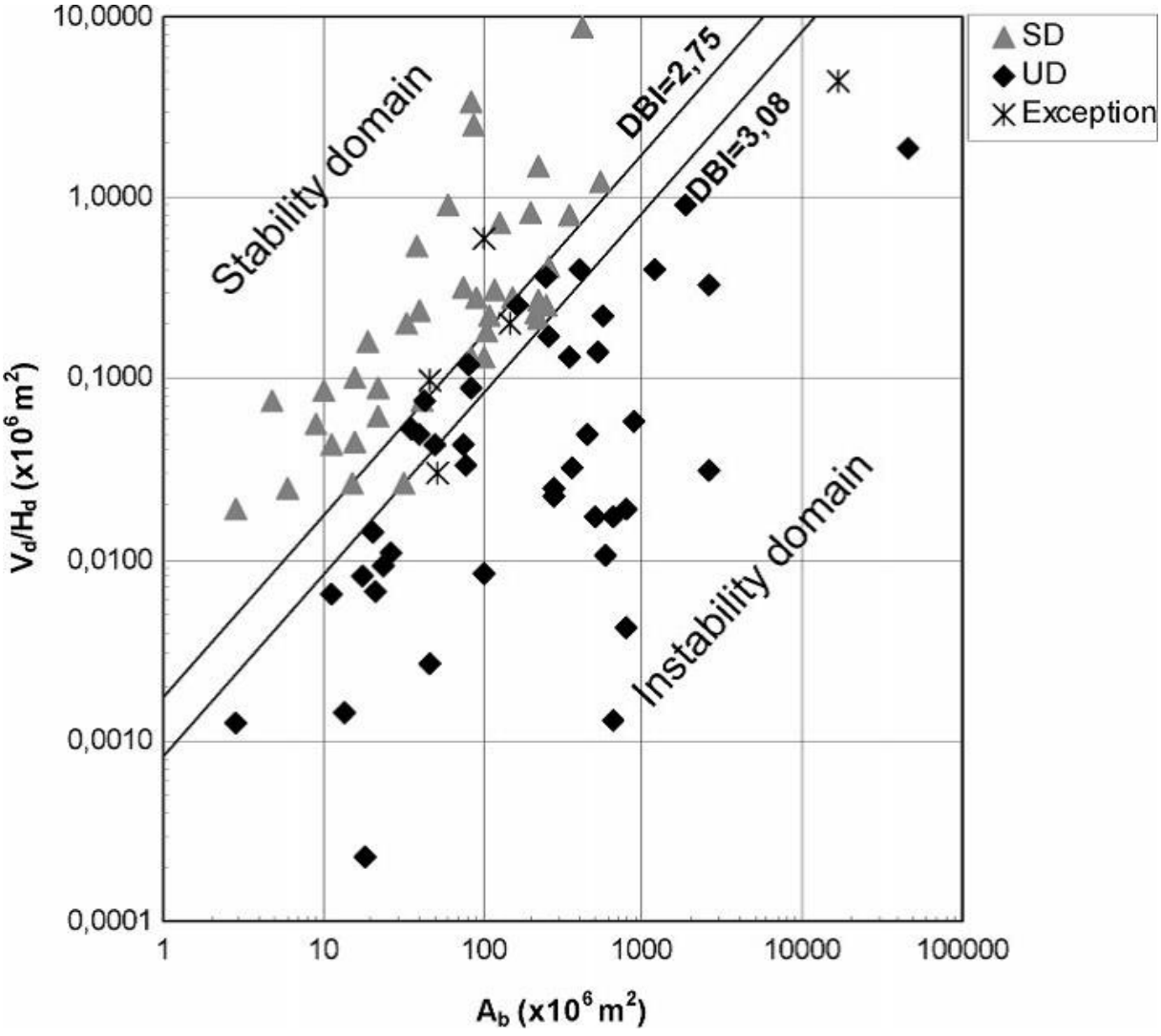

Figure 2.16: DBI plot of 84 landslide dams (Ermini & Casagli, 2003).

The main limitation of the DBI is that it only considers three parameters; the height of the landslide dam, the catchment area and the volume of the landslide dam. This is a simplification of the actual situation since factors such as the sedimentology of the landslide dam, the properties of the carapace, the climatic situation and the geomorphic setting all plays important roles considering the stability of landslide dams (Ermini & Casagli, 2003).

Work on rockslide dams in the southwestern part of Norway investigated and analyzed rockslide dams in the counties of Møre og Romsdal, Rogaland, Hordaland, and Sogn og Fjordane. Analysis on the DBI-situation resulted in Figure 2.17 (Jakobsen, 2015). These results were obtained from an analysis on rock avalanches, where the lower DBI-limit was defined by the breached dam with the lowest DBI, while the higher DBI-limit was defined by the stable dam with the highest DBI.

- Stability domain: DBI < 2,33
- Uncertain domain: 2,33 < DBI < 3,02
- Instability domain: DBI > 3,02

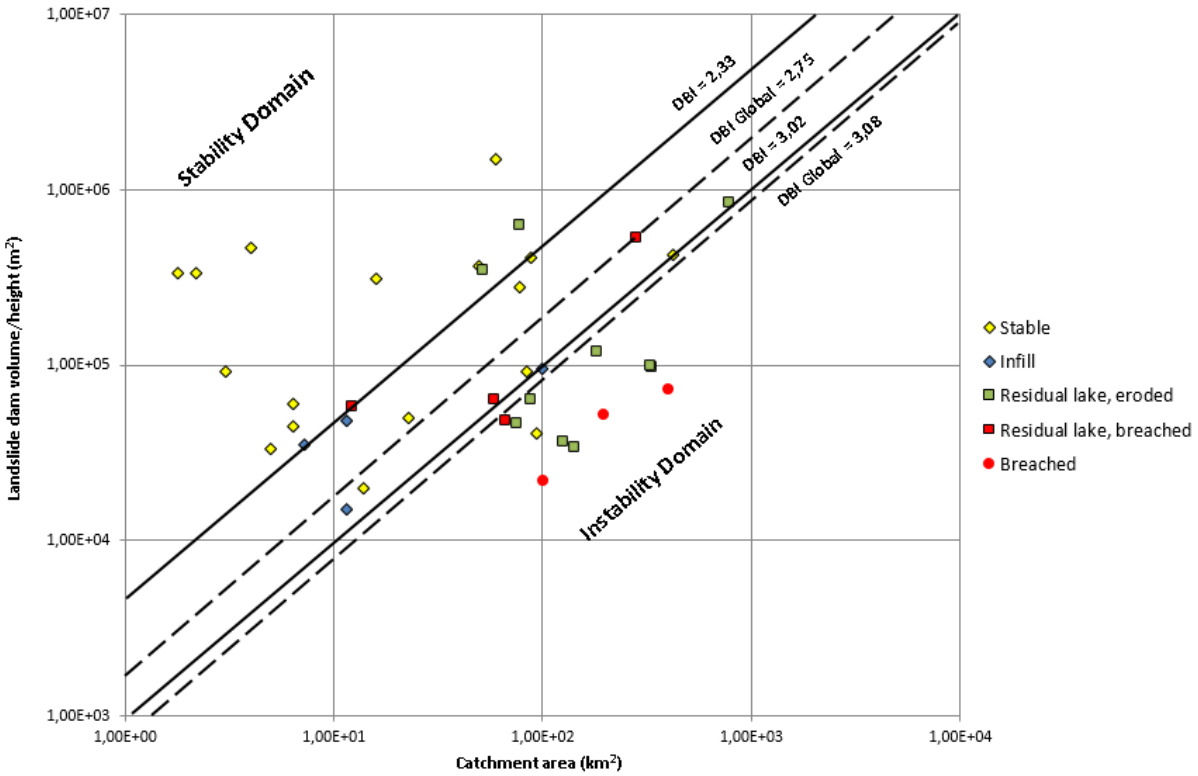

Figure 2.17: Regional study of landslide dams in the southern parts of Norway (Jakobsen, 2015).

A new plot was generated to illustrate the behavior of rockslide dams. The volume threshold was set to 10^6 m^3 to avoid negative influence from small volume rockslide dams. Each dam was characterized by its stability (Unstable, eroded, infill and stable), and plotted in a histogram where the x-axis indicates DBI-intervals of 0,5 while the y-axis indicates the number of occurring dams. The plot shows quite clearly that unstable rockslide dams are formed when the DBI-value is greater than two (Figure 2.18) (Jakobsen, 2015).

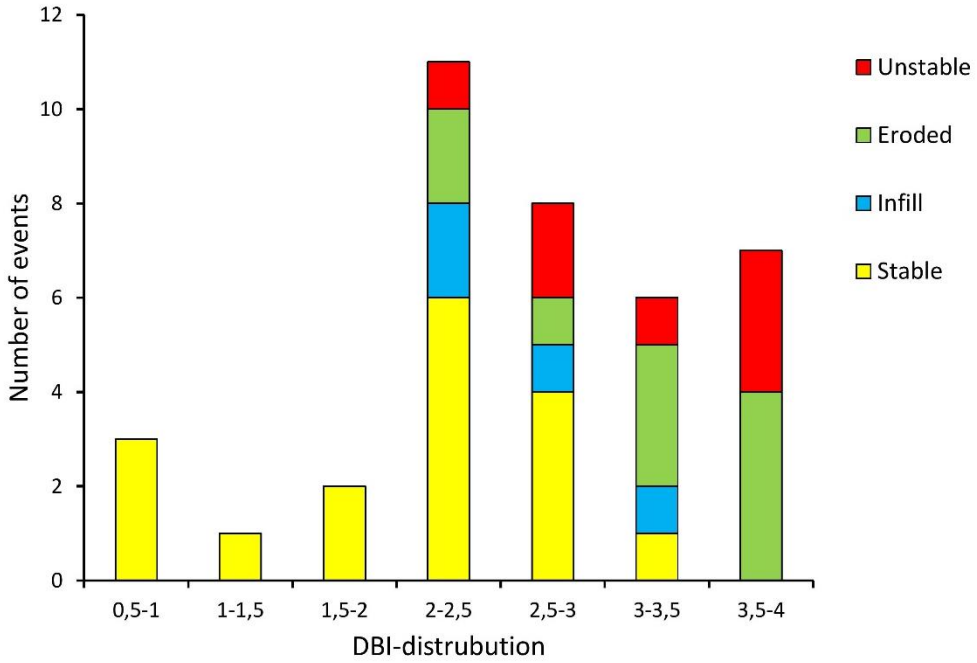

Figure 2.18: DBI-plot illustrating the relationship between DBI, and the stability of dams (Jakobsen, 2015).

3. Method

3.1. Remote Mapping and Investigation of Rockslide Dams

3.1.1 Mapping of Rockslide Dams

Systematic mapping of rockslide dams in the southwestern part of Norway was carried out in the project-thesis (Jakobsen, 2015). Geomorphic data from rockslide dams located in the southwestern parts of Norway were used in the analysis on the behavior of rockslide dams, both in creating an equation characterizing the height of future potential rockslide dams, and in the stability analysis of rockslide dams (Figure 3.4).

The southern parts of Finnmark, Troms and the northern parts of Norland were systematically mapped to locate suitable rockslide dams to test the results from the analysis (Chapter 4.2.2). The mapping was accomplished in an online ortophoto-database called "norgeibilder" (S. V. Kartverket, 2011). Waterbodies were used as an indicator for rockslide dams; it was further determined if the dam was impounded as a consequence of rock slope failure by analyzing debris in the surrounding area of the lake. Several rockslide dams have failed, knowledge about the geomorphology of rock avalanches is important to identify breached rockslide dams. The identified rockslide dams were implemented in the database created during the project thesis (Figure 3.3)(Jakobsen, 2015).

3.1.2 Geomorphic Investigation of Rockslide Dams

The geomorphic characteristics of the rockslide dams located in the northern parts of Norway were extracted in a similar way as in the project-thesis. Line features were drawn across and along the rockslide body in ARCMAP, and exported with information from a 10m digital elevation model provided by Kartverket. These line features represent the topography after rockslide dam formation, and can be used to investigate the morphometry of rockslide dams. (Figure 3.1 and Figure 3.2). To get an impression of the valley topography before rock slope failure, elevation contour-lines around the scar were interpolated to intersect with the across-valley profile. The topography before failure is represented by thick lines in the figures, while the present topography is represented by dashed lines (Figure 3.1 and Figure 3.2). In the case of the along-valley profile, the preexisting valley floor was assumed as a linear feature that can

be drawn with a starting point before the lake and an ending point after the rockslide dam (Figure 3.1 and Figure 3.2).

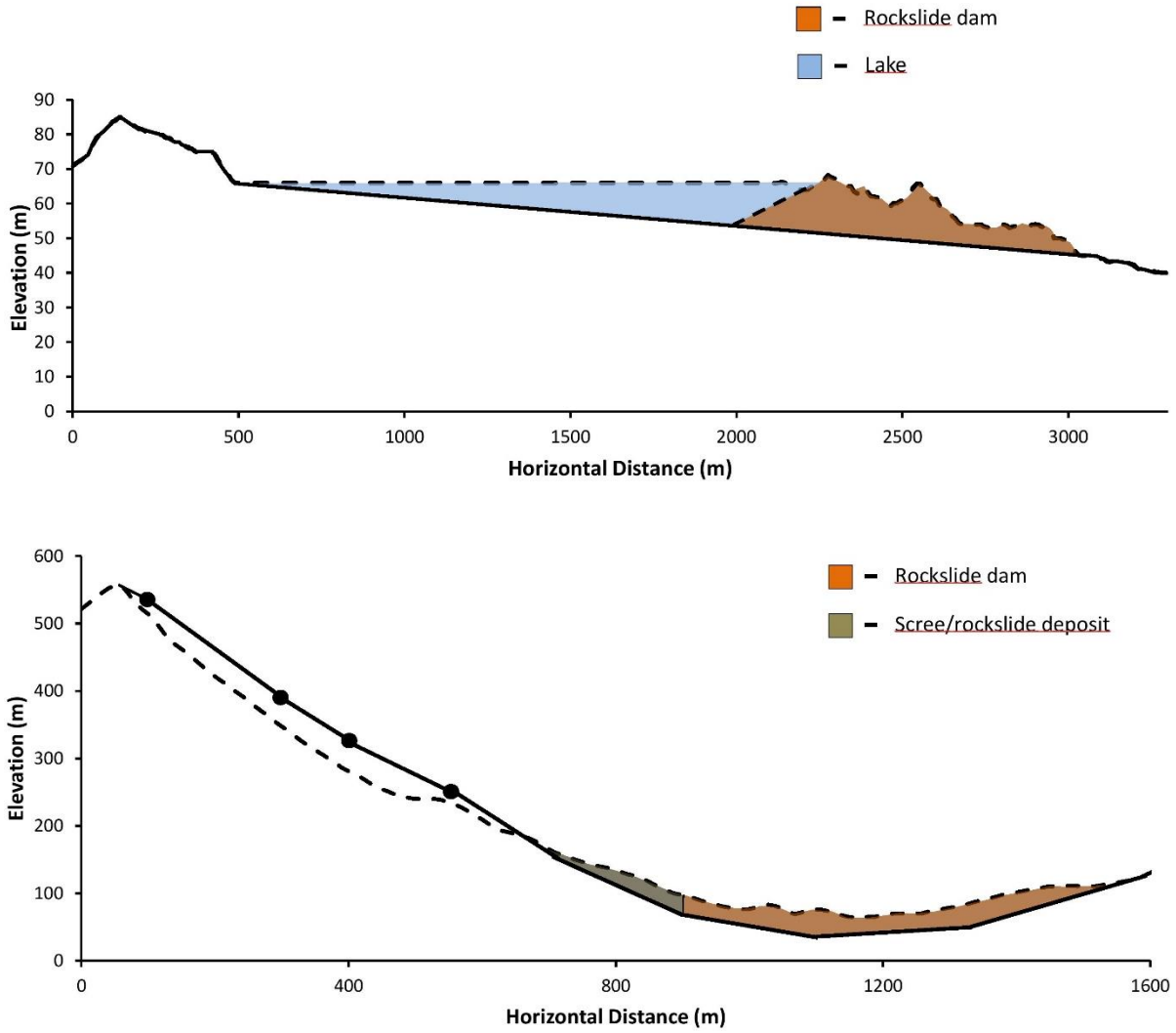

Figure 3.1: Rockslide dam nr. 145. Upper: along valley profile. Lower: cross-valley profile.

The profiles created can be used to estimate the morphometric parameters characterizing rockslide dams as mentioned in Chapter 2.3.2. ARCMAP offers tools that can be used to estimate the area of the polygon representing the periphery of a rockslide dam, while direct measurement tools can be used to assess the width of the valley. The volume of the rockslide dam was estimated by multiplying the mean height of the dam with the dam area.

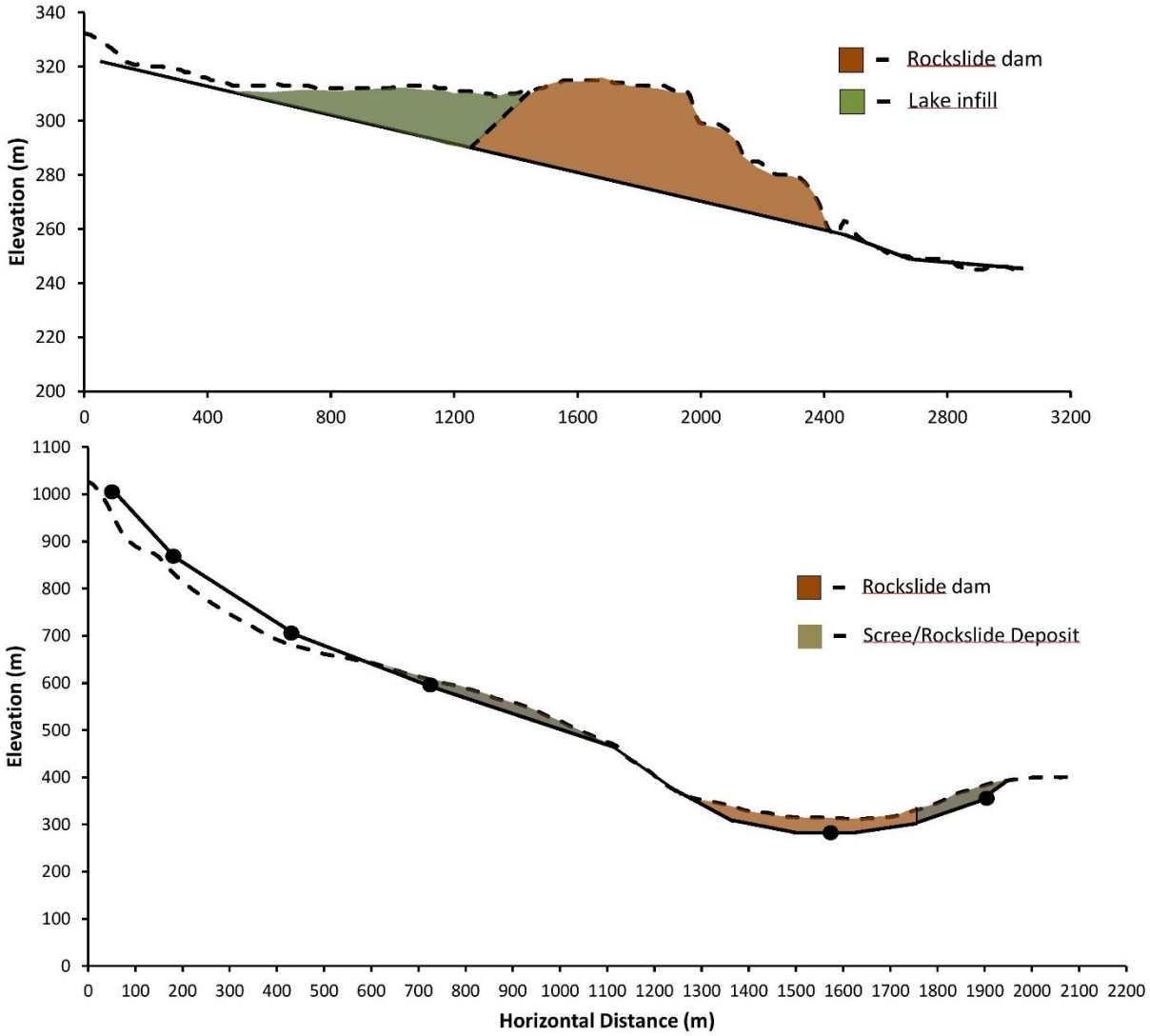

Figure 3.2: Rockslide dam nr. 155. Upper: along-valley profile. Lower: cross-valley profile.

The catchment area is used as a representative geomorphic parameter for river discharge and hence is the destabilizing factor in the DBI-equation (Ermini & Casagli, 2003). ARCMAP can be used to estimate the watershed, since it offers tools to predict flow accumulation towards a point. The tool "Flow Accumulation" returns the number of cells contributing drainage towards a point. If the point is placed in the direct vicinity of the flow-direction, the returning output represent the number of cells contributing to drainage. The number of cells can be multiplied with the resolution of the digital elevation model to calculate the size of the catchment area.

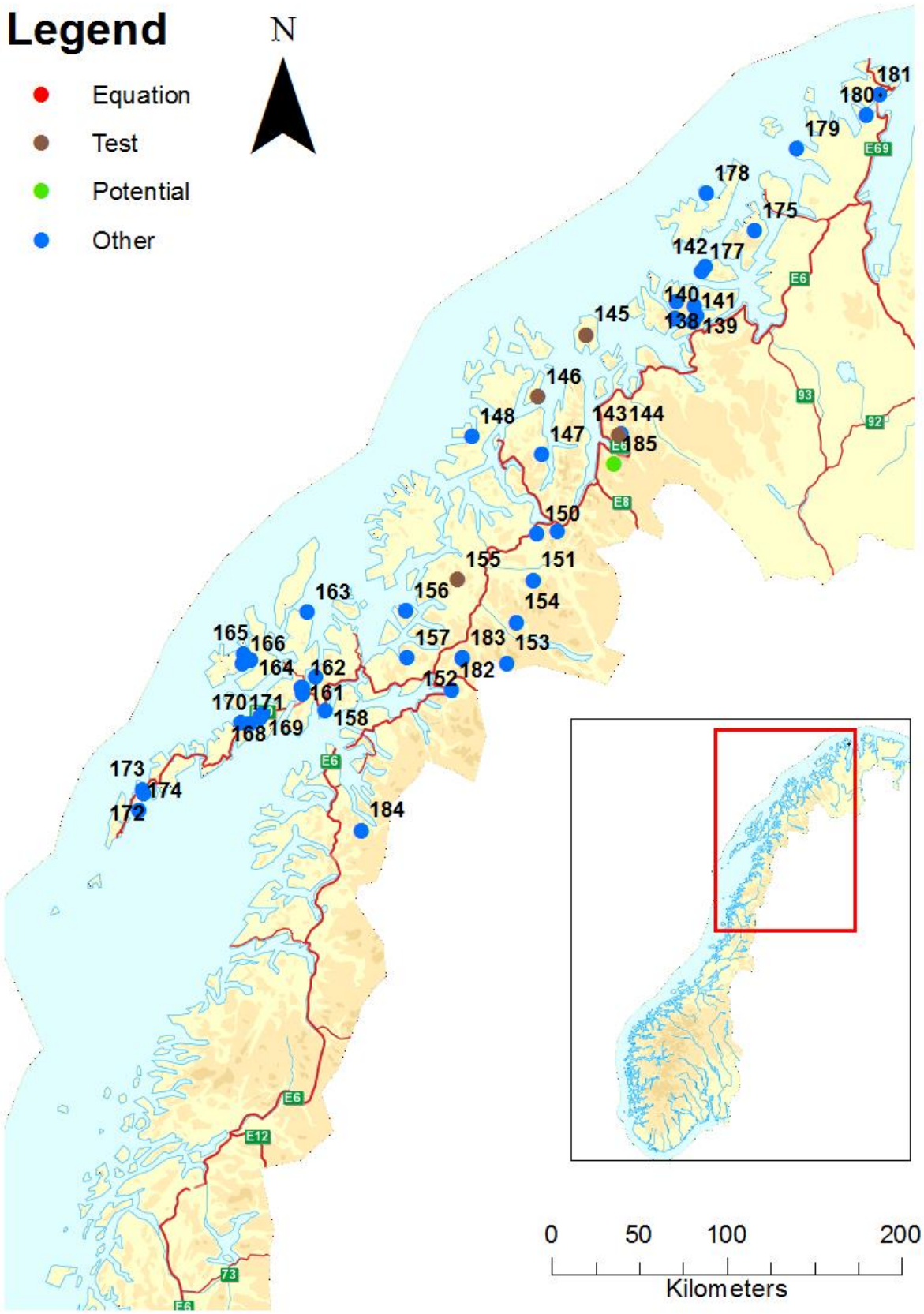

Figure 3.3: Map of the Northern parts of Norway. ***Equation*** *– illustrate the dams used in the equation.,* ***Test*** *– illustrates the dams that were tested against the equation.* ***Potential*** *– illustrates potential rockslide dams.* ***Other*** *dams were not used in the analysis.*

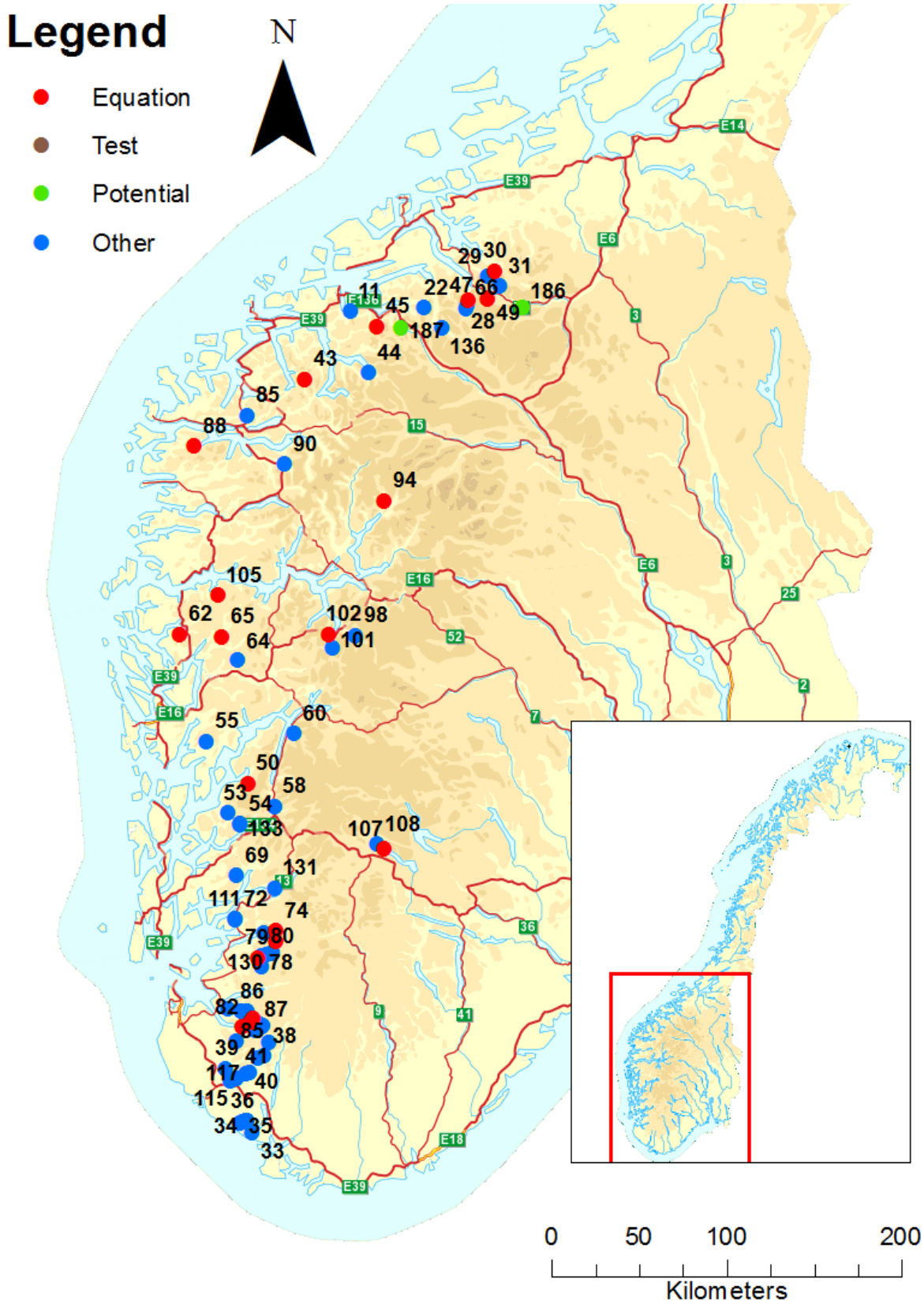

Figure 3.4: Map of the Southern parts of Norway. ***Equation*** *– illustrate the dams used in the equation.,* ***Test*** *– illustrates the dams that were tested against the equation.* ***Potential*** *– illustrates potential rockslide dams.* ***Other*** *dams were not used in the analysis.*

3.2. Field Mapping and Investigation of Rockslide Dams in Rogaland

Field work was carried out during the summer of 2015 in the southwestern parts of Rogaland. Grainsize analysis was carried out at two locations, namely; Månavatnet in Gjesdal and Gloppedalsura in Bjerkreimm.

3.2.1 Grainsize Analysis

Several methods can be applied to determine the sedimentological character of a rockslide deposit. The first technique is sampling grid by number, where a grid is placed onto the debris outcrop, and the particles beneath the grid points are sampled (Casagli, Ermini, & Rosati, 2003). Particles larger than 4mm are measured by rulers, while visual gauge are used for particles finer than 4mm (Casagli et al., 2003). Sieve analysis is a method that can be utilized if the amount of fines exceeds 12%. A bulk volume of the deposit is analyzed by standard volumetric sieve and pipette analysis (Casagli et al., 2003).

The coarse grained deposits located at Gloppedalsura and Månavatnet are of a character that makes it difficult to utilize the methods described above. The carapace is well developed, not heavily fragmented or damaged, with grainsizes varying between centimeters to tens of meters. It was decided to use an alternative method that focuses on analysis of the carapace, since investigation of the other facies is difficult, when good outcrops are absent, and because the carapace governs the stability of the dam against overtopping failure (Weidinger, 2011). The stepwise method is (Schleier, Hermanns, Rohn, & Gosse, 2015):

1. Assign domains to the rockslide dam. This allows us to analyze separate parts of the rockslide deposit, for example analysis on the stability or analysis on the rockslide source. Blocks within a specific domain should be of a uniform character, while the domains themselves should differ from each other. An example of this is illustrated in Figure 3.5.
2. The blocks within each respective domain should be bidimensional sampled based on the longest (a) and shortest axis (c) (Figure 3.6).
3. Approximate 100 blocks are to be measured within each domain. A block sampled must directly touch a previous measured block. This is to ensure consistency in the measurements, and to avoid selective data acquisition.
4. Block size data is collected from each of the domains.

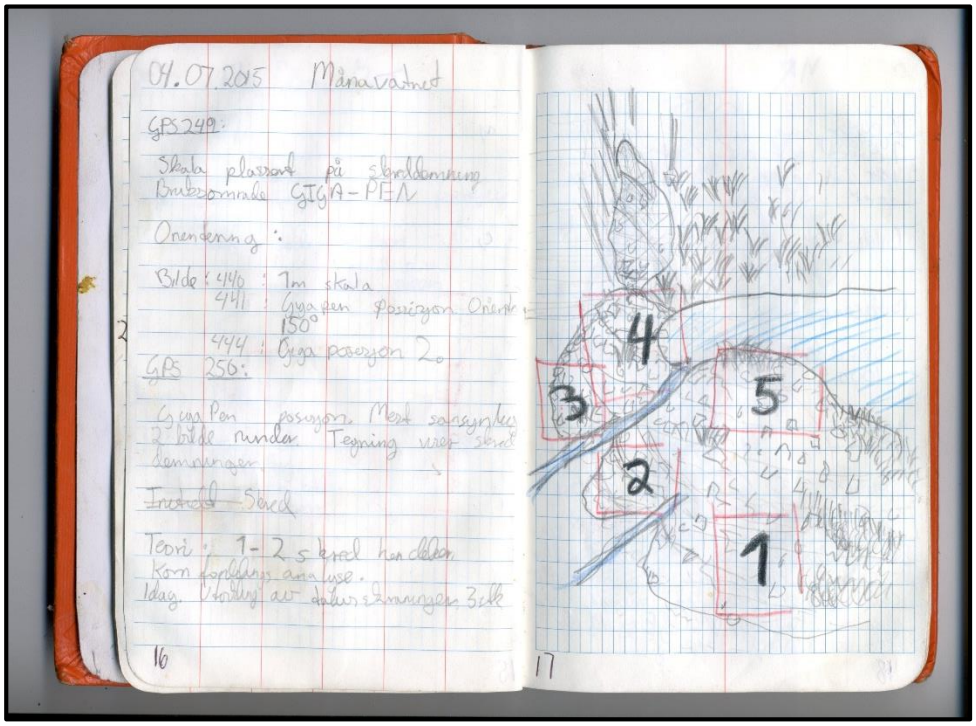

Figure 3.5: An example of how to select domain, from field book. Illustration of the rockslide deposit at Månavatnet.

Two grainsize analysis were carried out. MATLAB was used to illustrate the grainsize distribution by histogram, made up by the grainsize diameter on the x-axis, and the frequency of occurring blocks on the y-axis. This grainsize representation illustrate the most frequent occurring block size in each domain relative to the entire deposit. Each respective grainsize diagram can be compared with the longevity-block size diagram to get a crude impression of expected longevity of the respective rockslide dams (Figure 2.14) (Weidinger, 2011). EXCEL was used to generate conventional grainsize distribution curves, which represent all domain-curves within a single diagram. This distribution can also be compared to the longevity-block size diagram to get an impression of expected dam longevity (Figure 2.14).

Figure 3.6: Examples of block size data-acquisition with measuring tape. Upper: measurement of a-axis. Lower; measurement of c-axis.

3.3. Geomorphic Analysis

3.3.1 Significant Geomorphic Rockslide Dam Parameters

The features of rockslide dams can be characterized by the parameters listed in chapter 2.3.2. Some parameters are directly linked to the preexisting geomorphology and can be considered as independent. Other parameters are related to the morphometry of the subsequent rockslide dam; these are usually dependent on each other. This can be tested in a two-dimensional analysis, where dependency between parameters can be tested by plotting parameters against each other. The independent parameters describing the preexisting geomorphology are before two-dimensional testing believed to be,

- Valley width
- The rockslide volume
- The gradient of the valley
- The height of the release area above the valley floor
- Character of the rockmass

The dependent morphometric parameters characterizing the subsequent rockslide dam are before two-dimensional testing believed to be;

- Dam length
- Dam width
- Dam-area
- Dam height.

The difference between the independent- and codependent parameters is that independent parameters effect rockslide distribution, whereas codependent parameters characterize the morphometry of the rockslide dam.

3.3.2 Database Used to Investigate the Behavior of Rockslide Dams

Several datasets were attempted fitted to the geomorphic model. The different datasets are based on the original geodatabase containing 69 rockslide dams (Jakobsen, 2015). Rockslide dams with volume less than 10^6 m^3 were excluded from further analysis, because these rockslide dams usually only produce partial blockage of the drainage network. This leaves a database of 33 elements. Further refinement of the dataset; rockslides that have experienced an increase in mobility because of transportation across glaciers, or that have resulted in partial blockage have been excluded from further analysis. These dams do not represent the general trend of rockslide dams. This results in a dataset of 19 data entries. The following datasets have been used in the analysis.

- The original dataset where volumes [0, 10^6] m^3 have been excluded from further analysis. This dataset contains 33 data entries (Appendix. B-1).
- A refined dataset where asymmetric dams, and rockslides that have been influenced by glaciers have been excluded. This dataset contains 19 data entries (Appendix. B-2)
- The third dataset is similar to the second dataset. The difference is that all data-entries with volumes larger than 2 * 10^7 m^3 have been excluded. This is because most prone rockslide areas in Norway contain unstable volumes less than 2 * 10^7 m^3 (Oppikofer & Hermanns, 2015). This dataset consist of 18 data entries with the volume between [10^6, 2*10^7] m^3.
- The fourth dataset is similar to the third dataset. The difference is that rockslide dam volumes larger than 10 * 10^6 m^3 have been excluded from the analysis. This dataset contains 13 data entries with the volumes between [10^6, 10*10^6] m^3.

3.3.3 Equations Describing the Behavior of Rockslide Dams

The behavior of rockslide dams can be represented by plotting rockslide dam parameters. The datasets were plotted in MATLAB since the software offer opportunities for efficient processing and customization of the different plots. Two-dimensional plots illustrate the relationship between independent parameters and dependent-/codependent parameters (Equation 3.1). Examples of these plots are: “rockslide dam volume” against “rockslide dam height”, “valley width” against dam length” or “height of the release area” against the “rockslide dam area”. Two-dimensional data representation was used to test which parameters

control the behavior of rockslide dams, and can be used further in the three-dimensional analysis.

$$(3.1) \quad dependent\ parameter = f(independent\ varible)$$

MATLAB was used for the three-dimensional data representation, since it offers the desired plot-options, extensive customization of the plots and enables efficient processing of large data-sets. Three-dimensional plots allow representation of three rockslide dam parameters, and can be used to illustrate the relationship between a dependent-/codependent parameter, and two independent parameters (Equation 3.2). Examples of these plots are; "rockslide dam height" against "rockslide dam volume" and "valley width", or "rockslide dam area" versus "rockslide dam volume" and the "height of release area".

$$(3.2) \quad dependent\ variable = f(independent\ varible,\ \ independent\ variable)$$

The scatter plots can be fitted to a custom equation or a standard equation in MATLAB. MATLAB is able to determine the constants of a custom equation, making MATLAB adequate for this project. The desired behavior of the equation is that the dependent variables reacts in a logical way to changes in the independent variables. For example, "dam height" must increase if "dam volume" increases while "valley width" remain constant.

3.3.4 Power-Law Equations Describing the Behavior of Rockslide Dams

The general form of the equation is a power-law equation, where one independent parameter is multiplied with the exponential form of an independent parameter. Five different custom equations have been developed. From this point on, the parameter, "z" denotes rockslide dam height, the parameter "x", denotes rockslide dam volume and the parameter "y" denotes valley width. A, b, c, d and e are constants in the equations.

Equation 3.3 illustrates the crude form of the desired behavior of the rockslide dam. If the constant "b" in the exponential term is negative, the resulting "dam height" experience reduction with increasing "valley width", when the "rockslide dam volume" is constant.

$$(3.3) \quad z = x * exp^{by}$$

Equation 3.4 illustrates a modified form of equation 3.3. By multiplying the volume with constant "a", the fitted surface represents "rockslide dam height" as a fraction of the "rockslide dam volume".

$$(3.4.) \quad z = ax * exp^{by}$$

By adding a constant term, the constant "c" to the equation 3.4 forces the fitted curve to intersect with the "dam height"-axis, resulting in equation 3.5.

$$(3.5) \quad z = ax * exp^{by} + c$$

The constant "c" can be multiplied with the parameter "valley width" to create a longer equation (3.6), taking into account several polynomials, making the equation more flexible. The idea is that if the constants "b" and "c" are negative, the "valley width" will influence the "dam height" by reducing "dam height" with increasing "dam width".

$$(3.6) \quad z = ax * exp^{by} + cy$$

Equation 3.7 was produced by adding constant "d" to equation 3.6. This produces a longer chain of polynomials that is more flexible fitted to the different datasets.

$$(3.7) \quad z = ax * exp^{by} + cy + d$$

The equations listed above are to be fitted with the datasets listed in chapter 3.3.2, and compared with each other according to root-mean-square error (RMSE is a statistical operator described in Appendix. A-6).

3.4. Analysis in MATLAB

3.4.1 MATLAB-Script Created for the Geomorphic Analysis

The intent of the MATLAB script is to illustrate geomorphic relationships of rockslide dams in three-dimensions, and to find a satisfactory fit to the plotted data. Users of the script can plot geomorphic information in three dimensions, illustrate geomorphic relationship by emphasizing plot option and compute constants of the best fitted surface described in chapter 3.3.4. The data used in the MATLAB script is imported from an excel table. The general form of the function is;

```
function[Plot,f1,goodness]=threeauto(x,y,z,volumemin,volumemax
,plotoption, fitoption, sheet)
```

The scripts and notes on the script are found in Appendix. A-1 and Appendix. A-2. A data point was added at (2000 (x),2000 (y), 0(z)) to force the fitted surface through a rational point. This point represents a small rock fall volume, in a large valley that does not form a dam.

3.4.2 MATLAB Script Created to Predict the Stability of Potential Rockslide dams

The stability of potential rockslide dams can be assessed by using the DBI-equation described in chapter 2.4.3. The equations estimating rockslide dam height, described in chapter 3.3.4 can be used as input to the DBI-equation. This allows the user to predict the stability of future rockslide dams.

$$DBI = \log\left(\frac{A_b * z}{V_d}\right) \quad (3.8)$$

The script plots database 1 in the DBI-Diagram (Ermini & Casagli, 2003). Where the catchment area is plotted against the relationship between rockslide dam height and rockslide dam volume on a 2-dimensional double logarithmic diagram, for each element in the dataset. Rockslide dam status is highlighted to get an impression on how rockslide dams behave depending on the DBI-values. DBI-lines from the global analysis and the regional analysis are drawn in the diagram (Ermini & Casagli, 2003; Jakobsen, 2015). A DBI-value is illustrated by the intersection of a line with the gradient of 1 with the axis that represent the relationship between dam height and dam volume. Orthogonal vectors on the DBI-lines towards the upper left corner illustrate decreasing DBI-values, and the stable domain of the plot, while orthogonal vectors towards the lower right corner illustrates the increasing DBI-values and the instable domain of the plot. The script plots the global estimates of the stability-instability domains and regional stability domains of southwestern Norway described in chapter 2.4.3 (Ermini & Casagli, 2003; Jakobsen, 2015). Users of the script can plot geomorphic data to get an impression on the future stability situation relative to the other landslide dams from the southern parts of Norway.

The script and notes on the script are found in Appendix. A-3.

3.4.3 MATLAB Script Created for the Grainsize Analysis

The MATLAB script created for the grainsize analysis was influenced by the block size-longevity diagram proposed by Widinger (2011) (Figure 2.14). The goal of the grainsize analysis was to generate a grainsize distribution that can easily be compared to Figure 2.18, while at the same time gives an impression on the distribution of the rockslide. This was achieved by generating histograms for each domain (chapter 3.2.1), and compering each domain to the entire deposit. The histogram contains grainsize on the x-axis, and frequency of occurring blocks on the y-axis. Each histogram was split into 10 bins. A conventional grainsize distribution was also created to illustrate the distribution of blocks in the carapace.

```
function [h] = graintest()
```

The MATLAB script and notes on the script are found in Appendix. A-4.

4. Results

4.1. Two-Dimensional Geomorphic Analysis

4.1.1 Testing Independent Geomorphic Variable versus Dam Height

The independent variables; dam volume, valley width and height of the release area (described in chapter 3.3.1) were fitted against rockslide dam height to see which parameters affect rockslide dam height. A linear equation with 95% prediction bounds (representing the 95% uncertainty limit of the equation) was added to the plot to illustrate the different relationships (Figure 4.1, Figure 4.2, Figure 4.3). Dataset-1 was used in the two-dimensional analysis (Chapter 3.3.2).

Dam volume influence dam height, larger volumes result in higher dams. Dam volume does not give an optimal indicator of dam height (alone), because of high variation between recorded dam heights (Figure 4.1).

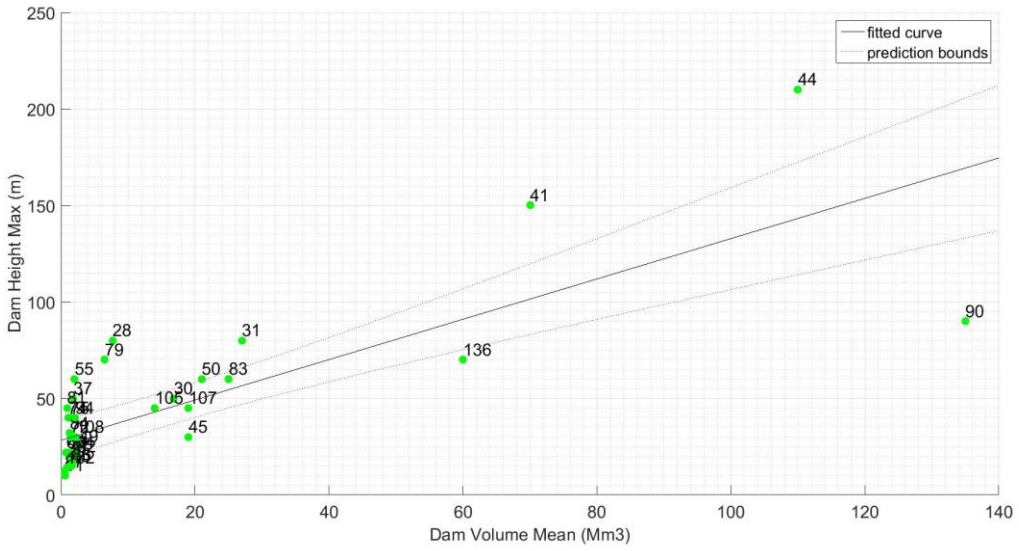

Figure 4.1: Two-dimensional scatter plot; dam height vs dam volume.

Dam height responds to changes in the valley width (Figure 4.2). Most dams are concentrated around the linear curve, but with high variation amongst the data points. The variation increases with increasing valley width.

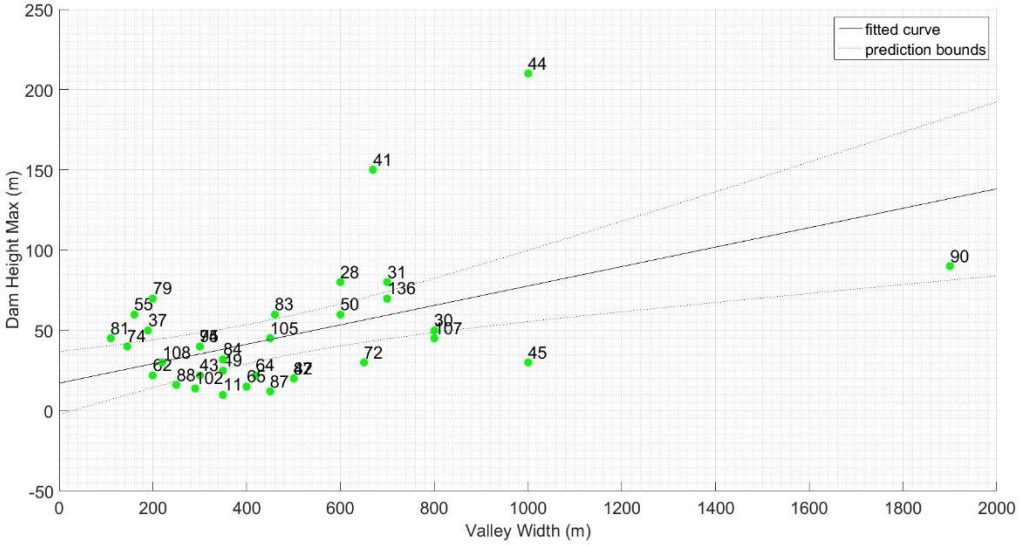

Figure 4.2: Two-dimensional scatter plot; dam height vs valley width.

The last independent geomorphic parameter, height of the release area shows extreme variation between the data-points (Figure 4.3). There seems to be no apparent control by height of release area on dam height.

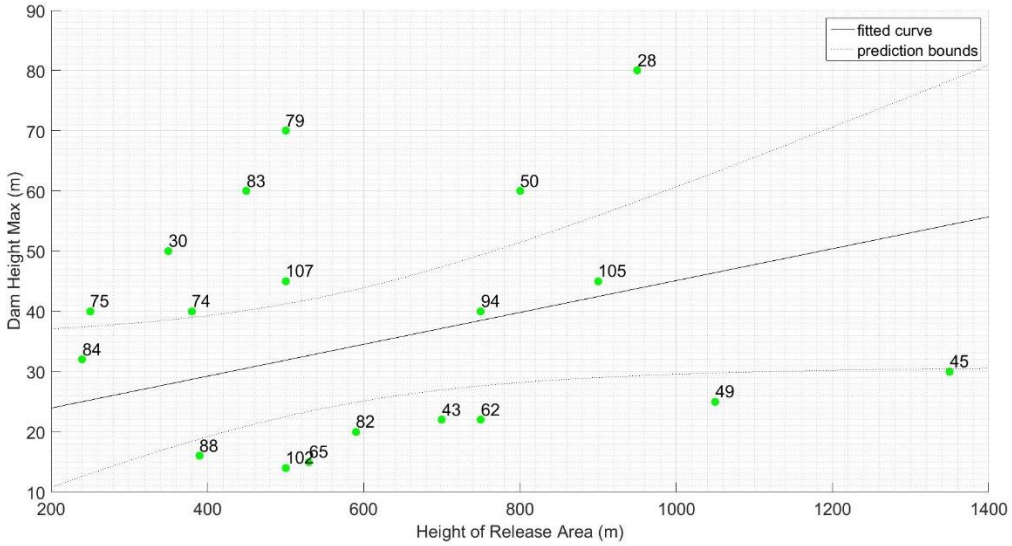

Figure 4.3: Two-dimensional scatter plot; dam height vs dam height of release area.

The two-dimensional analysis shows that "valley width", and "dam volume" are the two most important parameters controlling the resulting dam height (Figure 4.1, Figure 4.2, Figure 4.3). The three-dimensional analysis is therefore to incorporate "dam height" as a function of "valley width" and "dam volume".

4.2. Three-Dimensional Geomorphic Analysis

4.2.1 MATLAB Analysis of Equations

The equations proposed in chapter 3.3.4 were fitted to the different datasets presented in chapter 3.3.2. The MATLAB script (Appendix. A-2) was used to define which equation with its respective constant to use. The output from the scrip is a three-dimensional surface characterizing the specified equation, the best fitted constants composing the equation and the uncertainty (Root mean squared error (RMSE) Appendix. A-6) of fit. It is necessary to evaluate the respective uncertainty of each individual fit by different datasets to determine the most adequate equation to be used as a predictive tool. The variable "x" represent "rockslide dam volume" and the variable "y" represent "valley width".

Equation 4.1 is composed of a single power-term. The height of the dam increases when variable "x" increases and decreases when variable "y" increases. This relationship represents the conceptual behavior of landslide dams in valleys (Figure 4.4). As seen, the uncertainty varies between 26,7 meters and 19 meters for the different datasets (Table 4.2.1). Table 4.2.2 shows the 95% confidence bounds of the calculated constants.

$$z = ax * exp^{by} \quad (4.1)$$

Table 4.2.1:The estimated constants for equation 4.1, and the uncertainty of the fit.

	Dataset 1	**Dataset 2**	**Dataset 3**
a	4.633e-06	1.122e-05	1.8e-05
b	-0.001022	-0.002215	-0.002432
RMSE	26.7808	22.8718	19.4298

Table 4.2.2: 95% confidence bound of the fitted constants.

	Dataset 1	**Dataset 2**	**Dataset 3**
a	2.563e-06, 6.704e-06	1.525e-07, 2.229e-05	6.554e-06, 2.945e-05
b	-0.001503, -0.0005402	-0.004087, -0.0003431	-0.003621, -0.001243

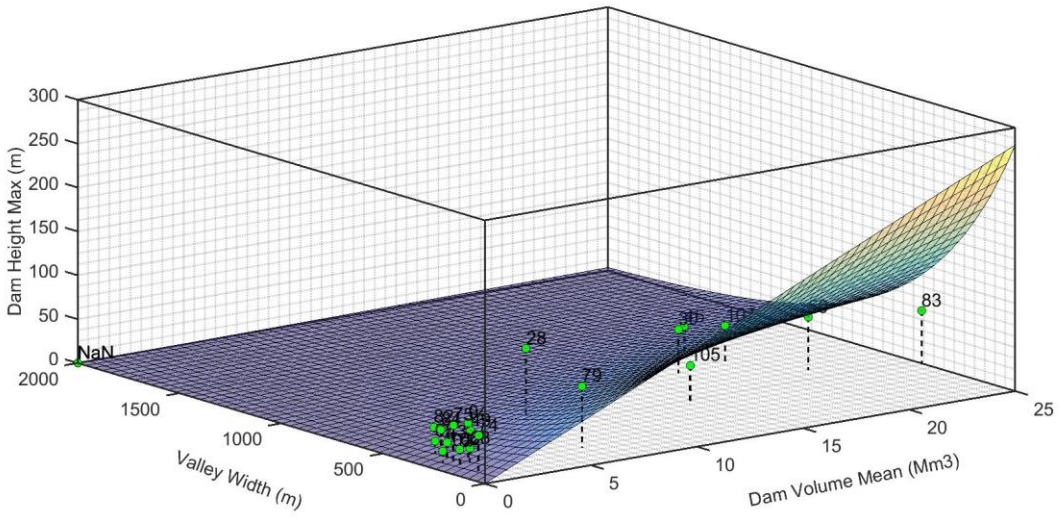

Figure 4.4: Dataset-2 fitted to equation 4.1.

The uncertainty of the fit in equation 4.1 originates from the fact that most data-points are plotted above the fitted surface in the x-interval [0, 0,5*10^7]. A constant was added to equation 4.1, to elevate the fitted surface, making the surface intersect with the scatter of data-points in the x-interval: [0, 0,5*10^7] resulting in equation 4.2. Table 4.2.3 shows the estimated constants in equation 4.2 for the different data-sets, and the uncertainty of the fit. As seen, the uncertainty varies between 20,3 meters and 16,1 meters for the different data-sets. Table 4.2.4 shows the 95% confidence bounds of the estimated constants. Figure 4.5 shows the fitted surface of equation 4.2 to data-set 1.

$$(4.2) \quad z = ax * exp^{by} + c$$

Table 4.2.3: The estimated constants for the different data-sets to equation 4.2, and the uncertainty of the fit.

	Dataset 1	**Dataset 2**	**Dataset 3**
a	3.264e-06	7.267e-06	1.229e-05
b	-0.0008797	-0.002353	-0.002504
c	20.47	19.93	15.46
RMSE	20.2946	16.9847	16.0682

Table 4.2.4: The calculated confidence bounds for each constant.

	Dataset 1	Dataset 2	Dataset 3
a	1.843e-06, 4.684e-06	-1.82e-06, 1.635e-05	1.734e-06, 2.284e-05
b	-0.001302, -0.0004569	-0.004692, -1.469e-05	-0.004016, -0.0009919
c	12.58, 28.36	9.892, 29.96	4.775, 26.14

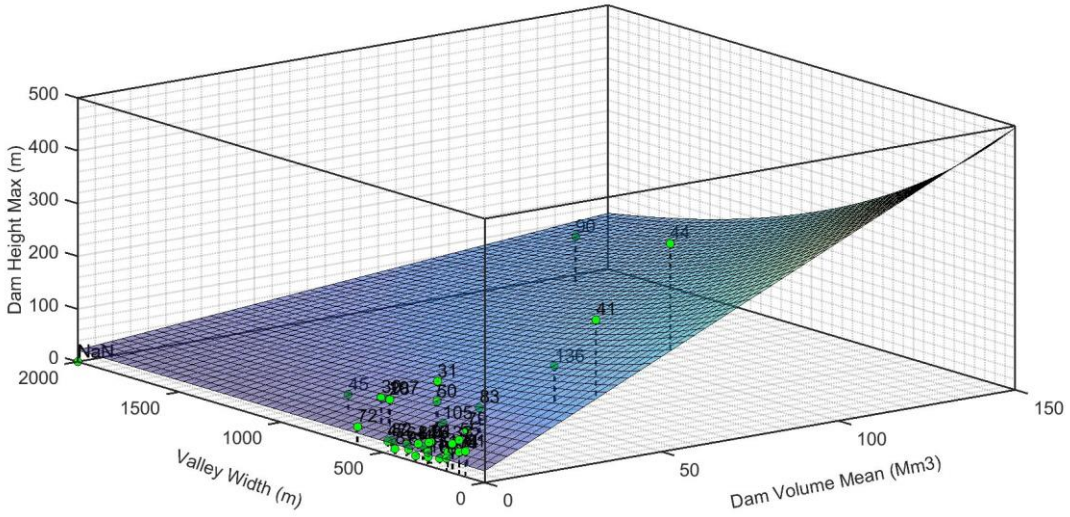

Figure 4.5: Dataset-1 fitted to equation 4.2

By adding a constant to equation 4.1, the uncertainty has been reduced for all the data-sets. The most evident inaccurate behavior of the fitted surface is that the "dam height" remains constant when the "dam volume" is insignificant and the "valley width" varies. This was attempted solved by multiplying the constant "c" with "valley width", producing equation 4.3. Table 4.2.5 shows the estimated constants in equation 4.3 for the different data-sets, and the uncertainty of the fit. As seen, the uncertainty varies between 26,5 meters and 19,6 meters for the different data-sets. Table 4.2.6 shows the 95% confidence bounds of the estimated constants. Figure 4.6 shows the fitted surface of equation 4.3 to dataset 3.

$$(4.3) \quad z = ax * exp^{by} + cy$$

Table 4.2.5: The estimated constants for the different data-sets to equation 4.3, and the uncertainty of the fit.

	Dataset 1	Dataset 2	Dataset 3
a	4.656e-06	1.363e-05	1.825e-05
b	-0.001095	-0.002774	-0.002559
c	0.007289	0.007588	0.004255
RMSE	26.4667	22.6279	19.6487

Table 4.2.6: The calculated 95% confidence bounds for each constant.

	Dataset 1	**Dataset 2**	**Dataset 3**
a	2.424e-06, 6.888e-06	7.158e-07, 2.798e-05	6.036e-06, 3.047e-05
b	-0.001635, -0.0005561	-0.004941, -0.0006069	-0.003887, -0.001232
c	-0.003536, 0.01811	-0.005248, 0.02042	-0.007285, 0.0158

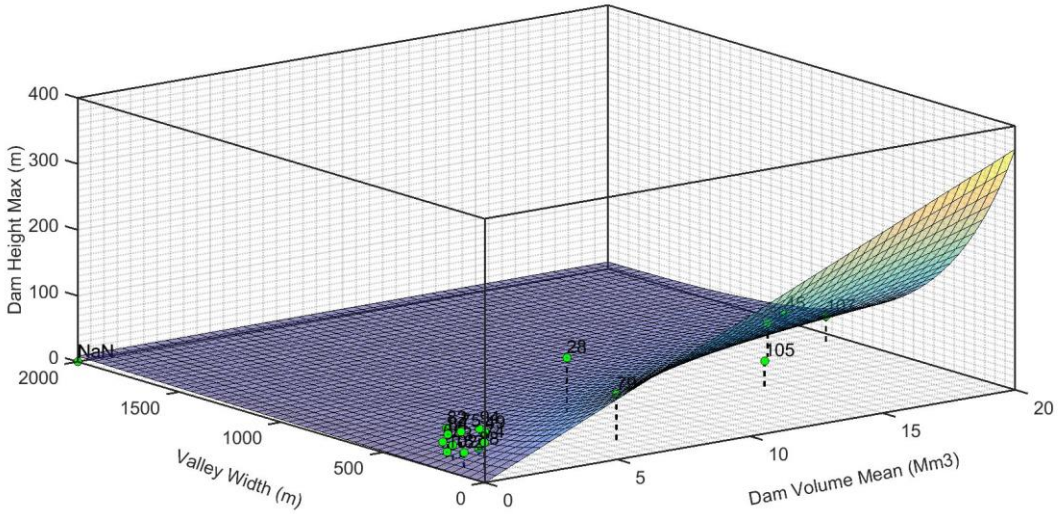

Figure 4.6: Surface produced by fitting dataset-3 to equation 4.3.

The uncertainty has increased when multiplying the constant term "c" to "valley width" in equation 4.2. This makes equation 4.3 less appropriate as a predictive tool for estimating rockslide dam height than equation 4.2. The behaviorally suitability of the surface characteristics in Figure 4.6 has as well been reduced. This is because the surface exhibits non rational behavior when the "dam volume" is close to zero, where "rockslide dam height" increases when "valley width" increases. The same argument about uncertainty is valid for equation 4.3 as used for equation 4.1, since the scatter of data-points in the x-interval [0, $0{,}5*10^7$] is located above the fitted surface. A fourth constant, constant "d" can be added to equation 4.3 as an attempt to produce a more suitable equation characterizing the formation of rockslide dams. Table 4.2.7 shows the estimated constants in equation 4.4 for the different data-sets, and the uncertainty of the fit. As seen, the uncertainty varies between 17,8 meters and 9,9 meters for the different data-sets. Table 4.2.8 shows the 95% confidence bounds of the estimated constants. Figure 4.7 and Figure 4.8 show the fitted surface of equation 4.4 to dataset 2 and 4.

$$(4.4) \quad z = ax * exp^{by} + cy + d$$

Table 4.2.7: The constants and the uncertainty of the fit calculated for each separate dataset to equation 4.4.

	Dataset 1	Dataset 2	Dataset 3	Dataset 4
a	2.783e-06	3.62e-06	8.091e-06	8.478e-06
b	-0.0006747	-0.001245	-0.001965	-2.71e-05
c	-0.01752	-0.01501	-0.0125	-0.008644
d	32.37	31.12	25.79	16.46
RMSE	17.8193	15.0774	14.7071	9.9573

Table 4.2.8: The calculated 95% confidence bounds for each constant.

	Dataset 1	Dataset 2	Dataset 3	Dataset 3
a	1.751e-06,	-1.301e-06,	-8.356e-07,	2.426e-06,
	3.814e-06	8.54e-06	1.702e-05	1.453e-05
b	-0.001017,	-0.003428,	-0.003603,	-0.001352,
	-0.0003327	0.000938	-0.0003277	0.001298
c	-0.02812,	-0.02752,	-0.02524,	-0.01784,
	-0.006913	-0.0025	0.000227	0.0005483
d	22.4,	18.3,	11.42,	5.124,
	42.35	43.94	40.16	27.8

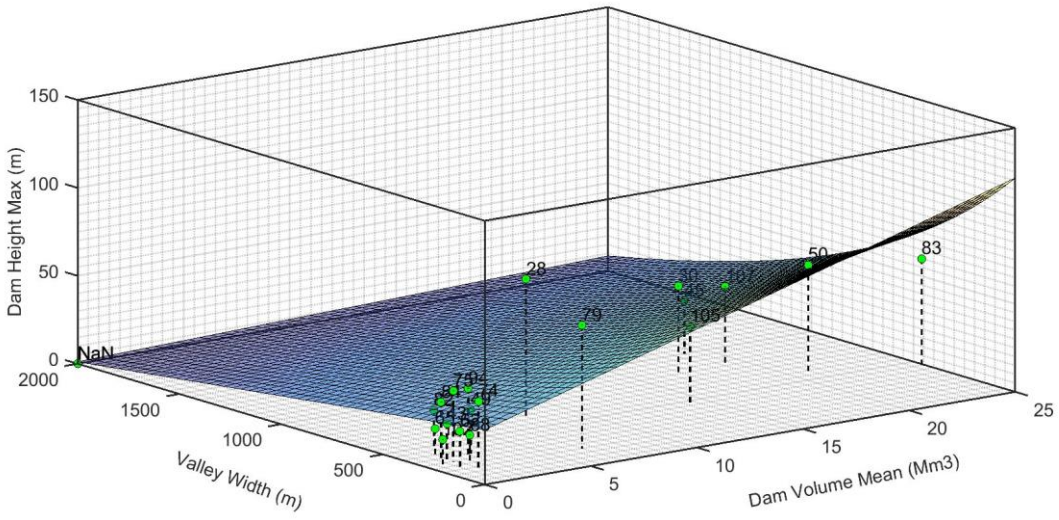

Figure 4.7: Surface produced by fitting dataset-2 to equation 4.4.

Figure 4.7 is based on data-set 2 and behaves as expected. The feature of Figure 4.7 that can be argued as irrational is the fact that a zero volume rockslide dam produce a non-zero dam height. This feature can be overlooked on the basis that only rockslide dams of volumes larger than 10^6 m^3 have been implemented in the data-sets, making the equation inadequate for predicting the formation of close to zero volume rockslides.

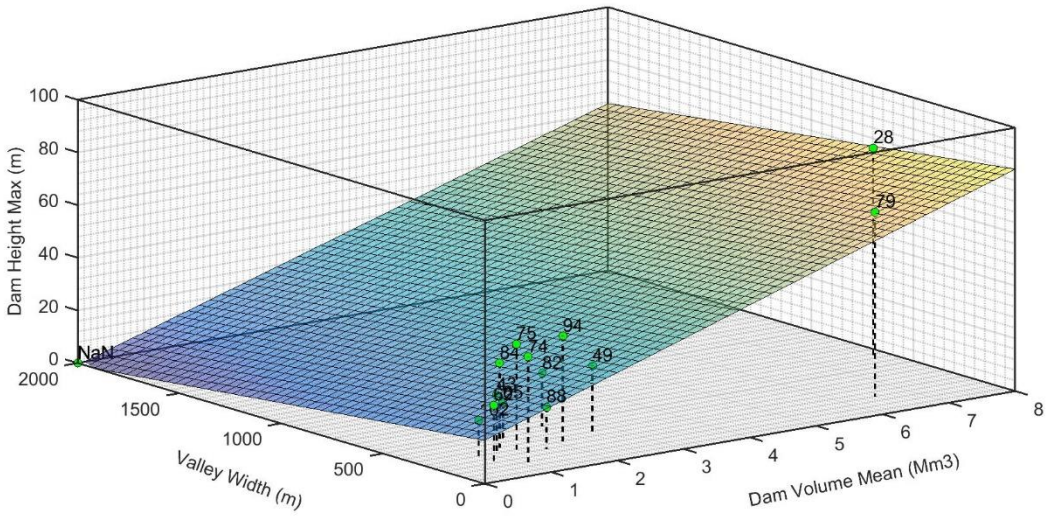

Figure 4.8: Surface produced by fitting dataset-4 to equation 4.4.

Figure 4.8 illustrates the surface fitted to equation 4.4 for dataset 4. The surface exhibits planar features compared to the other fitted surfaces. This is primarily because the dataset used contains fewer data points than the other datasets. Another negative aspect of the fitted surface is that the dam height is less affected by changes in the valley width.

4.2.2 Testing Equations against Inventory from the Northern Parts of Norway

The northern parts of Norway were systematically mapped for rockslide dams. These dams represent test samples for the equations presented in chapter 4.2.1 against. Equation 4.5 was deemed as the most promising, since it behaves as expected, where the width of the valley affects the resulting dam height. To evaluate the suitability of the equation and the datasets used to determine the constants of the equation, the measured height of the dams were compared to the calculated dam height, and Root mean squared error (RMSE) was calculated based on dam height difference.

$$z = ax * exp^{by} + cy + d \quad (4.5)$$

To decide which dataset is most ideal to determine the constants in equation 4.5, the estimated constants originating from the four different datasets were used in the equation, and evaluated against the test dams. Four test dams exhibit properties similar as the datasets used, and were therefor deemed satisfactory for testing. The locations of the test dams are illustrated in the map in Appendix. C-4.

Table 4.2.9: Height difference calculated by using dataset-1.

Test dam	Morphometric height (m)	Calculated Height (m)	Height difference (m)
143	60	52	-8
145	40	47	7
146	50	41	-9
155	40	50	10
RMSE			8,6

The results from dataset 1 (Table 4.2.9) illustrate that the measured morphometric dam height and the dam height calculated with equation 4.5 using constants from dataset 1 are similar. Results show that the difference varies between -8 meters (the calculated height is less than the morphometric height) and 10 meters. The difference in percent between the measured morphometric height and the calculated height is between 13% and 25%. The expected uncertainty of equation 4.5 with the constants from dataset 1 is 8,6 meters.

Table 4.2.10: Height difference calculated by using dataset-2.

Test dam	Morphometric height (m)	Calculated Height (m)	Height difference (m)
143	60	50	-10
145	40	45	5
146	50	40	-10
155	40	50	10
RMSE			9

The results from dataset 2 (Table 4.2.10) illustrate that the measured morphometric dam heights and the dam heights calculated by equation 4.5 using constants from dataset 2 are similar. Results show that the difference varies between 5 meters and 10 meters. The difference in percent between the measured morphometric height and the calculated height is between 12,5% and 25%. The expected uncertainty of equation 4.5 based on the constants calculated with dataset 2 is 9 meters.

Table 4.2.11: Height difference calculated by using dataset-3.

Test dam	Morphometric height (m)	Calculated Height (m)	Height difference (m)
143	60	58	-2
145	40	50	10
146	50	44	-6
155	40	61	21
RMSE			12,1

The results from dataset 3 (Table 4.2.11) illustrate that the measured morphometric dam heights, and the heights calculated with equation 4.5 using dataset 3 are similar when the valley is wide, but different when the valley width is narrow. Results show that the difference varies between 2 meters and 21 meters. The difference in percent varies between 3% and 53%. The expected uncertainty of equation 4.5 based on the constants calculated with dataset 3 is 12,1 meters.

Table 4.2.12: Height difference calculated by using dataset-4.

Test dam	Morphometric height (m)	Calculated Height (m)	Height difference (m)
143	60	151	91
145	40	135	95
146	50	94	44
155	40	113	73
RMSE			78,3

The results from dataset 4 (Table 4.2.12) illustrate that the measured morphometric dam height, and the height calculated with equation 4.5 using dataset 4 are different. Results show that the difference varies between 95 meters and 44 meters. The difference in percent varies between 47% and 70%. The expected uncertainty of equation 4.5 based on the constants calculated with dataset 4 is 78,3 meters.

4.2.3 Using Plot-Option to Emphasize Rockslide Dam Characteristics

Plot-option can be used to distinguish between rockslide dam properties (Appendix. A-2). This allows information to be presented in 4 dimensions. Three different plot options can be customized:

- DW/DL (Dam width/Dam length - Appendix. A-2): The relationship between dam width and dam length illustrate the morphometric relationship of the rockslide dam (Figure 4.9). The shape of the dam equals a quadrat if the DW/DL = 1, elsewise a rectangle.
- DL/VW (Dam length/Valley width - Appendix. A-2): The relationship between dam length and valley width (Figure 4.10). The rockslide deposit covers the entire valley floor (across valley) if DL/DW =1, or partly covers the valley floor if DL/VW is less than 1.
- 2D-Classification: Illustrate the geomorphic shape of the rockslide dam based on the classification introduced in chapter 2.2. (Figure 4.11).

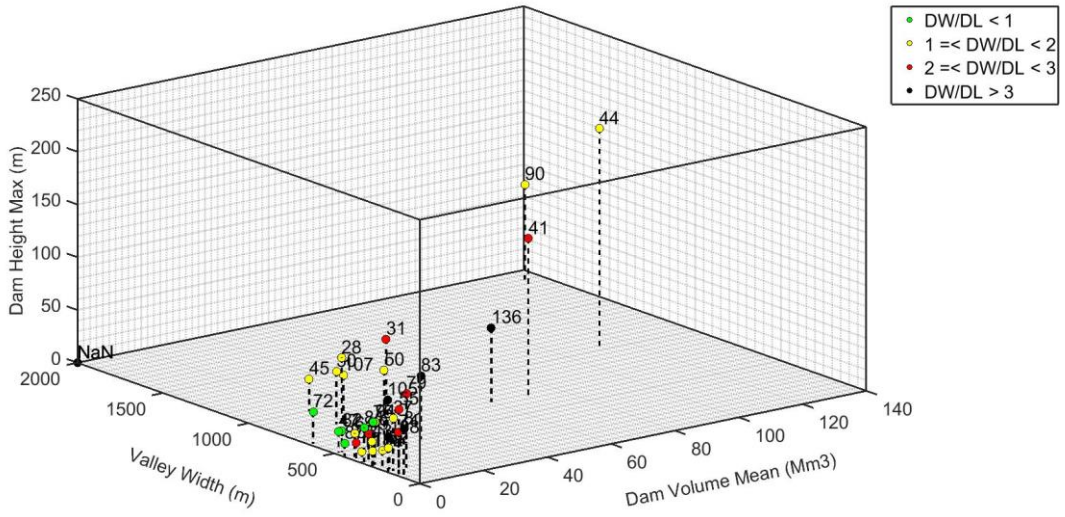

Figure 4.9: Figure illustrating the geomorphic distribution of dataset 1. The morphometric data plotted are; dam volume (m^3), valley width (m) and dam height (m).

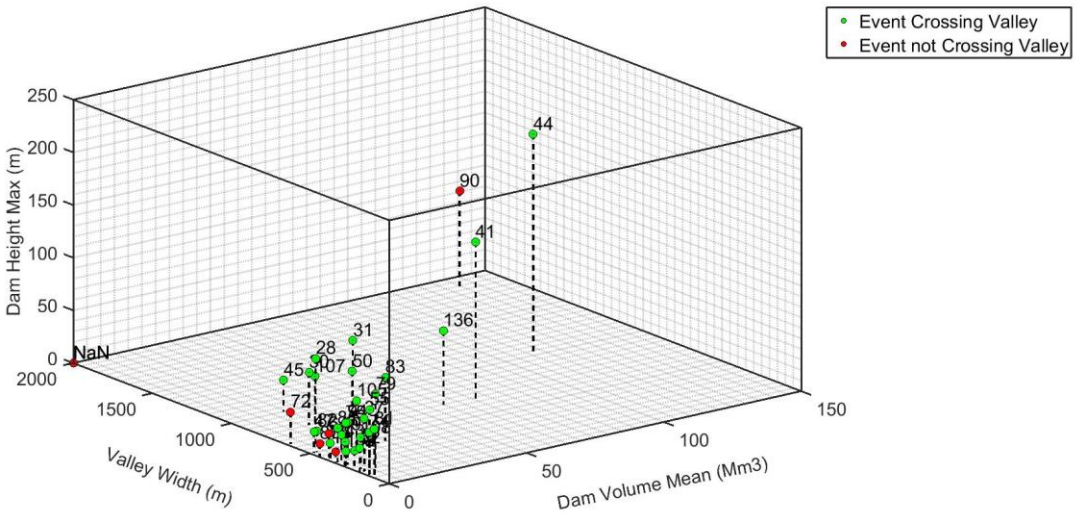

Figure 4.10. Figure illustrating the relationship between rockslide dam length and valley width.

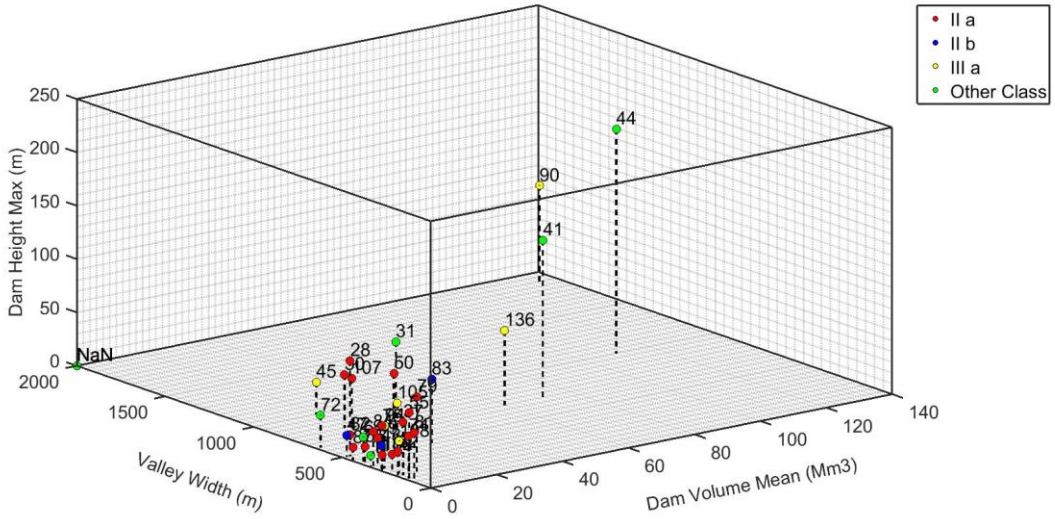

Figure 4.11: Figure illustrating the two-dimensional classification.

Most rockslide dams that are formed by singular rock slope failure are concentrated in the plot; Dam volume: [0, 10] Mm^3, Valley width: [0, 500] m (Figure 4.11). Larger rockslides are either classified as IIIa or Other class (complex rockslide dam formation).

4.3. Stability Analysis of Rockslide Dams

4.3.1 MATLAB Script Estimating the Stability of Rockslide Dams

The equations tested in chapter 4.2.2 can be used to assess the future stability of the rockslide dams by introducing the equations to the DBI-equation presented in chapter 3.4.2.

The script and notes on the script are found in Appendix. A-3.

4.3.2 DBI Plot Predicting the Behavior of Future Rockslide Events

Systematic mapping of the northern parts of Norway (Chapter 3.1.1) resulted in the identification of 4 ideal test-dams. The test-dams exhibit volumes that lies in the ranges of dataset-2, and have been formed by singular rockslide events. Some dams have been filled in, and some have partly been eroded but none have experienced breach. Geomorphic analysis of the test-dams established the input to the DBI-analysis (Table 4.3.1).

Table 4.3.1: Geomorphic input data to the geomorphic analysis.

Dam	Volume (m^3)	Width (m)	C-Area (m^2)	Type
145	15000000	670	4550000	1
146	10000000	580	17767000	1
143	16800000	620	29000000	1
155	12000000	440	21000000	1

The MATLAB script (Appendix. A-3) described in chapter 3.4.2 was used to illustrate the behaviur of the test-dams (Figure 4.12). As seen, all test-dams are plotted in the stable domain, in the upper left part of the plot.

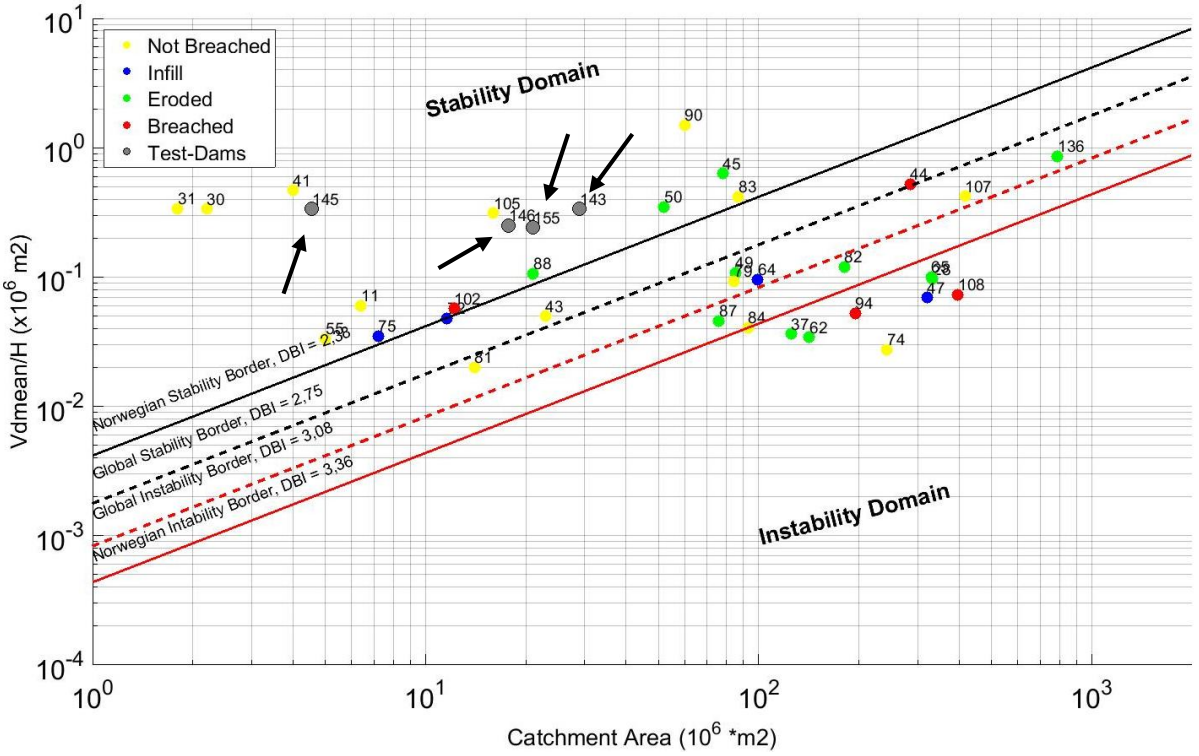

Figure 4.12: The resulting DBI-plot based on data from Appendix. B-1, and test-data from Table 4.3.1. The arrows indicate the test-dams.

The script returns the calculated dam height, and the estimated DBI for each element in the test-set (Table 4.3.2). This allows the user to inspect specific rockslide dams. The parameters in Table 4.3.2 were estimated by using the constant from dataset-2 in equation 4.5 (Table 4.2.7).

Table 4.3.2: The data output from the DBI-analysis.

Dam	Dam height (m)	DBI
145	44,64272	1,131671
146	39,99767	1,851649
143	49,91895	1,935354
155	49,6335	1,938813

4.4. Grainsize Analysis of Rockslide Dams in Rogaland

4.4.1 Gloppedalsura (nr. 41)

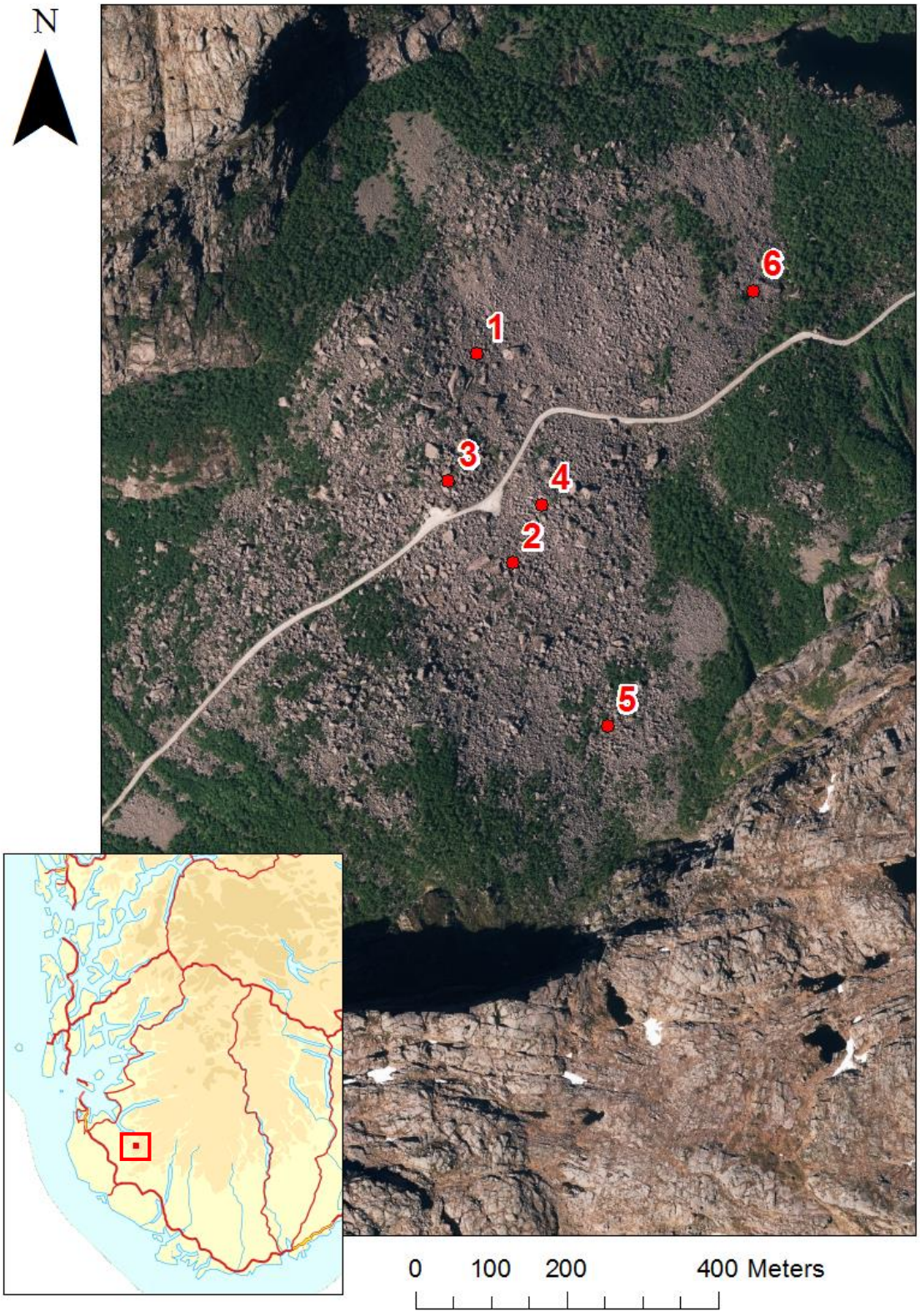

Figure 4.13: Illustration map of Gloppedalsura. The numbers represent the different grainsize domains (Chapter 3.2.1)

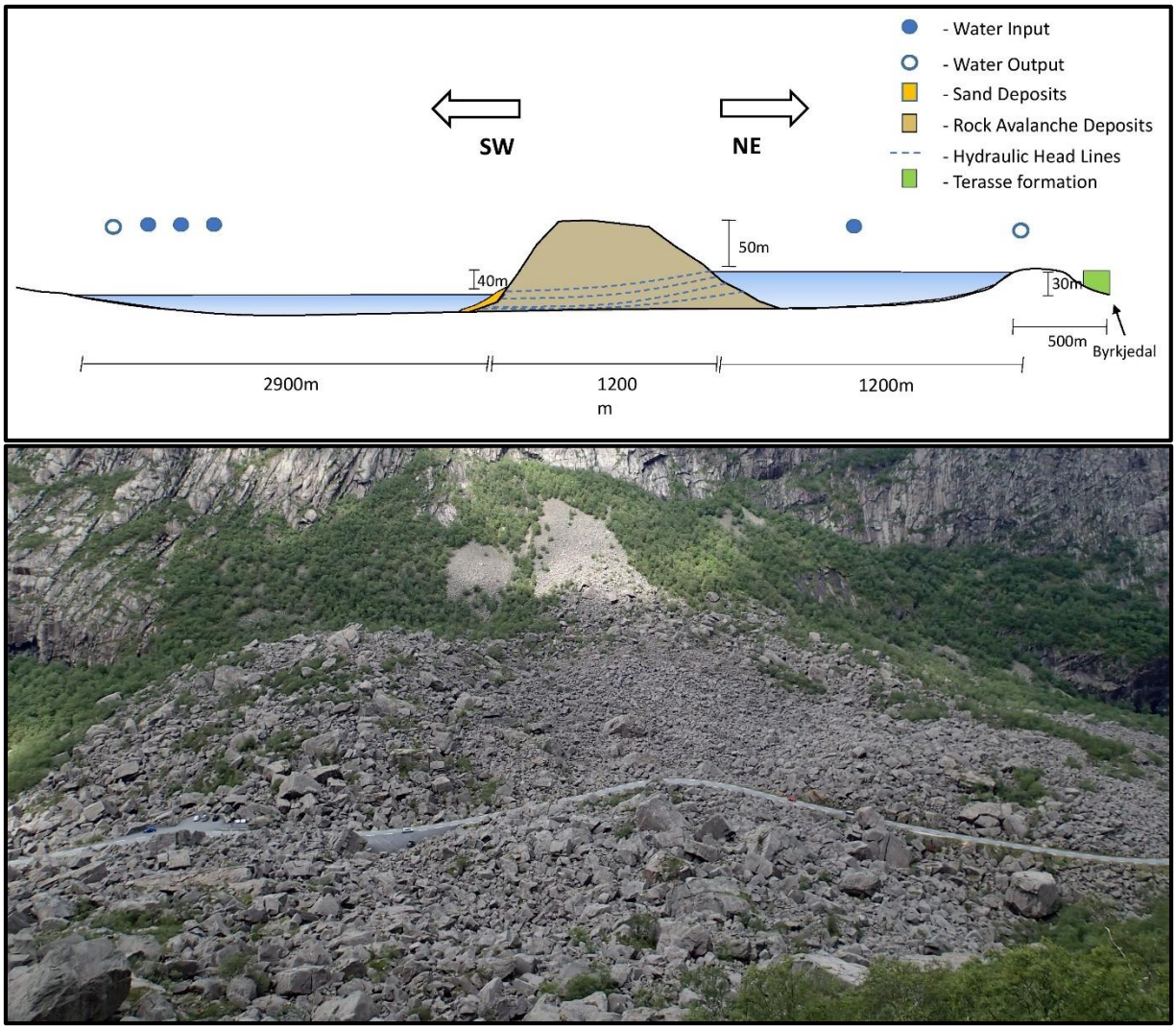

Figure 4.14: Upper: Conceptual sketch of Gloppedalsura. Lower: Overview of Gloppedalsura (taken towards north).

Gloppedalsura is located in the county of Rogaland, at the limit of Gjesheim and Bjerkheim. commune The deposit stands out of the landscape (Figure 4.13 and Figure 4.14), and is situated between the lakes; Gloppedalsvatnet (to the northeast) and Indra Vinjavatnet. The valley sides are composed of the lithologies (NGU, 2016);

Diorite to granitic gneiss	Northern valley side
Monzonite to quartz-monzonite	Southern valley side

While Gloppedalsura stands out as a massive rockslide formation, no surface drainage establish communication between the lakes. This implies that the deposit; Gloppedalsura forms a drainage divide. Gloppedalsvatnet would not have been a lake if a Gloppedalsura did not exist (Figure 4.14). This is also reflected by the small catchment area at Gloppedalsura, which is constituted by the direct vicinity of the rockslide deposit (Table 4.4.1). Beach-deposits are situated on the border between Gloppedalsura to Indra Vinjavatnet. This observation may

indicate communication between Gloppedalsvatnet to Indra Vinjavatnet through Gloppedalsura, as well as intense wind activity through Gloppedalen, resulting in wave-activity, and sorting of the material composing the deposit (Figure 4.14 and Figure 4.15).

Geomorphic analysis of Gloppedalsura resulted in Table 4.4.1

Table 4.4.1: Geomorphic parameters from Gloppedalsura (nr.41)

Type slide	Rock Avalanche
Glacial influence	No glacial influence
Stability status	Not breached
Two dimensional classification	V
Across valley classification	i
Along-valley classification	2
Valley width	670
Height of release area	550
Dam length	670
Dam width	1500
Dam area (m^2)	700000
Dam height max	150
Dam height mean	100
Dam volume	70000000
Catchment area	4000000

Figure 4.15: Upper: Beach deposits on the shore between Indra Vinjavatnet to Gloppedalsura. Lower: Gravel-boulder deposits on the shore between Indra Vinjavatnet and northern parts of Gloppedalsura.

4.4.2 Grainsize Analysis at Gloppedalsura

The grainsize analysis can be compared with the map illustrating the different domains (Figure 4.13). Each domain is compared to the grainsize analysis of the total deposit. Two grainsize analysis have been performed, one in MATLAB (histogram) and one in EXCEL (conventional grainsize analysis) (Figure 4.16 Figure 4.17).

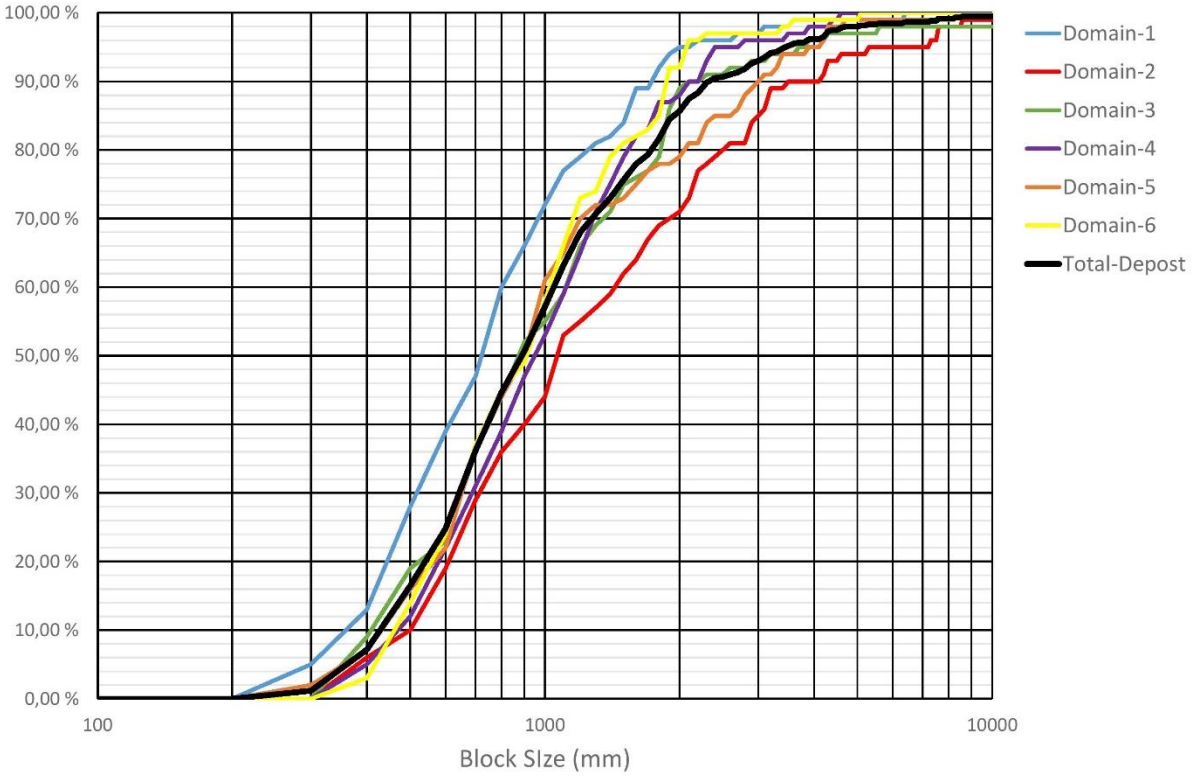

Figure 4.16: Conventional grainsize distribution of Gloppedalsura.

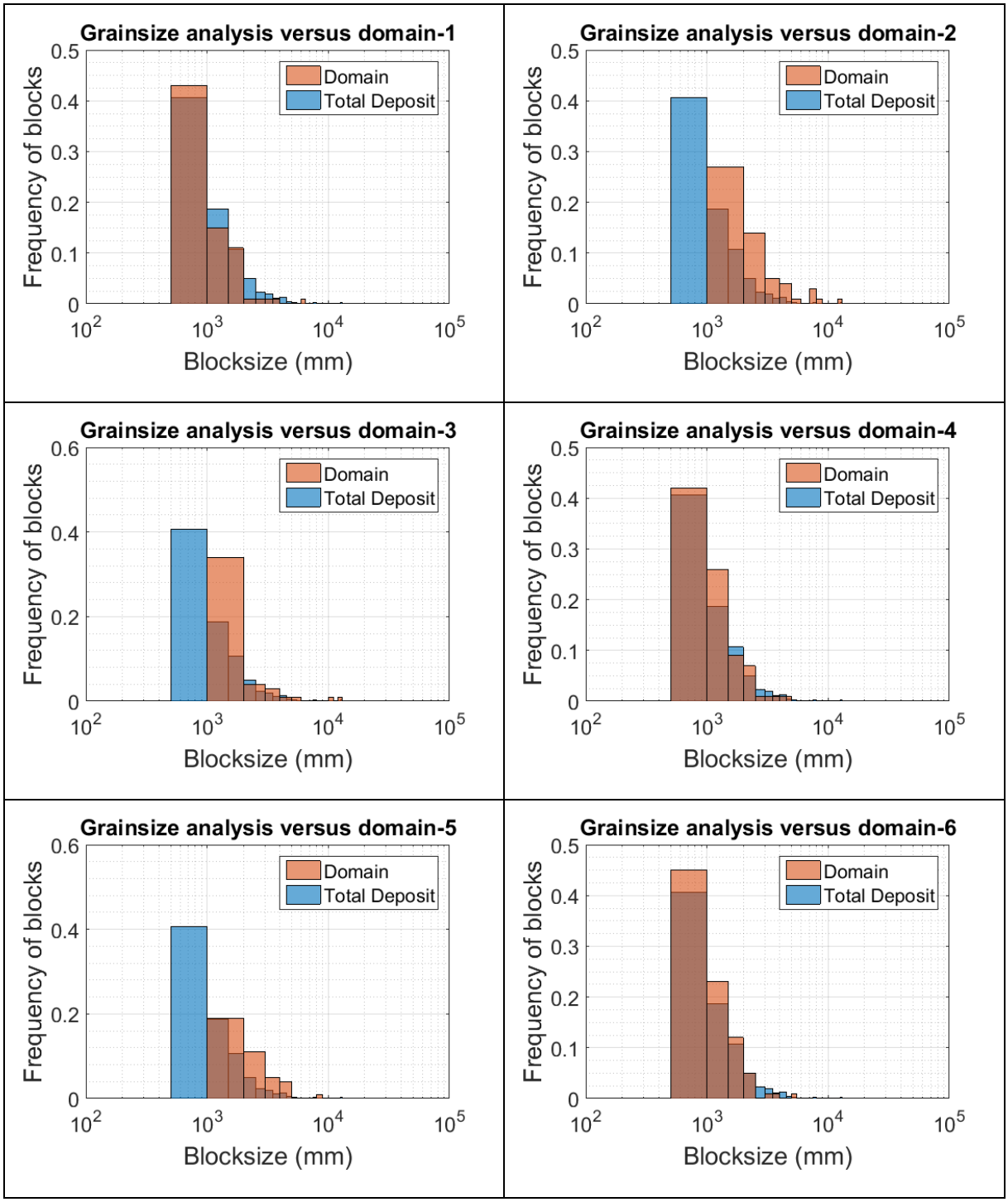

Figure 4.17: Grainsize distributions created in MATLAB.

4.4.3 Månavatnet (nr. 84)

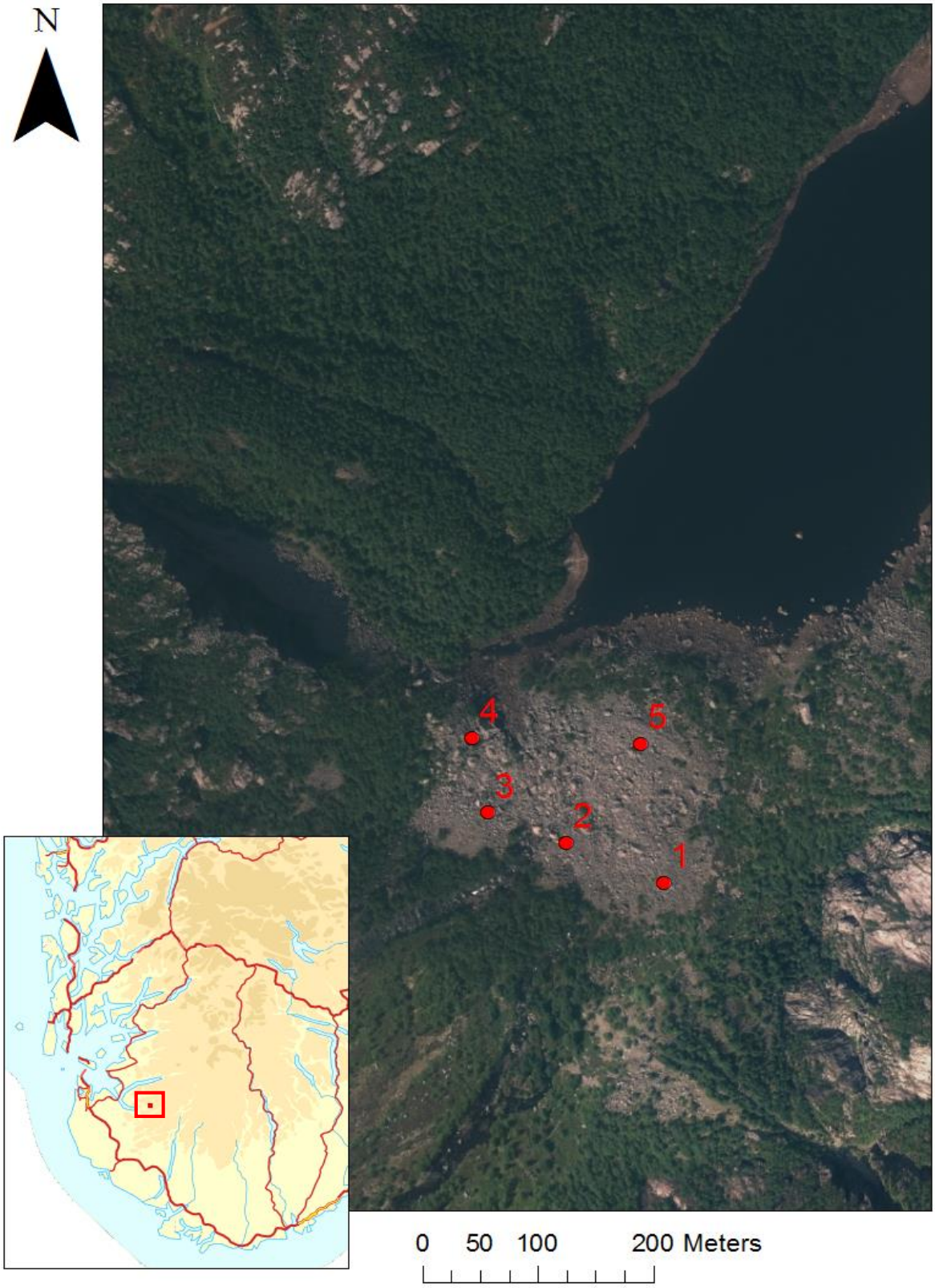

Figure 4.18: Grainsize domains at Månavatnet

Figure 4.19: Overview of Månavatnet. Picture is taken toward west.

Månavatnet is located in the regional county of Rogaland, northeast of Frafjord, in Månadalen (Figure 4.18). The rockslide dam originates from an evident scar on the western valley side (Figure 4.19). The valley sides are composed of the lithologies (NGU, 2016);

Diorite to granitic gneiss	Northwestern valley-side (scar)
Augengneis and granite	Southeastern valley-side

Field investigation of the deposit at Månavatnet showed that the grainsizes are finer to southwest, but retains its angular shape (Figure 4.19). The coarsest deposits were located in the northeastern parts of the deposit, close to the scar. This part has been influenced by continuous rock fall activity, and filtration of lake water since dam formation. River discharge varies greatly, and the lake responds quickly to changes in drainage (Figure 4.20). Drainage is concentrated through the dam. A fraction of the total drainage overflows when lake level reaches the dam rim (Figure 4.20).

Figure 4.20: Upper left: Picture of the overflowing channel. The picture is taken close to point 4(Figure 4.18). Upper right: Picture of lake level response to intense rainstorm. Lower: Picture illustrating outlet of drainage through the dam, the picture is taken between point 2 and 3 towards northeast (Figure 4.18).

Geomorphic analysis of Månavatnet resulted in Table 4.4.2.

Table 4.4.2: Results from the geomorphic analysis at Månavatnet.

Type slide	Rock Avalanche
Glacial influence	No
Stability status	Not Breached
Two dimensional classification	II A
Across valley classification	i
Along-valley classification	2
Valley width	350m
Height of release area	240m
Dam length	350m
Dam width	280m
Dam area (m^2)	82000
Dam height max	32m
Dam height mean	16m
Dam volume	13000000m^3
Catchment area	93000000

4.4.4 Grainsize Analysis at Månavatnet

The grainsize analysis can be compared with the map illustrating the different grainsize domains at Månavatnet (Figure 4.18). Each domain can be compared with the total deposit. Two grainsize analysis have been performed, one in MATLAB (histogram) and one in EXCEL (conventional grainsize analysis) (Figure 4.21 and Figure 4.22).

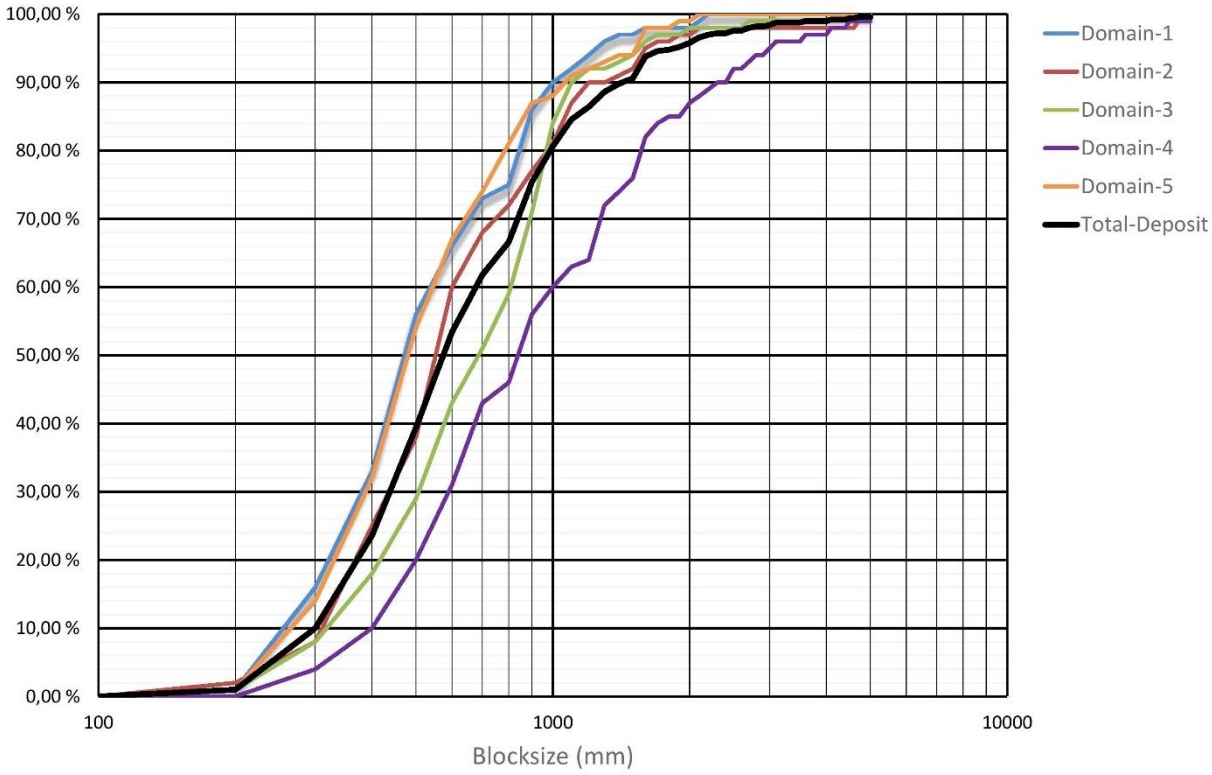

Figure 4.21: Conventional block size analysis in EXCEL.

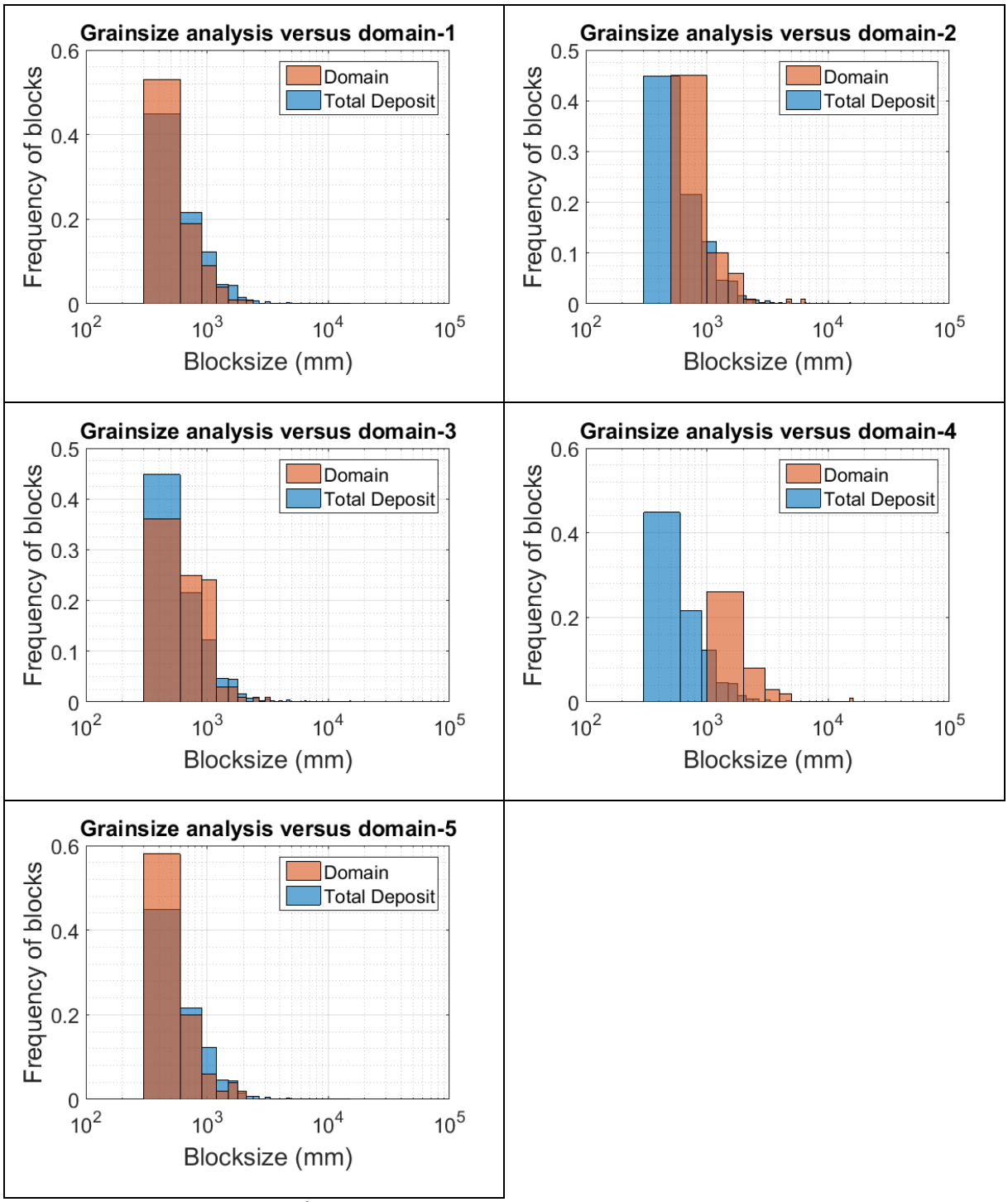

Figure 4.22: Block size analysis of Månavatnet in MATLAB.

5. Discussion

5.1. Tool that Predict Dam Height

Several different equations have been proposed where the input variables are "dam volume" and "valley width". The suggested equations have been fitted against different datasets to estimate the constants making up the equations. Equation 5.1 was deemed most promising based on the uncertainty of the fitted data, and the quality of the datasets.

$$z = ax * exp^{by} + cy + d \quad (5.1)$$

Each dataset was fitted to the different equations to determine which dataset represented the behavior of rockslide dams. The RMSE (Appendix. A-6)from using dataset 2 is approximately 15 meters. The uncertainty can be evaluated as moderate to high, but the shape of the fitted surface is logical based on the behavior of the variables (Figure 4.7). The main reason behind the high uncertainty is that several seemingly identical dams, regarding "dam volume" and "valley width", result in dams of different heights. In other words, "dam volume" and "valley width" does not totally represent the geomorphological situation determining the behavior of rockslide dam formation. Other factors that influences dam formation are for example; channelization of the rockslide, the energy involved in rock slope failure or the character of the substrate (Chapter 2.1.2).

It is reckoned that the constants from dataset 2 are most suitable for describing the behavior of rockslide dams based on testing of the equation against test-dams. Dataset 2 is the next largest dataset, comprising dams that exhibit a large variety of behaviors. The author's educated opinion is that rock slope failures suitable for the equation should contain volumes between [10^6, $25*10^6$]. One should use the constant from dataset-1 if larger rock slope failures are to be investigated.

$$dam\ height = \frac{dam\ Volume}{2{,}76E+05} e^{-\frac{valley\ width}{8{,}03E+02}} - \frac{valley\ width}{6{,}66E+01} + 31{,}12 \quad (5.2)$$

The potential rockslide areas; Gamanjunni, Mannen and Ivanasen were analyzed to investigate the secondary consequences of future rock slope failures.

5.1.1 Testing the Tool against Future Potential Rockslides

Gamanjunni is a large unstable rock slope located in Manndalen in Kåfjord. The unstable rock slope is located in Schist (NGU, 2016). dGPS measurements show that the unstable rock slope experience inhomogeneous deformation, varying form 5mm/y to 20mm/y (Bunkholt, 2011). The catchment area of Manndalselva is relative large, compared to other catchment areas in the database.

Table 5.1.1: Geomorphic input parameters to the tool, and resulting output parameters from the tool.

Unstable Rock Slope	Gamanjunni (nr.200)
Dam Volume (m^3)	21000000
Valley Width (m)	900
Catchment Area (m^2)	150000000
Predicted Dam Height (m)	42,4

Mannen is located in Rauma in Romsdalen. A large rock slope failure here may lead to secondary effects like damming of Rauma, and catastrophic flooding downstream when the dam fail. Two volumes of Mannen have been analyzed (Table 5.1.2 and Table 5.1.3) (Dahle et al., 2011). The catchment area of Rauma is the largest catchment area in the rockslide dam database (Appendix. B-1).

Table 5.1.2: Geomorphic input parameters to the tool, and resulting output parameters from the tool.

Unstable Rock Slope	Mannen (201)
Dam Volume (m^3)	18800000
Valley Width (m)	900
Catchment Area (m^2)	1200000000
Predicted Dam Height (m)	39,8

Table 5.1.3: Geomorphic input parameters to the tool, and resulting output parameters from the tool.

Unstable Rock Slope	Mannen (202)
Dam Volume (m^3)	2900000
Valley Width (m)	900
Catchment Area (m^2)	1200000000
Predicted Dam Height (m)	21

The unstable rock slope; Ivasnasen is located in Sunndalen, Møre og Romsdal. The site contains an historical rock avalanche deposit that may have resulted in blockage of the river Driva. The unstable rock slope is situated in augengneiss (Dreiås, 2012). Failure of Ivasnasen will result in blockage of Driva, which may result in dam-breach and downstream flooding.

Table 5.1.4: Geomorphic input parameters to the tool, and resulting output parameters from the tool.

Unstable Rock Slope	Ivasnasen (203)
Dam Volume (m^3)	4100000
Valley Width (m)	220
Catchment Area (m^2)	40000000
Predicted Dam Height (m)	39,1

5.1.2 Stability Analysis of Future Potential Rockslides

DBI can be used to assess dam stability of future rock slope failures by replacing dam height with the equation proposed in chapter 5.1. This allows us to get an impression of the future stability, and the consequences related to rockslide dam formation.

$$DBI = \log\left(\frac{A_b * \left(\frac{V_d}{2{,}76E+05}\, e^{\frac{W_v}{8{,}03E+02}} - \frac{W_v}{6{,}66E+01} + 31{,}12\right)}{V_d}\right) \quad (5.3)$$

Where A_b is the catchment (m^2) V_d is rockslide dam volume (m^3) and W_v is the width of the valley (m). It is possible to predict the behavior of future rock slope failures by using geomorphic data from potential rock slope failures in equation 9.3 (Table 5.1.1, Table 5.1.2, Table 5.1.3 and Table 5.1.4). The resulting DBI values and plot illustrate the future stability of the potential rockslide dams (Figure 5.1).

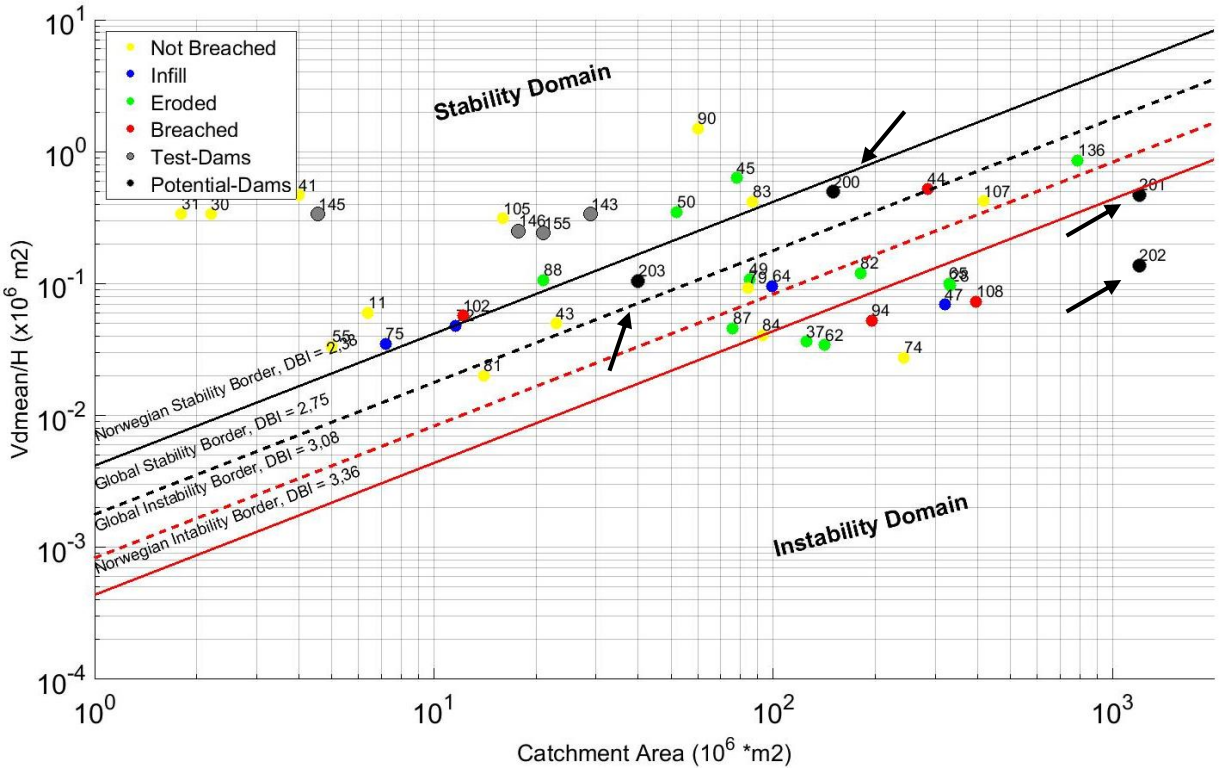

Figure 5.1: DBI-plot of general rockslide dams (from dataset-1), test-dams and potential rockslide dams. The arrows indicate the potential dams.

Rockslide	Gamanjunni (200)
Dam height (m)	42,4
DBI	2,5

The stability analysis of Gamanjunni indicates that the dam will lie in the stable-uncertain domain. This is primarily because Gamanjunni is restricted by a limited catchment area. However, fluctuation in weather condition (late snow melting, rainstorms) may periodically reduce the stability of the dam. The author predicts that Gamanjunni will remain stable based on Figure 5.1.

Rockslide	Mannen (201)
Dam height (m)	39,8
DBI	3,4
Rockslide	**Mannen (202)**
Dam height (m)	21
DBI	3,9

The two volume scenarios of Mannen (201 and 202) will both be unstable based on Figure 5.1. The large catchment area of Rauma will quickly fill the lake reservoir, and overtop. Continuous erosion of the carapace will progressively initiate failure by overtopping. The smallest volume scenario of Mannen (202) is least stable, while the larger scenario (201) is somewhat more stable. However, both dams will most likely fail.

Rockslide	Ivasnasen (203)
Dam height (m)	39,1
DBI	2,6

Ivasnasen is plotted in the stable-uncertain domain in Figure 5.1. The catchment area of Driva is relatively small, which is the primary reason Ivasnasen is plotted in the stable-uncertain domain. However, fluctuation in weather condition (late snow melting, rainstorms) may periodically reduce the stability of the dam. The author predicts that Ivasnasen will remain stable for a period of time based on Figure 5.1.

Equation 9.3 allows us to make predictions on the secondary consequences of rock slope failure. The equation considers catchment area, valley width and dam volume as the main factors affecting the stability of future landslide dams. The proposed equation is not an improvement of the original DBI-equation (Chapter 2.4.3), but in sorts an evolved version that can be used a predictive tool. Ermini and Casagli (2003) discussed future improvements of the dimensionless blockage index. They discussed improvements made by considering other variables such as the grain size distribution of the dam material, and setting up a wider database to reduce the statistical uncertainty of the relationship (Casagli et al., 2003). Rockslide dams from the southern parts of Norway have been implemented to database. While Norwegian dams have not been analyzed against the global database, they represent a regional trend on the behavior of landslide dams.

The destabilizing factor in the DBI-equation is the catchment area (Ermini & Casagli, 2003). While the catchment area account for the entire area of drainage, it does not consider fluctuation in drainage as a result of weather conditions (snow-melting or rain storms). High river discharge may result in considerable erosion of the dam material. Erosion of the dam material depends on the character of the rockslide deposit and the river discharge. While the carapace's role on dam stability has not yet been implemented in the stability model (equation 5.3), it is recognized that the dam material plays a crucial role concerning dam stability. Therefore, a separate longevity model (Figure 2.14) has been constructed to get an idea of the stability at Gloppedalsura and Månavatnet (Weidinger, 2011). The model is discussed in chapter 5.2.3.

5.1.3 Data Uncertainties

The proposed equation gives the user the opportunity to get an impression of the possible secondary consequences of rock slope failure in Norwegian valleys. However, there are several uncertainties that influences the proposed equation.

- First and foremost: The morphometric analysis is based on a 10-meter digital elevation model. This means that the terrain is divided into pixel cells of 10*10 meters, and an elevation value is given to the center of the cell. Height values are weighed to the area between the cell-centers by method called triangulated irregular network (TIN). The accuracy of the DEM, hence the accuracy of the morphometric analysis increases with decreasing DEM-resolution. However, work on creating a new national DEM with a resolution of 2-points/m^2 started in 2015. The DEM is planned to be available in 2019 (Kartverket, 2013). This rises the opportunity of improving the tool (equation 5.2) when the new DEM is released by repeating the morphometric analysis.
- Second: The morphometric analysis is based on subjective interpretations of the geomorphic situation. The quality of the geomorphic data is therefore highly dependent on the understanding of the geomorphic situation of each landslide dam. The data available for interpretation from the method (described in chapter 3.1.2) is limited, since it consists of 2-profiles. Therefore, the author assumes that the uncertainty of the morphometric data can be as high as 30% for some landslide dams.
- Third; Several parameters affect dam formation. The equation proposed regards only two parameters, and therefore simplifies the actual situation where several more parameters affect the formation of landslide dams. This is highlighted by the fact that several landslide dams of identical "volume" in valleys with equal "valley width" produce dams of different height. However, difficulties arise when incorporating a fourth parameter to the proposed equation since it is difficult to visualize the effect of the fourth parameter on the equation.

- Fourth: While a large amount of data exists for small rockslide dams in narrow valleys, few dams exhibit the behavior of large volume in narrow or wide valleys. This rises the uncertainty of the accuracy of the behavior of large rockslides/rock avalanches. This can be illustrated by comparing Figure 4.7 and Figure 4.8. Where the dataset used in Figure 4.7 incorporates large rockslides while Figure 4.8 is created from using dams smaller than $10^7 m^3$. The latter figure is therefore ill equipped as a tool when the volume exceeds $10^7 m^3$. This is illustrated in Table 4.2.12 where the RMSE is 78 meters, because the volume of the test dams exceeds $10^7 m^3$.
- Fifth: The uncertainty of the datasets fitted to the different equations determines the accuracy of the tool. The RMSE of the datasets fitted to the different equations exceed 10 meters, with the exception of dataset 4 fitted to equation 4.5 (Table 4.2.1, Table 4.2.3, Table 4.2.5 and Table 4.2.7). While the RMSE of equation 4.5 with the constants computed from dataset-2 (equation 5.2), versus the test dams is 9 meters. The author would therefor argue that Equation 5.2 is most suitable as a tool for describing the secondary consequences of rock slope failures.

Several uncertainties influence the accuracy of the final equation, as mentioned above. The final equation is a few-step method that allows the user to easily assess the consequences of future rock slope failures. The author recommend that the tool is to be used as a preliminary tool to give an impression of expected dam height and dam stability before further analysis are conducted.

5.2. Grainsize Analysis

5.2.1 Grainsize Analysis at Månavatnet (nr. 84)

The grainsize distribution of Månavatnet is illustrated in chapter 4.4.4 and the map of the assigned domains in Appendix. C-1.The coarsest part of the of the deposit are domain; 4 (close to the scar) and 2 (in the middle of the deposit). Domain 3 is somewhat coarser than the total deposit, domain 1 and 5 are the finest (located furthest from the scar). All domains are characterized by unwheatered angular blocks.

The domains that are located furthest from the scar are finer grained because of longer transportation and higher grade of mechanical disintegration. The blocks get coarser progressing towards the scar. The coarsest part of the deposit is located directly below the vicinity of the scar. Drainage is located between domain 2 and 3. Drainage is concentrated trough the deposit during dry periods (as illustrated in Appendix. C-1), while overflow during periods of intense snow-melting or rainstorms (Figure 4.20).

The block size interval [minimum block size, maximum block size] can be plotted in the block size-longevity diagram to get an impression on the longevity of landslide dams (Figure 5.2)(Weidinger, 2011). The grainsize-longevity diagram indicates that Månavatnet will remain stable.

The DBI-value of Månavatnet is plotted on the border to the unstable domain, and indicates that dam failure is a possibility (Figure 5.1). However, this contradicts the results from the grainsize analysis. The author would therefore argue that the actual situation is somewhere in between. DBI-does not consider grainsize as a factor influencing dam stability, while the longevity-block size diagram only considers block-size as a factor. The author's educated opinion is that Månavatnet will remain stable, while progressively becoming more influenced by continuous erosion, reducing the capacity of the lake.

5.2.2 Grainsize Analysis at Gloppedalsura

Gloppedalen is a valley with bad GPS coverage. This was experienced firsthand when plotting GPS data after finished field work. Several GPS-points that should have indicated domains in the deposit were located around the deposit. One of the goals at Gloppedalsura was to investigate the different domains, this is however impossible because of the high uncertainty considering the location of the GPS-points.

The average grainsize of Gloppedalsura can be used to illustrate the hypothetical stability of Gloppedalsura as a conventional dam, not a drainage divide. Because of the extreme coarse carapace, Gloppedalsura will remain stable for several millennia. The author believes Gloppedalsura will remain a geomorphic feature in the landscape until the next glacial age.

5.2.3 Block Size Characteristics Versus Lifespan of the Lakes

The stability diagram proposed by Weidinger (2011) considers the block size of the carapace as the stabilizing factor (Weidinger, 2011). The dams in the diagram follow a quite clear trend, where increasing block size results increasing dam longevity. By continuing the trend (grey dashed line in Figure 5.2) the longevity of landslide dams can be assessed by plotting the grainsize interval describing the block size of the carapace constituting the dam.

First, this is a simplification of the actual situation since other factors influence the stability of the dam. Second, the diagram is based on the stability situation of landslide dams in the Himalayas; where both the geomorphologic and climatic setting differ from Norway. Making the diagram unsuitable for predicting dam longevity in Norway.

However, the diagram illustrates the important role the carapace plays considering the stability of the dam, and should therefore be included in the stability analysis.

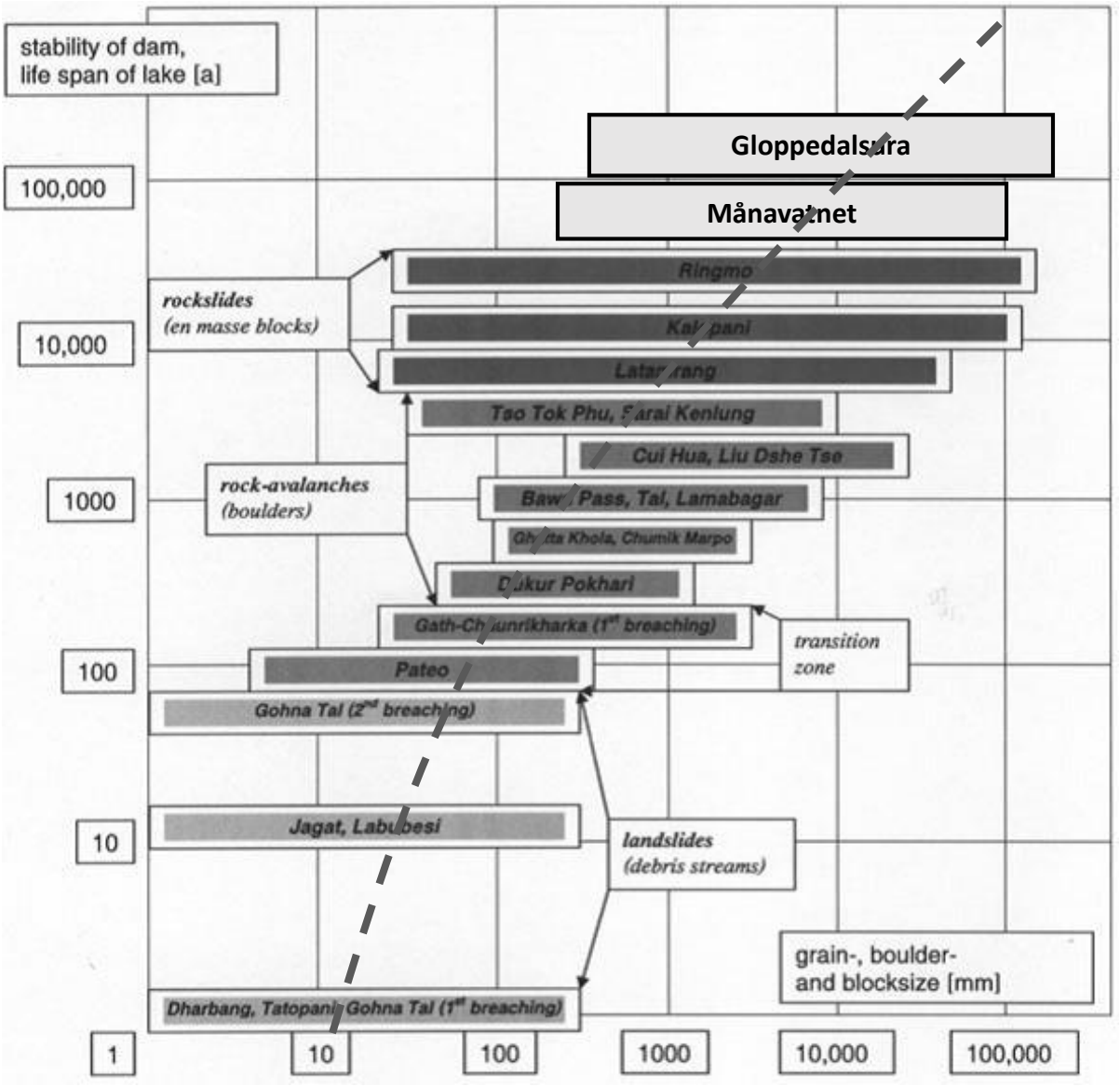

Figure 5.2: Gloppedalsura and Månavatnet plotted in the block size-longevity diagram (Weidinger, 2011). The line indicates longer longevity the coarser the carapace..

6. Conclusion

Rockslide dams poses a threat to people living beneath dams if catastrophic breaching occur. The tools proposed in this master thesis allows us to make predictions on the secondary consequences of future rock slope failures. The tools are easy to use, and the ideal purpose of the tools is to use them as preliminary forecast on the potential secondary consequences of future rock slope failures. The equation predicting future dam height can easily be used in the starting phase of a project to get an impression of the dam height of rock slope failure, and hence the lake volume. The tool can further be combined with run-out models to get a better understanding of the rockslide deposit.

$$dam\ height = \frac{dam\ Volume}{2{,}76E+05}\, e^{-\frac{valley\ width}{8{,}03E+02}} - \frac{valley\ width}{6{,}66E+01} + 31{,}12$$

DBI was originally used as a tool that assess landslide dam stability. It is possible to assess future dam stability by replacing dam height with the tool proposed above. This is also an easy tool to use in the early phases of a project to get an idea of the future stability situation.

$$DBI = \log\left(\frac{A_b * \left(\frac{V_d}{2{,}76E+05}\, e^{\frac{W_v}{8{,}03E+02}} - \frac{W_v}{6{,}66E+01} + 31{,}12\right)}{V_d}\right)$$

There are several other parameters that influence both dam height and dam stability as discussed earlier (chapter 5.1.3 and chapter 5.2.3). The geomorphology, the fall height and the substrata all influence the formation of rockslide deposits. While the grainsize distribution of the deposit influences the stability of the dam, as discussed in chapter 5.2.

7. Further Work

The author recommends a further analysis with a larger dataset to get a better a representation on the behavior of rockslide dams. Other parameters than “valley width” and dam “volume influence rockslide dam formation”. Parameters like; geomorphic channelization of the rockslide, fall height and the substrate influence the final deposit. In other words, there are ways to improve the equation. The author recommends to do a statistical analysis that incorporates more parameters, rather than plotting the parameters to visualize the effect of the different parameters.

The grainsize distribution of rockslide dams influences the longevity of rockslide dams. The developers of the Dimensionless blockage index (DBI) have discussed further work on the equation, and have commented on the role of the grainsize distribution on dam longevity (Ermini & Casagli, 2003). The author agrees with Ermini and Casagli. Work should be done on incorporating the grainsize character in the DBI. However, little to no data exist on the grainsize character of rockslide dams. So field visits are necessary.

The author recognizes the potential on research on fragmentation of rock slope failure. This can be used to predict the future grainsize distribution of rockslide dams, and hence make it possible to predict how the grainsize affect the stability of future rockslide dams.

8. Bibliography

Bunkholt, H. O., Per Terje; Redfield, Tim; Oppikofer, Thierry; Eiken, Trond; Hermanns, Reginald; Lauknes, Tom Rune. (2011). *ROS Fjellskred i Troms: status og analyser etter feltarbeid 2010*. Retrieved from Norges Geologiske Undersøkelse:

Canuti, P., Casagli, N., & Ermini, L. (1998). Inventory of landslide dams in the Northern Apennine as a model for induced flood hazard forecasting. *CNR-GNDCI-UNESCO (IHP): Managing Hydro-Geological Disasters in a Vulnerable Environment for Sustainable Development, Publ*(1900), 189-202.

Casagli, N., & Ermini, L. (1999). Geomorphic analysis of landslide dams in the Northern Apennine. *Transactions of the Japanese Geomorphological Union, 20*(3), 219-249.

Casagli, N., Ermini, L., & Rosati, G. (2003). Determining grain size distribution of the material composing landslide dams in the Northern Apennines: sampling and processing methods. *Engineering geology, 69*(1), 83-97.

Clague, J. J. E., S G. (1994). Formation and failure of natural dams in the Canadian Cordillera. *Geological Survey of Canada, Bulletin 464*, 40.

Coleman, S. E., Webby, M. G., & Andrews, D. P. (2002). Overtopping breaching of Noncohesive Homogeneous Embankments. *Journal of Hydraulic Engineering, 128*(9), 829-838. doi:doi:10.1061/(ASCE)0733-9429(2002)128:9(829)

Corominas, J. (1996). The angle of reach as a mobility index for small and large landslides. *Canadian Geotechnical Journal, 33*(2), 260-271. doi:10.1139/t96-005

Costa, J. E., & Schuster, R. L. (1988). The formation and failure of natural dams. *Geological Society of America Bulletin, 100*(7), 1054-1068.

Cruden, D. M. (1996). Landslide types and processes. *Landslides-investigation and mitigation-*.

Dahle, H., Bjerke, P. L., Crosta, G. B., Hermanns, R. L., Anda, E., & Saintot, A. (2011). *Fresoner for utløp, oppdemming og flom som følge av fjellskredfare ved mannen*. Retrieved from NGU

Dreiås, G. M. (2012). *Engineering geological assessment, and structural comparison of the Vollan and Ivasnasen rockslioe at Sunndal, Norway*(Master), NTNU-Trondheim, NTNU.

Dunning, S., Petley, D., & Strom, A. (2005). The morphologies and sedimentology of valley confined rock-avalanche deposits and their effect on potential dam hazard. *Landslide Risk Management. AT Balkema, Amsterdam*, 691-704.

Dunning, S. A., & Armitage, P. (2011). The grain-size distribution of rock-avalanche deposits: implications for natural dam stability *Natural and artificial rockslide dams* (pp. 479-498): Springer.

Ermini, L., & Casagli, N. (2003). Prediction of the behaviour of landslide dams using a geomorphological dimensionless index. *Earth Surface Processes and Landforms, 28*(1), 31-47.

Evans, S. G., Delaney, K. B., Hermanns, R. L., Strom, A., & Scarascia-Mugnozza, G. (2011). The formation and behaviour of natural and artificial rockslide dams; implications for engineering performance and hazard management *Natural and artificial rockslide dams* (pp. 1-75): Springer.

Heim, A. (1932). *Bergsturz und menschenleben*: Fretz & Wasmuth.

Hermanns, R. L., Dahle, H., Bjerke, P. L., Crosta, G. B., Anda, E., Blikra, L. H., . . . Longva, O. (2013). Rockslide Dams in Møre og Romsdal County, Norway *Landslide Science and Practice* (pp. 3-12): Springer.

Hermanns, R. L., Hewitt, K., Strom, A., Evans, S. G., Dunning, S. A., & Scarascia-Mugnozza, G. (2011). The classification of rockslide dams *Natural and Artificial Rockslide Dams* (pp. 581-593): Springer.

Hsü, K. J. (1975). Catastrophic debris streams (sturzstroms) generated by rockfalls. *Geological Society of America Bulletin, 86*(1), 129-140.

Hungr, O. (2006). Rock avalanche occurrence, process and modelling *Landslides from Massive Rock Slope Failure* (pp. 243-266): Springer.

Hungr, O., Leroueil, S., & Picarelli, L. (2014). The Varnes classification of landslide types, an update. *Landslides, 11*(2), 167-194.

Jakobsen, V. U. (2015). *Investigation of Rockslide Dams in the Southwestern Part of Norway.* Norwegian University of Science and Technology.

Kartverket. (2013). *Forposjekt "nasjonal, detaljert høydemodell"*. Retrieved from Kartverket.no: http://www.kartverket.no/globalassets/kart/nasjonal-hoydemodell/nasjonal-detaljert-hoydedatamodell---satsingsforslag.pdf?_ga=1.82566422.1611796079.1453799845

Kartverket, S. V. (2011). NorgeiBilder. Retrieved from http://www.norgeibilder.no/?zoom=3&lat=7210000&lon=795000&srs=EPSG:32632

Korup, O. (2004). Geomorphometric characteristics of New Zealand landslide dams. *Engineering geology, 73*(1), 13-35.

NGU (Cartographer). (2016). Berggrunns Kart (1:250000). Retrieved from http://geo.ngu.no/kart/berggrunn/

Nicoletti, P. G., & Sorriso-Valvo, M. (1991). Geomorphic controls of the shape and mobility of rock avalanches. *Geological Society of America Bulletin, 103*(10), 1365-1373.

Oppikofer, T., & Hermanns, R. L. (2015). [Rockslide prone areas in Norway].

Richards, K. S., & Reddy, K. R. (2007). Critical appraisal of piping phenomena in earth dams. *Bulletin of Engineering Geology and the Environment, 66*(4), 381-402.

Schleier, M., Hermanns, R. L., Rohn, J., & Gosse, J. C. (2015). Diagnostic characteristics and paleodynamics of supraglacial rock avalanches, Innerdalen, Western Norway. *Geomorphology*.

Stead D, E., E. (2013). Understanding the mechanics of large landslides. *Italian Journal of Engineering Geology and Environment, 6*, 108. doi:10.4408/IJEGE.2013-06.B-07

Stefanelli, C. T., Catani, F., & Casagli, N. (2015). Geomorphological investigations on landslide dams. *Geoenvironmental Disasters, 2*(1), 1-15.

Swanson FJ, O. N., Tominaga M. (1986). Landslide dam in Japan. *Landslide Dam: Process and risk Mittigation*.

Swanson, F. J., Oyagi, N., & Tominaga, M. (1986). *Landslide dams in Japan.* Paper presented at the Landslide Dams@ sProcesses, Risk, and Mitigation.

Varnes, D. J. (1978). Slope movement types and processes. *Transportation Research Board Special Report*(176).

Weidinger, J. (2011). Stability and life span of landslide dams in the Himalayas (India, Nepal) and the Qin Ling Mountains (China) *Natural and Artificial Rockslide Dams* (pp. 243-277): Springer.

Appendix. A MATLAB

Appendix. A-1. MATLAB Script for Plotting 2D-Data

```
function [Plot,f1,goodness] = toauto(x,y,volumemin,volumemax,plotoption,fitoption,sheet)

    [num,txt] = xlsread('Refined.xlsx', sheet);

    xname=txt(1,x);
    yname=txt(1,y);

    w=size(num);

    figure('Name', '2D-Plot','NumberTitle','on');

    if plotoption == 1

        Plot = zeros(1,4);

        for i = 1:w(1,1)

            if num (i,18) < volumemax && num(i,18) >= volumemin

                label = num2str(num(i,1)','%d');

                if (num(i,14) >= 0) && (num(i,14) < 1)

                    Plot(1,1) = scatter(num(i,x),num(i,y), 'g', 'filled','SizeData',
100,'DisplayName', 'DW/DL < 1');

                elseif (num(i,14) >= 1) && (num(i,14) < 2)

                    Plot(1,2) = scatter(num(i,x),num(i,y), 'y', 'filled','SizeData', 100,
'DisplayName', '1 =< DW/DL < 2');

                elseif (num(i,14) >= 2) && (num(i,14) < 3)

                    Plot(1,3) = scatter(num(i,x),num(i,y), 'r', 'filled','SizeData', 100,
'DisplayName', '2 =< DW/DL < 3');

                else

                    Plot(1,4) = scatter(num(i,x),num(i,y), 'k', 'filled','SizeData', 100,
'DisplayName', 'DW/DL > 3');

                end

                text(num(i,x),num(i,y),label, 'horizontal','left', 'vertical','bottom',
'fontsize',22);

            end

        hold on

        end

        legend(Plot(1:4),'DW/DL < 1','1 =< DW/DL < 2','2 =< DW/DL < 3','DW/DL > 3');

    elseif plotoption == 2

        Plot = zeros(1,2);

        for i = 1:w(1,1)

            if num (i,18) < volumemax && num(i,18) >= volumemin

                label = num2str(num(i,1)','%d');

                if num(i,12) >= 1

                    Plot(1) = scatter(num(i,x),num(i,y), 'g', 'filled','SizeData',
100,'DisplayName', 'Event Crossing Valley');
```

```
                else

                    Plot(2) = scatter(num(i,x),num(i,y), 'r', 'filled','SizeData',
100,'DisplayName', 'Event not Crossing Valley');

                end

                text(num(i,x),num(i,y),label, 'horizontal','left', 'vertical','bottom',
'fontsize',22);

            end

        hold on

        end

        legend(Plot(1:2),'Event Crossing Valley', 'Event not Crossing Valley')

    elseif plotoption == 3

        for i = 1:w(1,1)

            if num (i,18) < volumemax && num(i,18) >= volumemin

                label = num2str(num(i,1)','%d');

                class = num(i,6);

                switch(class)

                    case{21}

                        Plot(1) = scatter(num(i,x),num(i,y), 'g', 'filled','SizeData',
100,'DisplayName', 'II a');

                    case{22}

                        Plot(2) = scatter(num(i,x),num(i,y), 'y', 'filled','SizeData',
100,'DisplayName', 'II b');

                    case{31}

                        Plot(3) = scatter(num(i,x),num(i,y), 'r', 'filled','SizeData',
100,'DisplayName', 'III a');

                    case{42}

                        Plot(4) = scatter(num(i,x),num(i,y), 'b', 'filled','SizeData',
100,'DisplayName', 'IV b');

                    otherwise

                        Plot(5) = scatter(num(i,x),num(i,y), 'h', 'filled','SizeData',
100,'DisplayName', 'Other Classification');

                end

            text(num(i,x),num(i,y),label, 'horizontal','left', 'vertical','bottom',
'fontsize', 22);

            end

        hold on

        end

        legend(Plot(1:5),'II a', 'II b', 'III a', 'IV c', 'Other Class')

    else

        for i = 1:w(1,1)

            if num(i,18) >= volumemin  && num (i,18) < volumemax

                label = num2str(num(i,1)','%d');
```

```
                Plot = scatter(num(i,x),num(i,y), 'g', 'filled','SizeData', 100);

                text(num(i,x),num(i,y),label, 'horizontal','left', 'vertical','bottom',
'fontsize',22);

            end

        hold on

        end

    end

    count = teller(volumemin, volumemax,sheet);
    aa = 0;
    antall = zeros(count,2);
    w = size(num);

    for j = 1:w(1,1)

        if num (j,18) < volumemax && num(j,18) >= volumemin

            aa = aa +1;

            antall(aa,1) = num(j,x);
            antall(aa,2) = num(j,y);

        end

    end

    xcol = antall(:,1);
    ycol = antall(:,2);

    if fitoption == 1

        lft = fittype(@(a,b,x) a*x+b , 'independent', {'x'}, 'dependent', 'y' );

        [f1,goodness] = fit( xcol, ycol, lft, 'Normalize', 'off', 'StartPoint', [0,0]);

        plot(f1,'k','predfunc');

    elseif fitoption == 2

        lft = fittype(@(a,b,x) a*log(x)+b*x, 'independent', {'x'}, 'dependent', 'y' );

        [f1,goodness] = fit( xcol, ycol, lft, 'Normalize', 'off', 'StartPoint', [0,0]);

        plot(f1,'k','predfunc');

    end

    grid on
    grid minor

    set(gca,'fontsize',22);

    xlabel(xname,'fontsize', 22);
    ylabel(yname,'fontsize',22);

    disp(f1)
    disp(goodness)
end
```

```
function[count] = teller(volumemin, volumemax, sheet)
[num] = xlsread('Refined.xlsx', sheet);
count = zeros(1,1);
w = size(num);
for i = 1:w(1,1)
     if num (i,19) < volumemax && num(i,19) >= volumemin
    count = count + 1;
     end
end
```

Appendix. A-2. MATLAB Script for Plotting and Fitting 3D-Data

```
function[Plot,f1,goodness]=threeauto(x,y,z,volumemin,volumemax,plotoption,
fitoption, sheet)
```

The role of the input/output-parameters are listed below:

- **x**: allows the user to define the first independent variable of the scatter-plot. The input variable is a numeric value, and refer to the column-number in the spreadsheet-file where the desired data is situated.
- **y**: allows the user to define the second independent variable of the scatter-plot. The input variable is a numeric value, and refer to the column-number in the spreadsheet-file where the desired data is situated.
- **z**: allows the user to define the dependent variable of the scatter-plot. The input variable is a numeric value, and refer to the column-number in the spreadsheet-file where the desired data is situated.
- **volumemin-volumemax**: allows the user to define the volume interval that is desired investigated.
- **plotoption**: allows the user to define which additional rockslide dam characteristics to be illustrated. The input parameter is a numeric value between 1 and 3.
    1. Illustrates the morphometric relationship between rockslide dam length and rockslide dam width.
    2. Illustrate the geomorphic relationship between the valley width and the rockslide dam length.
    3. Illustrates the two-dimensional classification of the rockslide dam.
    0. Does nothing.
- **fitoption**: allow the user to define which surface should fit the scatter plot, the different equations are illustrated in chapter 3.3.4. The input parameter is a numeric value between 1 and 4.
    1. Fit the scatter-plot to equation 4.3
    2. Fit the scatter-plot to equation 4.4
    3. Fit the scatter-plot to equation 4.5
    4. Fit the scatter-plot to equation 4.6
    0. Does nothing.
- **sheet**: allow the user to define which excel sheet to import data from. The input parameter is a numeric value that refer to the excel sheet-number.

- **Plot**: returns a 3-dimensional scatter plot of the data set clarified by; **volumemin-volumemax** and the **sheet,** with the **plotoption** emphasized by the user.
- **f1**: returns a surface fitted to the scatter plot clarified by the dataset selected by the user and the **fitoption** chosen.
- **f1**: returns the constants of the equation clarified by the **fitoption**, characterizing the surface-plot created.
- **goodness**: returns the 95% confidence bounds of the constants in **f1**, characterizing the fitted equation.
- **goodness**: returns the statistical operators of the fit, **f1**. The statistical operators can be found in table Statistical Operators in MATLAB.

Presenting data in three dimensions does not illustrate the entire geomorphic situation of rockslide dams, since more than 2 variables can affect the rockslide dam height. The geomorphic plot in MATLAB allows the user to illustrate different geomorphic characteristics, and ultimately allow illustration of information in more than 3-dimensions. The following customization options are offered in the script:

- The morphometric situation (DL/DW – Dam length/Dam width) of the rockslide dam is illustrated by the relationship between rockslide dam width and rockslide dam length.
- The geomorphic correlation between the rockslide deposit and the valley floor is illustrated by the relationship between rockslide dam length and valley width (DL/VW). The rockslide does not cross the valley floor if the divergent is less than 1.
- The general shape of the rockslide dam is represented by the two dimensional classification of the rockslide deposit, described in chapter 2.2.

```
function [Plot,f1,goodness] = threeauto(x,y,z,volumemin,volumemax,plotoption, fitoption,
sheet)

[num,txt] = xlsread('Refined.xlsx', sheet);

xname=txt(1,x);
yname=txt(1,y);
zname=txt(1,z);

w = size(num);

figure('Name', '3D-Plot','NumberTitle','on');

if plotoption == 1

    Plot = zeros(1,4);

    for i = 1:w(1,1)

        if num (i,19) < volumemax && num(i,19) >= volumemin

            label = num2str(num(i,1)','%d');

            if (num(i,14) >= 0) && (num(i,14) < 1)

                Plot(1) = scatter3(num(i,x),num(i,y),num(i,z), 'LineWidth',1,
'MarkerEdgeColor','k','MarkerFaceColor','g', 'SizeData', 100,'DisplayName', 'DW/DL < 1');

            elseif (num(i,14) >= 1) && (num(i,14) < 2)

                Plot(2) = scatter3(num(i,x),num(i,y),num(i,z), 'LineWidth',1,
'MarkerEdgeColor','k','MarkerFaceColor','y', 'SizeData', 100, 'DisplayName', '1 =< DW/DL <
2');

            elseif (num(i,14) >= 2) && (num(i,14) < 3)

                Plot(3) = scatter3(num(i,x),num(i,y),num(i,z), 'LineWidth',1,
'MarkerEdgeColor','k','MarkerFaceColor','r', 'SizeData', 100,'DisplayName', '2 =< DW/DL < 3');

            else

                Plot(4) = scatter3(num(i,x),num(i,y),num(i,z), 'LineWidth',1,
'MarkerEdgeColor','k','MarkerFaceColor','k', 'SizeData', 100,'DisplayName', 'DW/DL > 3');

            end

            text(num(i,x),num(i,y),num(i,z),label, 'horizontal','left', 'vertical','bottom',
'fontsize',22);

        end

        hold on

    end

    h_legend = legend(Plot(1:4),'DW/DL < 1','1 =< DW/DL < 2','2 =< DW/DL < 3','DW/DL > 3');
    set(h_legend, 'FontSize', 22);

elseif plotoption == 2

    Plot = zeros(1,2);

    for i = 1:w(1,1)

        if num (i,19) < volumemax && num(i,19) >= volumemin

            label = num2str(num(i,1)','%d');

            if num(i,12) >= 1

                Plot(1) = scatter3(num(i,x),num(i,y),num(i,z), 'LineWidth',1,
'MarkerEdgeColor','k','MarkerFaceColor','g','SizeData', 100,'DisplayName', 'Event Crossing
Valley');

            else
```

```
                Plot(2) = scatter3(num(i,x),num(i,y),num(i,z), 'LineWidth',1,
'MarkerEdgeColor','k','MarkerFaceColor','r','SizeData', 100,'DisplayName', 'Event not Crossing
Valley');


            end

            text(num(i,x),num(i,y),num(i,z),label, 'horizontal','left', 'vertical','bottom',
'fontsize',22);

        end

        hold on

    end

    h_legend = legend(Plot(1:2),'Event Crossing Valley', 'Event not Crossing Valley');
    set(h_legend, 'FontSize', 22);

elseif plotoption == 3

    Plot = zeros(1,4);

    for i = 1:w(1,1)

        if num (i,19) < volumemax && num(i,19) >= volumemin

            label = num2str(num(i,1)','%d');

            if num(i,6) == 21;

                    Plot(1) = scatter3(num(i,x),num(i,y),num(i,z), 'LineWidth',1,
'MarkerEdgeColor','k','MarkerFaceColor','r','SizeData', 100, 'DisplayName', 'II a');

            elseif num(i,6) == 22

                    Plot(2) = scatter3(num(i,x),num(i,y),num(i,z), 'LineWidth',1,
'MarkerEdgeColor','k','MarkerFaceColor','b','SizeData', 100,'DisplayName', 'II b');

            elseif num(i,6) == 31

                    Plot(3) = scatter3(num(i,x),num(i,y),num(i,z), 'LineWidth',1,
'MarkerEdgeColor','k','MarkerFaceColor','y','SizeData', 100,'DisplayName', 'III a');
            else

                    Plot(4) = scatter3(num(i,x),num(i,y),num(i,z), 'LineWidth',1,
'MarkerEdgeColor','k','MarkerFaceColor', 'g','SizeData', 100,'DisplayName', 'Other
Classification');

            end

            text(num(i,x),num(i,y),num(i,z),label, 'horizontal','left',
'vertical','bottom','fontsize',22);

        end

        hold on

    end

    h_legend = legend(Plot(1:4),'II a', 'II b', 'III a','Other Class')% 'III a','IV c', );
    set(h_legend, 'FontSize', 22);

elseif plotoption == 0

    for i = 1:w(1,1)

        if num(i,19) >= volumemin  && num (i,19) < volumemax

            label = num2str(num(i,1)','%d');

            Plot = scatter3(num(i,x),num(i,y),num(i,z),'LineWidth',1, 'MarkerEdgeColor', 'k',
'MarkerFaceColor', 'g', 'SizeData', 100);

            text(num(i,x),num(i,y),num(i,z),label, 'horizontal','left',
'vertical','bottom','fontsize',22);
```

```
        end

        hold on

    end

end

count = teller(volumemin, volumemax, sheet);
aa = 0;
antall = zeros(count,3);
w = size(num);

for j = 1:w(1,1)

    if num (j,19) < volumemax && num(j,19) >= volumemin

        aa = aa +1;

        antall(aa,1) = num(j,x);
        antall(aa,2) = num(j,y);
        antall(aa,3) = num(j,z);

    end

end

xcol = antall(:,1);
ycol = antall(:,2);
zcol = antall(:,3);

stem3(xcol,ycol,zcol, 'LineStyle','--', 'LineWidth',2 ,'Color','black','Marker','none');

if fitoption == 1

    lft = fittype(@(a,x,y) x.*exp(a*y), 'independent', {'x', 'y'}, 'dependent', 'z' );

    [f1,goodness] = fit( [xcol, ycol], zcol, lft, 'Normalize', 'off', 'StartPoint', [0]);
    plot( f1)

    disp(goodness)
    disp(f1)

elseif fitoption == 2

    lft = fittype(@(a,b,x,y) a*x.*exp(b*y), 'independent', {'x', 'y'}, 'dependent', 'z' );

    [f1,goodness] = fit( [xcol, ycol], zcol, lft, 'Normalize', 'off', 'StartPoint', [0,0]);
    plot( f1);
    alpha(0.5)

    disp(goodness)
    disp(f1)

elseif fitoption == 3

    lft = fittype(@(a,b,c,x,y) a*x.*exp(b*y) + c, 'independent', {'x', 'y'}, 'dependent', 'z'
);

    [f1,goodness] = fit( [xcol, ycol], zcol, lft, 'Normalize', 'off', 'StartPoint', [0,0,0]);
    plot( f1);
    alpha(0.5)

    disp(goodness)
    disp(f1)

elseif fitoption == 4

    lft = fittype(@(a,b,c,x,y) a*x.*exp(b*y) + c*y, 'independent', {'x', 'y'}, 'dependent',
'z' );

    [f1,goodness] = fit( [xcol, ycol], zcol, lft, 'Normalize', 'off','StartPoint', [0,0,0] );
    plot( f1)
    alpha(0.5)

    disp(goodness)
    disp(f1)
```

```
elseif fitoption == 5

    lft = fittype(@(a,b,c,d,x,y) a*x.*exp(b*y) + c*y + d, 'independent', {'x', 'y'},
'dependent', 'z' );

    [f1,goodness] = fit( [xcol, ycol], zcol, lft, 'Normalize', 'off', 'StartPoint',
[0,0,0,0]);
    plot( f1 );
    alpha(0.5)

    disp(goodness)
    disp(f1)

end

grid on
grid minor

set(gca,'fontsize',22);

zlim([0 100]);

xlabel(xname,'fontsize', 22);
ylabel(yname,'fontsize',22);
zlabel(zname,'fontsize',22);

rotx = get(gca,'xlabel');
set(rotx,'rotation',11, 'position', [4 -500 0] )
roty = get(gca,'ylabel');
set(roty,'rotation',340)

box on

ax = gca;
ax.BoxStyle = 'full';
ax.LineWidth = 2;

end
```

Appendix. A-3. **: MATLAB Script for the Stability Analysis**

. The MATLAB script opens an excel sheet with geomorphic data organized like:

Dam	Volume (m^3)	ValleyWidth (m)	Catchment Area (m^3)	Type

- Nr: The numeric identification number of the rockslide dam.
- Volume (m^3): Described in chapter 2.3.2.
- Valley width (m): Described in chapter 2.3.1.
- Catchment area (m^2): Described in chapter 3.1.2.
- Type: Indicates if the dam is a test dam (2) or a potential dam (1).

The DBI-values of each separate data-element is plotted against the DBI-points of dataset-1 (Appendix. B-1). This gives the user the opportunity to analyze where the separate rockslide dams are plotted relative to other dams, and the stability domains. The computed data are stored in a second excel-sheet with the name; *resultdam.xlsx*. The second excel-sheet is organized like:

Dam	Dam height (m)	DBI

```
[num,txt] = xlsread('Refined.xlsx', 3);
[test] = xlsread('predictdam.xlsx',1);

figure('Name', 'DBI-Plot','NumberTitle','on');

x = size(test);
Result = zeros(x(1,1), 10);
Result(:,1:5) = test;

for i = 1:x(1,1)

    Result(i,6) = analyzis(Result(i,2), Result(i,3), 2);
    Result(i,7) = (Result(i,2)./Result(i,6));
    Result(i,8) = log10(Result(i,4)./Result(i,7));
    Result(i,9) = Result(i,7)/10^6;
    Result(i,10) = Result(i,4)./10^6;

end

Alpha = zeros(x(1,1),3);
Alpha(:,1) = Result(:,1);
Alpha(:,2) = Result(:,6);
Alpha(:,3) = Result(:,8);

filetest = 'xxx.xlsx';
xlswrite(filetest,Result,1);
filename = 'resultdam.xlsx';
xlswrite(filename,Alpha,1);

Plot = zeros(1,6);

w = size(num);

for i = 1:w(1,1)

    label = num2str(num(i,1)','%d');

    if (num(i,27) == 1)

        Plot(1) = scatter(num(i,22),num(i,24),'LineWidth',1, 'MarkerEdgeColor', 'yellow',
'MarkerFaceColor', 'yellow', 'SizeData', 100 , 'DisplayName', 'Not Breached');

    elseif (num(i,27) == 2) || (num(i,27) == 5)

        Plot(2) = scatter(num(i,22),num(i,24),'LineWidth',1, 'MarkerEdgeColor', 'blue',
'MarkerFaceColor', 'blue', 'SizeData', 100 ,'DisplayName', 'Infill');

    elseif (num(i,27) == 3)

        Plot(3) = scatter(num(i,22),num(i,24),'LineWidth',1, 'MarkerEdgeColor', 'green',
'MarkerFaceColor', 'green', 'SizeData', 100 ,'DisplayName', 'Eroded');

    elseif (num(i,27) == 4) || (num(i,27)== 6)

        Plot(4) = scatter(num(i,22),num(i,24),'LineWidth',1, 'MarkerEdgeColor', 'red',
'MarkerFaceColor', 'red', 'SizeData', 100 ,'DisplayName', 'Breached');

    end

    text(num(i,22),num(i,24),label, 'horizontal','left', 'vertical','bottom', 'fontsize',14);

    hold on

end

for i = 1:x(1,1)

    label2 = num2str(Result(i,1)','%d');

    if Result(i,5) == 1

        Plot(5) = scatter(Result(i,10),Result(i,9),'LineWidth',1, 'MarkerEdgeColor', 'black',
'MarkerFaceColor', '[0.5 0.5 0.5]','SizeData', 150 , 'DisplayName', 'Test-Dams');

    elseif Result(i,5) == 2
```

```
        Plot(6) = scatter(Result(i,10),Result(i,9), 'LineWidth',1, 'MarkerEdgeColor', '[0.5
0.5 0.5]', 'MarkerFaceColor', 'black', 'SizeData', 150 , 'DisplayName', 'Potential-Dams');

    end

    text(Result(i,10),Result(i,9),label2, 'horizontal','left', 'vertical','bottom',
'fontsize',14);

    hold on

end
grid off
grid minor

ax = gca;
ax.GridLineStyle = '-';
ax.MinorGridLineStyle = '-';

set(gca,'xcolor',[0 0 0]);
set(gca,'ycolor',[0 0 0]);
set(gca,'GridColor',[0 0 0]);
set(gca,'LineWidth',1);

set(gca,'XScale','log', 'fontsize',24);
set(gca,'YScale','log', 'fontsize',24);

cmarea = logspace(0,3.3);
SG = cmarea/(10^2.75);
USG = cmarea/(10^3.08);
SR = cmarea/(10^2.38);
USR = cmarea/(10^3.36);

Plot1 = loglog(cmarea,SG);
set(Plot1,'color','black','LineStyle','--','linewidth',2)%,'DisplayName','Stable Global - DBI
= 2,75');

Plot2 = loglog(cmarea,USG);
set(Plot2,'color','red','LineStyle','--','linewidth',2)%,'DisplayName','Unstable Global - DBI
= 3,08');

Plot3 = loglog(cmarea,SR);
set(Plot3,'color','black','LineStyle','-','linewidth',2)%,'DisplayName','Stable Regional - DBI
= 2,38');

Plot4 = loglog(cmarea,USR);
set(Plot4,'color','red','LineStyle','-','linewidth',2)%'DisplayName','Unstable Regional - DBI
= 3,36');

st1=text(10, 2, 'Stability Domain','fontsize',20,'fontweight','bold');
set(st1,'rotation',14)
st2=text(100, 1e-3, 'Instability Domain','fontsize',20,'fontweight','bold');
set(st2,'rotation',14)

t1=text(1, 7e-3, 'Norwegian Stability Border, DBI = 2,38', 'fontsize',14);
set(t1,'rotation',14);
t2=text(1, 3e-3, 'Global Stability Border, DBI = 2,75', 'fontsize',14);
set(t2,'rotation',14);
t3=text(1, 1.45e-3, 'Global Instability Border, DBI = 3,08', 'fontsize', 14);
set(t3,'rotation',14);
t4=text(1, 7e-4, 'Norwegian Intability Border, DBI = 3,36', 'fontsize',14);
set(t4,'rotation',14);

xname=txt(1,22);
yname=txt(1,24);
xlabel(xname, 'fontsize',20);
ylabel(yname, 'fontsize',20);

xlim([0 2*10^3])

h_legend = legend(Plot(1:6),'Not Breached','Infill','Eroded','Breached','Test-
Dams','Potential-Dams','Location','northwest');
set(h_legend, 'FontSize', 18);
```

```
function[heightmax] = analyzis(damvolume,valleywidth,alternative)

x = damvolume;
y = valleywidth;

if alternative == 1

    a = 2.783e-06 ;
    b = -0.0006747;
    c = -0.01752  ;
    d = 32.37     ;

elseif alternative == 2

    a = 3.62e-06 ;
    b = -0.001245;
    c = -0.01501 ;
    d = 31.12    ;

elseif alternative == 3

    a = 8.091e-06;
    b = -0.001965;
    c = -0.0125  ;
    d = 25.79    ;

elseif alternative == 4

    a = 8.478e-06;
    b = -2.71e-05;
    c = -0.008644;
    d = 16.46    ;

end

heightmax = a*x.*exp(b*y)+c*y+d;

end
```

Appendix. A-4. **MATLAB Script for the Grainsize Analysis**

To use the script, the only change you have to do is to change the file-name, and make sure the excel-file is located in the same folder as the MATLAB-file. The filename in the script is; *gloppematlab2.xlsx*.

```
function [h] = graintest()

diameter = 4;

[type, number_sheets] = xlsfinfo('gloppematlab2.xlsx');

sheets_mx = size(number_sheets);
sheets_n = sheets_mx(1,2);

[alpha] = xlsread('gloppematlab2',1);
beta = size(alpha);

grain_m = zeros(beta(1,1),sheets_n-1);

for i = 1:sheets_n-1

    [sheet_d] = xlsread('gloppematlab2.xlsx', i);

    grain_m(:,i) = sheet_d(:,diameter);

end

[gamma] = xlsread('gloppematlab2', sheets_n);
grain_t = gamma(:,diameter);

%figure('Name', 'Grainsize analysis','NumberTitle','on');

for i = 1:sheets_n-1

    figure('Name', 'Grainsize analysis','NumberTitle','on');
    %subplot(3,2,i);
    grain_fm = grain_m(:,i);

    h(2) = histogram(grain_t,'normalization', 'probability');
    hold on
    h(1) = histogram(grain_fm,'normalization','probability');

    title(['Grainsize analysis versus domain-',num2str(i)]);

    l = cell(1,2);
    l{1}='Domain'; l{2}='Total Deposit';

    legend(h,l,'location','northeast')

    grid on
    grid minor

    set(gca,'fontsize',18)
    set(gca, 'XScale', 'log');

    xlabel('Blocksize (mm)', 'fontsize',22);
    ylabel('Frequency of blocks', 'fontsize',22);

end

end
```

Appendix. A-5. **Functions used in MATLAB**

Several build in functions were used in the MATLAB script. The most important functions used are listed in table (**Feil! Fant ikke referansekilden.**). MATLAB functions based on statements such as "for-loop", "while loop" and "if/case-statements" are not represented in the table.

Function	**Description**
xlsread (filename, sheet)	Read Microsoft Excel spreadsheet file
scatter(X,Y)	Creates a scatter plot with circles at the locations specified by the vectors x and y. This type of graph is also known as a bubble plot.
scatter3(X,Y,Z)	Displays circles at the locations specified by the vectors X, Y, and Z.
hist(x)	`hist(x)` creates a histogram bar chart of the elements in vector `x`. The elements in `x` are sorted into 10 equally spaced bins along the *x*-axis between the minimum and maximum values of `x`. `hist` displays bins as rectangles, such that the height of each rectangle indicates the number of elements in the bin.
plot(X,Y)	Creates a 2-D line plot of the data in Y versus the corresponding values in X.
fit(X,Y,Z,fitType)	Creates the fit to the data in x and y with the model specified by fitType.
fitType(libraryModelName)	Creates the fit type object for the model specified by libraryModelName.
fittype(expression)	Creates a fit type for the model specified by the MATLAB® expression.
gof [()]	Goodness-of-fit statistics, returned as the gof structure including the fields in table **Feil! Fant ikke referansekilden.**

Appendix. A-6. **Statistical Operators in MATLAB**

MATLAB offers several options to assess the uncertainty of the fit. By using the function "gof" listed in **Feil! Fant ikke referansekilden.**, the statistical operators listed in **Feil! Fant ikke referansekilden.** are returned. The statistical operator "root mean squared error" is used in this for the evaluation of different equations in this master-thesis.

Statistical Operator	**Description**
SSE	Sum of squares due to error.
rsquare	R-squared (coefficient of determination).
DFE	Degrees of freedom in the error.
adjrsquare	Degree-of-freedom adjusted coefficient of determination.
RMSE	Root mean squared error (standard error).

Appendix. B Databases

Appendix. B-1. **Database 1**

nr	Type Slide	Dam Failure	Glacial Influence	Two Dimensional Classification	Cross-Valley Classification	Along-Valley Classification
11	Rock Avalanche	Not Breached	Possible Glacial Influence	42	Type iv	Type 3
28	Rock Avalanche	Residual Lake, Erosion	No Glacial Influence	21	Type iv	Type 2
30	Rock Avalanche	Not Breached	No Glacial Influence	21	Type i	Type 1
31	Rock Avalanche	Not Breached	Possible Glacial Influence	25	Type iv	Type 1
37	Rock Avalanche	Residual Lake, Erosion	No Glacial Influence	21	Type ii	Type 2
41	Rock Avalanche	Not Breached	No Glacial Influence	20	Type i	Type 2
44	Rock Avalanche	Residual Lake, Breach	No Glacial Influence	25	Type i	Type 2
43	Rock Avalanche	Not Breached	No Glacial Influence	22	Type i	Type 1
45	Rock Avalanche	Residual Lake, Erosion	Possible Glacial Influence	31	Type i	Type 2
47	Rock Avalanche	Residual Lake, Infill	No Glacial Influence	22	Other	Other
49	Rock Avalanche	Residual Lake, Erosion	No Glacial Influence	21	Type i	Type 1
50	Rock Avalanche	Residual Lake, Erosion	No Glacial Influence	21	Type i	Type 1
55	Rock Avalanche	Not Breached	No Glacial Influence	21	Type i	Type 2
62	Rock Avalanche	Residual Lake, Erosion	No Glacial Influence	21	Type i	Type 2
64	Rock Avalanche	Infill	Possible Glacial Influence	23	Type ii	Type 1
65	Rock Avalanche	Residual Lake, Erosion	No Glacial Influence	21	Type iii	Type 1
72	Rock Avalanche	Infill	No Glacial Influence	42	Type iii	Type 1
74	Rock Avalanche	Not Breached	No Glacial Influence	21	Type ii	Type 2
75	Rock Avalanche	Infill	No Glacial Influence	21	Type ii	Type 1
79	Rock Avalanche	Not Breached	No Glacial Influence	21	Type i	Type 2
81	Rock Avalanche	Not Breached	No Glacial Influence	21	Type iv	Type 2
82	Rock Avalanche	Residual Lake, Erosion	No Glacial Influence	21	Type i	Type 1

83	Rock Avalanche	Not Breached	No Glacial Influence	22	Type i	Type 2
84	Rock Avalanche	Not Breached	No Glacial Influence	21	Type i	Type 2
87	Rock Avalanche	Residual Lake, Erosion	Possible Glacial Influence	21	Type i	Type 1
88	Rock Avalanche	Residual Lake, Erosion	No Glacial Influence	21	Type i	Not Specified
90	Rock Avalanche	Not Breached	No Glacial Influence	31	Type i	Type 1
94	Rock Avalanche	Breach, No Residual Lake	No Glacial Influence	31	Type i	Type 1
102	Rock Avalanche	Residual Lake, Breach	No Glacial Influence	21	Type i	Type 1
105	Rock Avalanche	Not Breached	No Glacial Influence	31	Type iii	Type 1
107	Rock Avalanche	Not Breached	No Glacial Influence	21	Type i	Type 2
108	Rock Avalanche	Breach, No Residual Lake	No Glacial Influence	31	Type ii	Type 2
136	Rock Avalanche	Residual Lake, Erosion	No Glacial Influence	31	Type ii	Type 2

nr	Valley Width (m)	Height of Release Area (m)	Dam Length (m)	D_L/V_W	Dam Width (m)	D_W/D_L	Dam Area (m^2)
11	350	450	250	0,71	350	1,40	100000
28	600	950	600	1,00	900	1,50	220000
30	800	350	800	1,00	1200	1,50	672000
31	700	650	700	1,00	1900	2,71	760000
37	190	400	190	1,00	350	1,84	73000
41	670	550	670	1,00	1500	2,24	700000
44	1000	1100	1000	1,00	1400	1,40	970000
43	300	700	300	1,00	500	1,67	100000
45	1000	1350	1000	1,00	1300	1,30	1260000
47	500	570	500	1,00	400	0,80	173000
49	350	1050	350	1,00	820	2,34	270000
50	600	800	600	1,00	600	1,00	470000
55	160	400	160	1,00	380	2,38	50000
62	200	750	200	1,00	300	1,50	50000
64	420	380	360	0,86	370	1,03	130000
65	400	530	400	1,00	800	2,00	190000
72	650	360	400	0,62	380	0,95	120000
74	145	380	145	1,00	300	2,07	55000
75	300	250	300	1,00	240	0,80	47000
79	200	500	200	1,00	530	2,65	130000
81	110	180	110	1,00	330	3,00	30000
82	500	590	500	1,00	420	0,84	200000

83	460	450	460	1,00	1400	3,04	630000
84	350	240	350	1,00	280	0,80	82000
87	450	400	400	0,89	300	0,75	93000
88	250	390	250	1,00	430	1,72	140000
90	1900	1050	1600	0,84	2200	1,38	2700000
94	300	750	300	1,00	300	1,00	70000
102	290	500	290	1,00	380	1,31	100000
105	450	900	450	1,00	1400	3,11	450000
107	800	500	800	1,00	900	1,13	630000
108	220	250	220	1,00	700	3,18	110000
136	700	900	700	1,00	2800	4,00	1500000

nr	Dam Height Max (m)	Dam Height Mean (m)	Dam Volume Maximum (m^3)	Dam Volume Mean (m^3)	Catchment Area (m^2)
11	10	6	1000000	600000	6400000
28	80	35	17600000	7700000	333000000
30	50	25	33600000	16800000	2200000
31	80	35	60000000	27000000	1800000
37	50	25	3650000	1820000	125000000
41	150	100	110000000	70000000	4000000
44	210	110	210000000	110000000	285000000
43	22	11	2200000	1100000	22900000
45	30	0	38000000	19000000	78000000
47	20	8	3460000	1384000	320000000
49	25	10	6750000	2700000	85000000
50	60	45	28000000	21000000	52000000
55	60	40	3000000	2000000	5000000
62	22	15	1100000	750000	142000000
64	22	15	2900000	2100000	99500000
65	15	8	2900000	1500000	330000000
72	30	12	3600000	1440000	11600000
74	40	20	2200000	1100000	243000000
75	40	30	1900000	1400000	7200000
79	70	50	9100000	6500000	84300000
81	45	30	1400000	900000	14000000
82	20	12	4000000	2400000	181000000
83	60	40	38000000	25000000	87000000
84	32	16	2600000	1300000	93000000
87	12	6	1100000	550000	76000000
88	16	12	2200000	1700000	21000000
90	90	50	243000000	135000000	60000000
94	40	30	2800000	2100000	195000000

102	14	8	1400000	800000	12200000
105	45	30	20000000	14000000	16000000
107	45	30	28000000	19000000	417000000
108	30	20	3300000	2200000	396000000
136	70	40	105000000	60000000	790000000

Appendix. B-2. **Database 2**

nr	Dam Failure	Glacial Influence	Two Dimensional Classification	Cross-Valley Classification	Along-Valley Classification
28	Residual Lake, Erosion	No Glacial Influence	21	Type iv	Type 2
30	Not Breached	No Glacial Influence	21	Type i	Type 1
43	Not Breached	No Glacial Influence	22	Type i	Type 1
45	Residual Lake, Erosion	Possible Glacial Influence	31	Type i	Type 2
49	Residual Lake, Erosion	No Glacial Influence	21	Type i	Type 1
50	Residual Lake, Erosion	No Glacial Influence	21	Type i	Type 1
62	Residual Lake, Erosion	No Glacial Influence	21	Type i	Type 2
65	Residual Lake, Erosion	No Glacial Influence	21	Type iii	Type 1
74	Not Breached	No Glacial Influence	21	Type ii	Type 2
75	Infill	No Glacial Influence	21	Type ii	Type 1
79	Not Breached	No Glacial Influence	21	Type i	Type 2
82	Residual Lake, Erosion	No Glacial Influence	21	Type i	Type 1
83	Not Breached	No Glacial Influence	22	Type i	Type 2
84	Not Breached	No Glacial Influence	21	Type i	Type 2
88	Residual Lake, Erosion	No Glacial Influence	21	Type i	Not Specified
94	Breach, No Residual Lake	No Glacial Influence	31	Type i	Type 1
102	Residual Lake, Breach	No Glacial Influence	21	Type i	Type 1
105	Not Breached	No Glacial Influence	31	Type iii	Type 1
107	Not Breached	No Glacial Influence	21	Type i	Type 2

nr	Valley Width (m)	Height of Release (m)	Dam Length (m)	D_L/V_W	Dam Width (m)	D_W/D_L	Dam Area (m^2)
28	600	950	600	1,00	900	1,50	220000
30	800	350	800	1,00	1200	1,50	672000
43	300	700	300	1,00	500	1,67	100000
45	1000	1350	1000	1,00	1300	1,30	1260000
49	350	1050	350	1,00	820	2,34	270000
50	600	800	600	1,00	600	1,00	470000
62	200	750	200	1,00	300	1,50	50000

65	400	530	400	1,00	800	2,00	190000
74	145	380	145	1,00	300	2,07	55000
75	300	250	300	1,00	240	0,80	47000
79	200	500	200	1,00	530	2,65	130000
82	500	590	500	1,00	420	0,84	200000
83	460	450	460	1,00	1400	3,04	630000
84	350	240	350	1,00	280	0,80	82000
88	250	390	250	1,00	430	1,72	140000
94	300	750	300	1,00	300	1,00	70000
102	290	500	290	1,00	380	1,31	100000
105	450	900	450	1,00	1400	3,11	450000
107	800	500	800	1,00	900	1,13	630000

nr	Dam Height Max (m)	Dam Height Mean (m)	Dam Volume Maximum (m^3)	Dam Volume Mean (m^3)	Catchment Area (m^2)
28	80	35	17600000	7700000	333000000
30	50	25	33600000	16800000	2200000
43	22	11	2200000	1100000	22900000
45	30	0	38000000	19000000	78000000
49	25	10	6750000	2700000	85000000
50	60	45	28000000	21000000	52000000
62	22	15	1100000	750000	142000000
65	15	8	2900000	1500000	330000000
74	40	20	2200000	1100000	243000000
75	40	30	1900000	1400000	7200000
79	70	50	9100000	6500000	84300000
82	20	12	4000000	2400000	181000000
83	60	40	38000000	25000000	87000000
84	32	16	2600000	1300000	93000000
88	16	12	2200000	1700000	21000000
94	40	30	2800000	2100000	195000000
102	14	8	1400000	800000	12200000
105	45	30	20000000	14000000	16000000
107	45	30	28000000	19000000	417000000

Appendix. C Maps

Appendix. C-1. **Grainsize Distribution Map of Månavatnet**

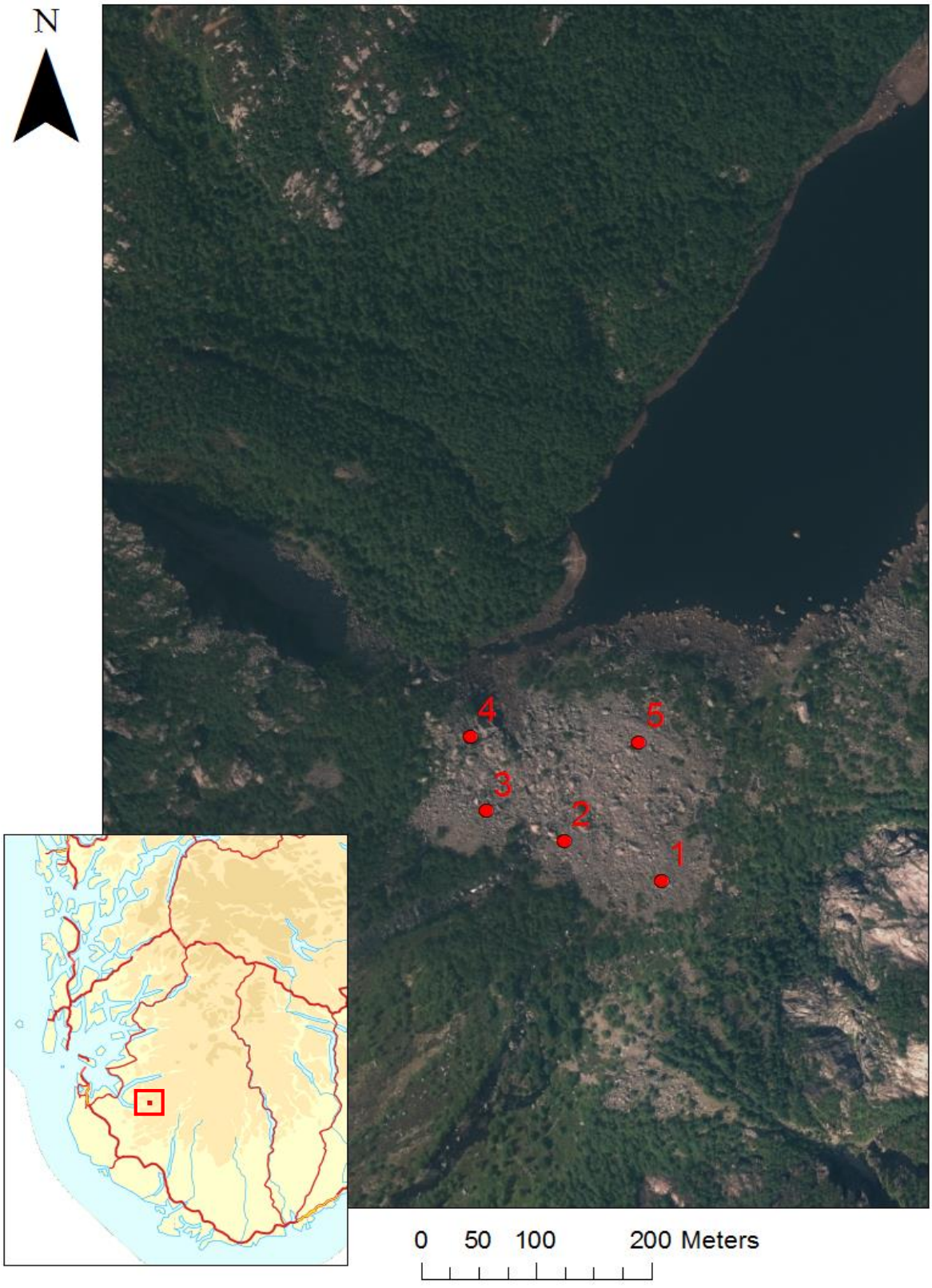

Appendix. C-2. **Grainsize Distribution Map of Gloppedalsura**

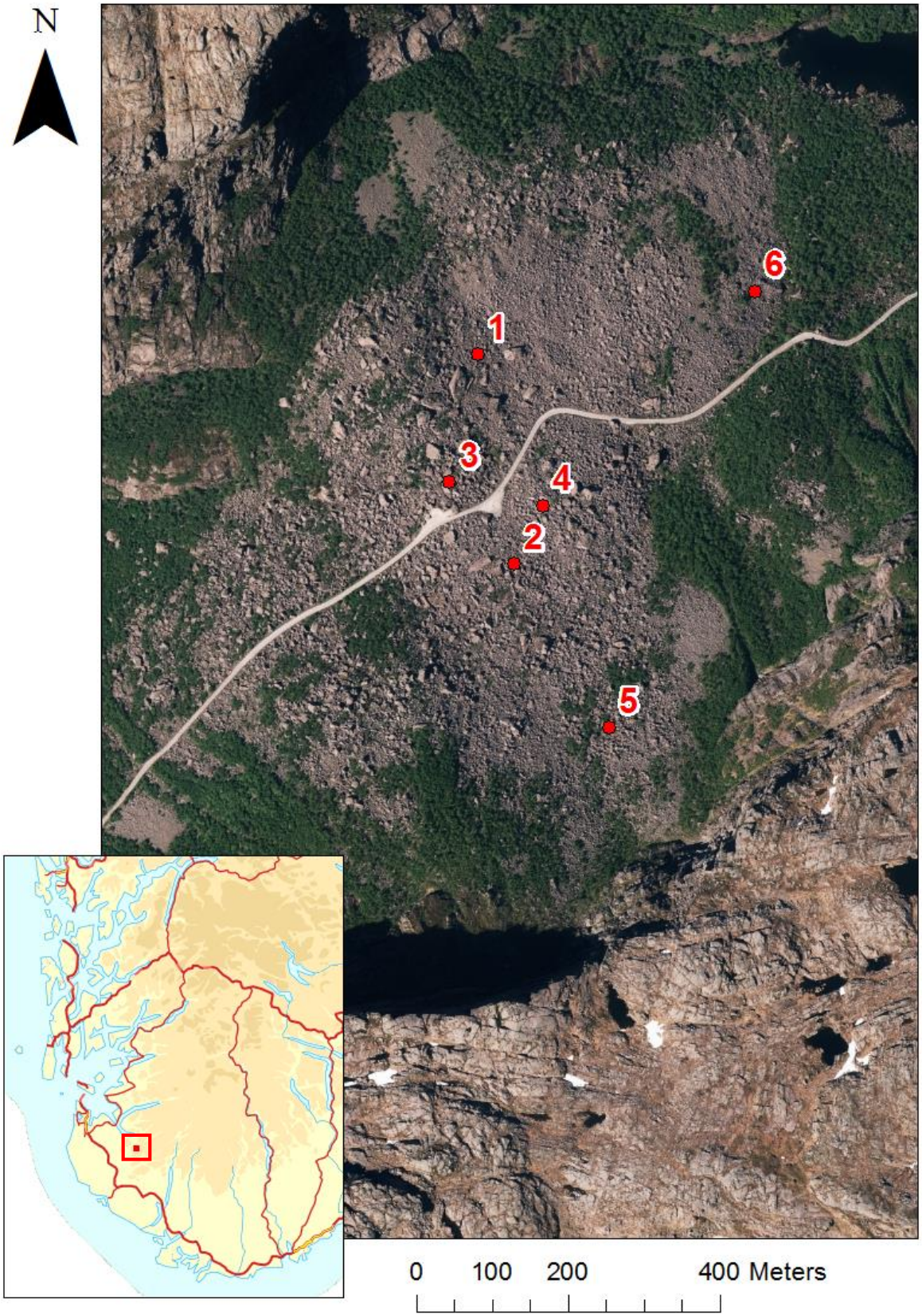

Appendix. C-3. **Regional Map of Southern Norway**

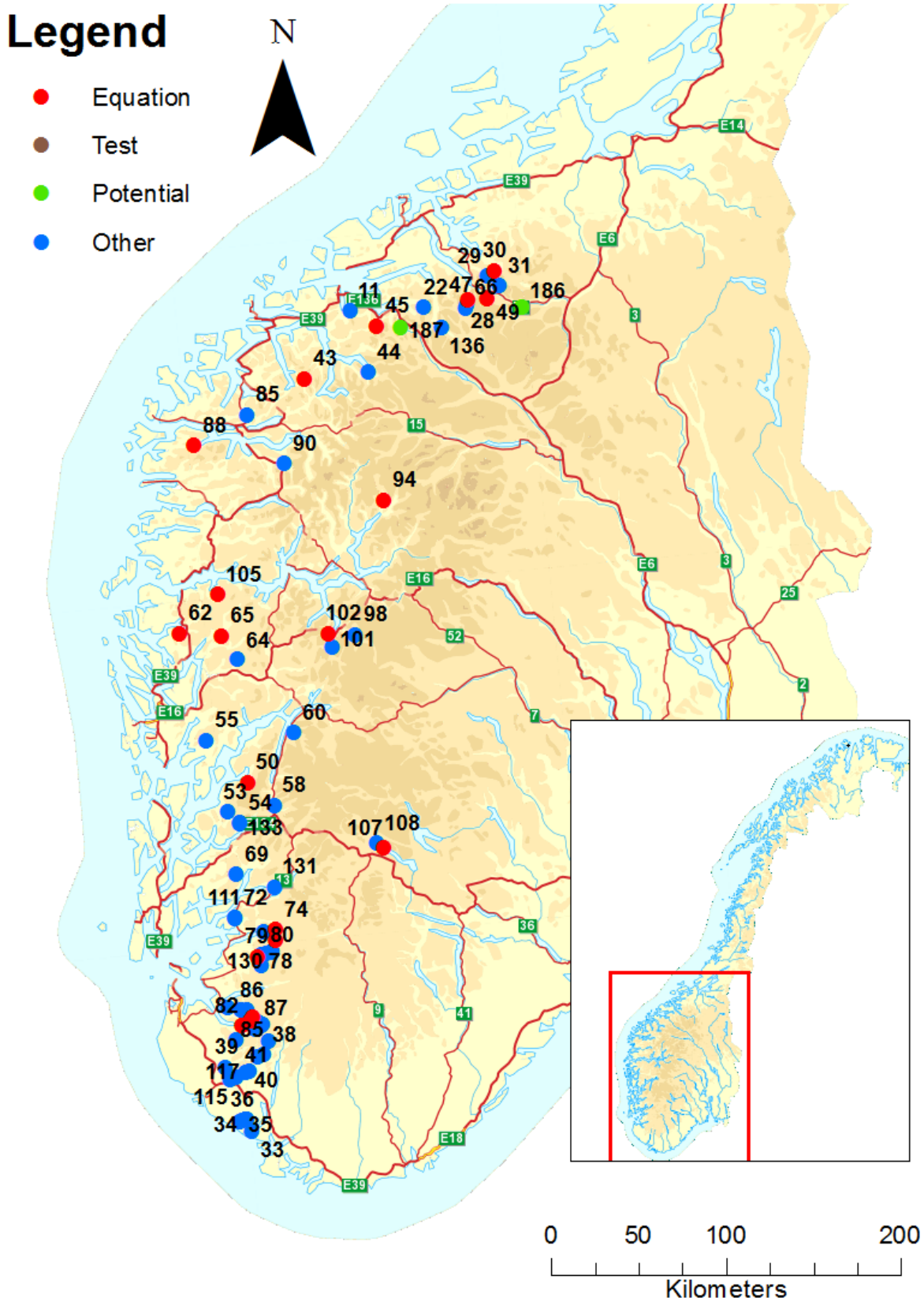

Appendix. C-4. **Regional Map of Northern Norway**